E2F1-induced IL6 mediates cancer-immune cell crosstalk by modulating T cell response in tumor microenvironment that regulates metastatic properties in melanoma

Dissertation

to obtain

the academic degree

Doctor rerum humanarum (Dr. rer. hum)

at the Medical Faculty

University of Rostock

Submitted by

Prabir Dhar

Born on 16.10.1987 in Chittagong, Bangladesh

Rostock, April 2025

https://doi.org/10.18453/rosdok_id00005667

Reviewers

Prof. Dr. rer. nat. Stefanie Scheu, Universität Rostock, Institut für Immunologie

PD Dr. rer. nat. Hugo Murua Escobar, Universität Rostock, Institut für Medizinische Genetik

PD Dr. rer. nat. Josef Mautner, Helmholtz Zentrum München, Institut für Virologie

Year of submission: 2025

Year of defense: 2026

Table of Contents

Abbreviations

$CD4^+$ T cells ..... T helper cells
$CD8^+$ T cells ..... Cytotoxic T cell
CCL1 ..... Chemokine (C-C motif) ligand 1
CCL2 ..... Chemokine (C-C motif) ligand 2
CXCL1 ..... Chemokine (C-X-C motif) ligand 1
C5/C5a ..... Complement component 5a
CXCL10 ..... C-X-C motif chemokine ligand 10
ChIP ..... Chromatin immunoprecipitation
DGEs ..... Differentially expressed genes
EMT ..... Epithelial-mesenchymal transition
ELISA ..... Enzyme-linked immunosorbent assay
GSEA ..... Gene Set Enrichment Analysis
GM-CSF ..... Granulocyte-macrophage colony-stimulating factor
IL2 ..... Interleukin 2
IL6 ..... Interleukin 6
IL10 ..... Interleukin 10
IFN-γ ..... Interferon-gamma
ICI ..... Immune checkpoint inhibitors
ng/ml ..... Nanogram per milliliter
PD-1 ..... Programmed cell death protein 1
PBMCs ..... Plasma and peripheral blood mononuclear cells
PHA ..... Phytohemagglutinin
pg/ml ..... Picogram per milliliter
qPCR ..... Quantitative polymerase chain reaction
TIME ..... Tumor immune microenvironment
Th1 ..... Type 1 T helper cells
Th2 ..... Type 2 T helper cells
Tc1 ..... Type 1 $CD8^+$ T cells

List of Tables

List of figures

Summary

Melanoma is the most aggressive and malignant type of skin cancer, which arises from the uncontrolled proliferation of melanocytes. A key player in melanoma pathology is the transcription factor E2F1 that affects tumor progression by regulating invasiveness, DNA repair, cell cycle, and apoptosis. In addition, E2F1 induces metastatic transformation by orchestrating epithelial mesenchymal transition (EMT), neoangiogenesis and extravasation, chemoresistance as well as evasion of immune surveillance.

This study investigated whether E2F1 regulates the immunomodulatory melanoma secretome and whether E2F1-regulated secreted factor modulate the melanoma-immune cell communication. To this aim, a trans-well co-culture system was established that permits studying the effect of the E2F1-regulated melanoma secretome on the transcriptional profile of immune cells, and vice versa, the effect of immune cell-derived factors on melanomas. When pairs of melanoma cell lines with high and low E2F1 expression were co-cultured with $CD4^+$ or $CD8^+$ T cells, changes in the pattern of secreted cytokines were detected, indicating that E2F1-regulated factors indeed impacted on immune cells. To predict putative E2F1 target genes with immunomodulatory function, an in silico pipeline, utilizing transcriptomics data and bioinformatics analysis, was employed. These analyses identified E2F1-dependent gene regulatory network with IL6 as a hub factor that mediates EMT and immune regulation. E2F1-induced activation and secretion of IL6 led to an autocrine forward-feedback loop that exacerbated IL6 secretion, promoting invasiveness and epithelial-to-mesenchymal transition. Mechanistically, E2F1 was found to bind to the IL6 promoter and transcriptionally regulate the IL6 expression. In neighboring $CD4^+$ and $CD8^+$ T cells, IL6 induced the expression of IL10 as well as changes in the secretome profile. Although known as immunosuppressive cytokine, IL10 exerted an antimetastaic feedback effect on melanoma cells. IL10 reduced their migratory activity, invasiveness as well as expression of genes involved in EMT, and this effect was further enhanced when combined with a knockdown of E2F1. In combination with clinical data from TCGA, this study suggests a new melanoma cancer-specific molecular signature, low-E2F1/high-IL10/low-IL6, which is associated with a favourable clinical outcome.

These findings highlight a novel gene regulatory network by which E2F1-induced factor IL6 modulates the melanoma microenvironment by altering $CD4^+$ or $CD8^+$ T cell responses. Further characterization of this tumor-immune cell crosstalk may contribute to the rational design of personalized therapies.

1. Introduction

Cancer is the second leading cause of mortality worldwide, responsible for one of every six deaths, according to the World Health Organization (Cancer 2024). Cancer is a disease characterized by uncontrolled proliferation of transformed cells (Brown et al. 2023). Abnormally proliferating cells may form a tumor that can be cancerous (malignant) or not cancerous (benign). Malignant tumor can invade the surrounding tissues as well as spread to other organs resulting in metastasis. Multiple factors play a role in the development and progression of cancer. However, cancer is generally caused by molecular changes in three types of genes - proto-oncogenes, tumor suppressor genes, and DNA repair genes (Cooper and Adams 2023). The body's immune system is also a crucial factor that is closely linked to cancer development and progression. Furthermore, cancer progression and development are profoundly influenced by bidirectional communication between cancer cells and the tumor immune microenvironment (TIME) (Anderson and Simon 2020). In recent years, cancer research has made impressive advances. However, numerous genetic and biological mechanisms that regulate cancer initiation and progression remain unknown. A more comprehensive understanding of uncontrolled cell proliferation and cancer-immune cells communication is needed to develop effective therapies that ultimately will make cancer become a curable disease.

1.1 Melanoma

Melanoma is the most aggressive type of skin cancer and one of the common cancers worldwide. The incidence of melanoma has gradually increased over the last decade and is projected to raise with a clear upwards trend in Australia, Europe and North America. According to the American Cancer Society, the number of new cases of melanoma rose to 97,610 in 2023, and caused 7990 deaths in the United States alone (Figure 1) (Siegel et al. 2023).

Introduction

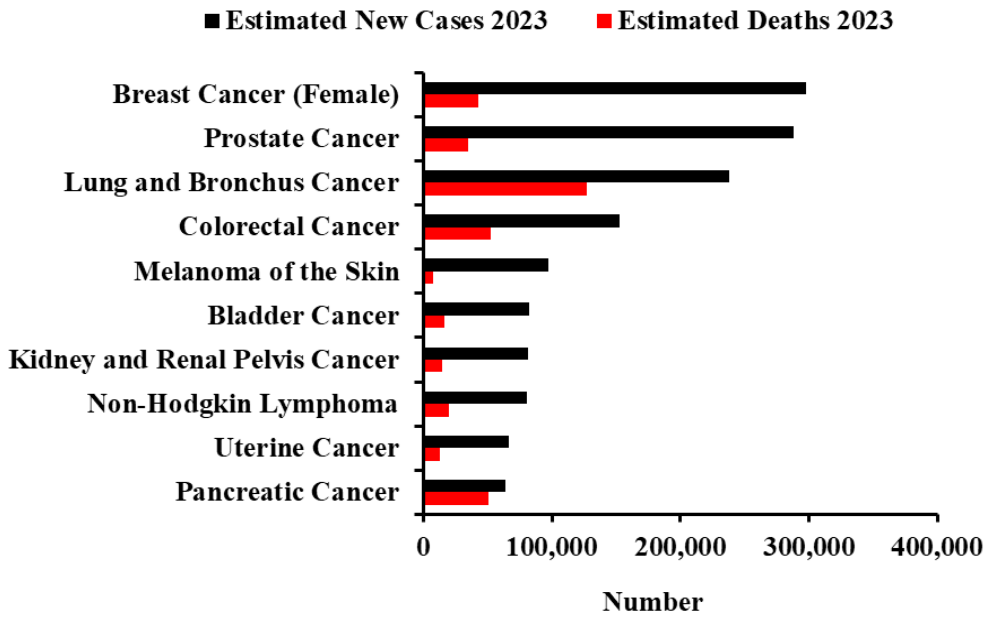

Figure 1: Estimated number of newly diagnosed cancer cases and cancer-associated deaths in USA (Siegel et al. 2023).

Melanoma arises from the uncontrolled proliferation of melanocytes, anatomically located in the lower layers of the epidermis (Matthews et al. 2017). Figure 2 illustrates the anatomy of skin, including epidermis, dermis, hypodermis, and subcutaneous layer as well as local development of melanoma as a result of uncontrolled growth of melanocyte. Melanoma affects both women and men but men more frequently. The risk of melanoma increases with age; the average age at diagnosis is 66 years. Nevertheless, melanoma is one of the most common cancers in young adults but death rates are usually higher among the middle-aged and elderly. Ultraviolet radiation (UVR) is a major environmental risk factor for melanoma development. UVR causes DNA damage including somatic mutations. Besides, lighter skin color and heredity predisposition are additional risk factors for melanoma (Tímár and Ladányi 2022). Once it reaches a metastatic stage, melanoma is one of the most lethal cancers. Treatment options for melanoma include surgery, chemotherapy, radiation, immunotherapy, and targeted therapy such as BRAF and MAPK kinase inhibitors (McArthur et al. 2014). If diagnosed early, simple surgery can solve the problem. However, due to its aggressive nature, melanoma has often already spread to other organs at the time of diagnosis, primarily the lungs, liver, and brain (Zbytek et al. 2008). In case of advanced melanoma, management is complex, particularly in those patients with cerebral metastases.

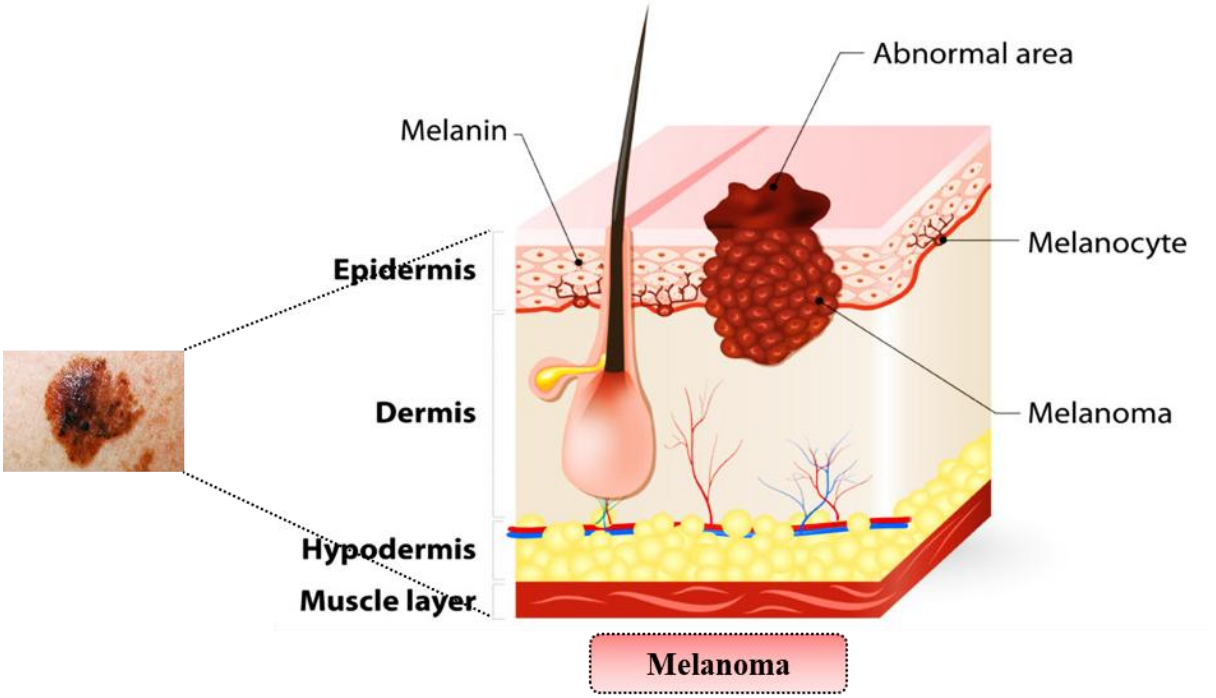

Figure 2: Schematic skin section and melanoma development. Anatomical overview of the skin including the three layers epidermis, dermis and hypodermis. Melanoma develops from melanocytes that reside in the epidermis (outermost layer). (Strazzulla et al. 2019). The figure was adapted from aimatmelanoma.org.

1.2 Overview of immune system

In broad sense, the immune system allows a living organism to discriminate between "self" and "nonself". It consists of two lines of defense: the innate and the adaptive immune system. The innate immune system comprises physical and anatomical barrier as well as effector cells, antimicrobial peptides, soluble mediators, and cellular receptors (Basset et al. 2003). Cells of the innate immune system utilize evolutionary conserved structures on pathogens; termed pathogen-associated molecular patterns (PAMPs) and to identify invaders using pattern recognition receptors (PRRs). Cells of the innate immune response, such as granulocytes, macrophages, and dendritic cells (DCs), are mostly phagocytic and able to present antigen to cells of the adaptive immune system (Akira et al. 2006; Medzhitov and Janeway Jr 2000). When an intruder is encountered, the innate immune system responds immediately by recruiting immune cells to sites of infection through the production of cytokines and chemokines (Marshall et al. 2018; Song et al. 2018). When the innate immune system is unable to clear the infection, the adaptive immune system takes over. The adaptive immune response is also known as an acquired or specific immune response. The core cellular players in adaptive immunity are lymphocytes, specifically T cells and B cells (Chi et al. 2024). With their clonotypic antigen receptors they can specifically recognize antigen, e.g.

neutralizing antibodies produced by B cells that bind to and thereby block infection by viruses. Traditionally, T cells are classified as $CD4^+$ helper T cells and $CD8^+$ cytotoxic T cells. The effector functions of $CD4^+$ T cells are mediated by both soluble factors and cell-to-cell interactions. $CD8^+$ T cells act primarily through the killing of specific target cells. While protecting the host from infections and cancer, failures in the self/non-self-discrimination by the immune system can lead to pathophysiological conditions such as autoimmunity (Chi et al. 2024; Tan et al. 2022)

1.3 Hallmarks of cancer

Cancer is a very heterogeneous disease, characterized by genetic mutations leading to abnormal cell division with the potential to invade local tissue or spread eventually into distant organ via the bloodstream or the lymphatic system by a process known as metastasis (Leong et al. 2022). The hallmarks of cancer, introduced by Hanahan and Weinberg more than two decades ago, are a logical framework that interprets the complex nature of cancer phenotypes and genotypes to understand the pathology of cancer (Hanahan 2022). As illustrated Figure 3, the ten hallmarks currently comprise genomic instability and mutation, tumor promoting inflammation, sustaining proliferative signaling, evading growth suppressors, resisting cell death, replicative immortality, inducing angiogenesis, invasion and metastasis, deregulating cellular energetics and finally avoiding immune destruction (Broertjes 2015). The tumor microenvironment (TME) plays an integral role in the functioning of these hallmarks. Genomic instability is an important hallmark for the development of malignant tumors that potentiates other hallmarks and eventually drives tumor progression. Normally, genomic integrity and mutation are closely monitored by several surveillance mechanisms including DNA damage checkpoint, DNA repair machinery and mitotic checkpoint. When DNA damage is recognized, the cell cycle is halted until the damage is repaired. If the DNA damage is beyond repair, tumor suppressor proteins such as p53 induce senescence or apoptosis (Yao and Dai 2014). Tumor promoting inflammation, another important hallmark, has been identified as another key player in cancer development. In healthy tissue, the innate and adaptive immune cells carry out their designated task by engulfing and/or destroying foreign invaders. However, during chronic inflammation, cancer cells hijack inflammatory mechanisms (i.e secretion of signaling molecules, enzymes and reactive oxygen species (ROS) into the tumor microenvironment) to promote their own growth and survival (Roncati and Figueiredo 2023). Another important hallmark of cancer is that tumor cells acquire the ability to sustain proliferative signaling in multiple ways, e.g. by

producing their own growth factors and the corresponding receptor molecules, resulting in autocrine stimulation. Alternatively, malignant cells may produce paracrine signals to stimulate tumor-associated cells, which in turn produce various factors to support their growth. Moreover, cancer cells become hyper-responsive due to elevated growth factor receptor levels or altered receptor signaling cascades. Last but not least, constitutive activation of multiple signaling pathways (e.g. Wnt, Notch, IGF, PI3K/Akt, NF-κB) may promote uncontrolled proliferation. Between 40- 60% of all melanomas carry activating BRAF mutations that ultimately regulate the RAS/RAF/MEK/ERK pathways and cause excessive proliferation (Feitelson et al. 2015; Gutschner and Diederichs 2012). Besides, sustaining proliferative signaling, evading growth suppression is a highly complementary feature of cancer. A number of tumor suppressive protein (e.g. Tp53, PTEN or RB) have been identified that inhibit diverse signaling pathways driving cell proliferation or mediate resistance to programmed cell death. Such tumor suppressor proteins are often inactivated or rapidly degraded in tumor cells following binding to oncoproteins. One such example is the human papilloma virus (HPV) encoded oncogenes E6 and E7, which are often expressed in human cervical cancers and are known to interact with Tp53 and RB leading to their inactivation (Subramanya and Grivas 2008). Continuous proliferation is an important feature of malignant cells and replicative immortality is caused by increased telomerase reverse transcriptase (TERT) expression. Mutations in the TERT promoter region or alternative splicing of the TERT transcript in cancer cells endow them with unlimited replicative capacity (Dratwa et al. 2020). The ability of cancer cells to induce angiogenesis is an additional hallmark of cancer. The formation of new blood vessels, induced by tumor cells, secures not only the supply with nutrients and oxygen but also allows tumors to dispose of their metabolic (toxic) wastes. Vascular endothelial growth factor A (VEGF-A) and its receptors (VEGFR1 and R2) play important roles in tumor angiogenesis. Moreover, some angiogenic factors (VEGF-A, FGF-2 and IL8) are strongly correlated with poor clinical outcome in melanoma patients (Ugurel et al. 2001). Activation of tumor cell invasion and metastasis is a multistep process, which starts with local invasion of tumor cells into the surrounding stroma, followed by intravasation into the vasculature and eventually extravasation at distant organs or sites. As cancer cells grow in a fast and uncontrolled manner, deregulating cellular energetics to sustain energy metabolism is essential. An emerging characteristic of cancer is avoiding immune attack. Cancer cells evolved several mechanisms to evade immune surveillance. For instance malignant cells often down-regulate the expression of MHC class I molecules as well as immunogenic antigens, thereby rendering

the cancer cells invisible to $CD8^+$ T lymphocytes. Also, up-regulation of immune inhibitory molecules such as PDL1 on cancer cells averts immune destruction by inducing T cells exhaustion (T_{ex}). In addition, tumor cell may induce an immunosuppressive microenvironment by secreting suppressive cytokines (e.g. TGF-β) or by recruiting immunosuppressive cells into the tumor microenvironment, such as myeloid-derived suppressor cells (MDSCs), which strongly inhibit the effector T cell response and promote the differentiation of regulatory T cells (T_{reg}) (Kim and Cho 2022).

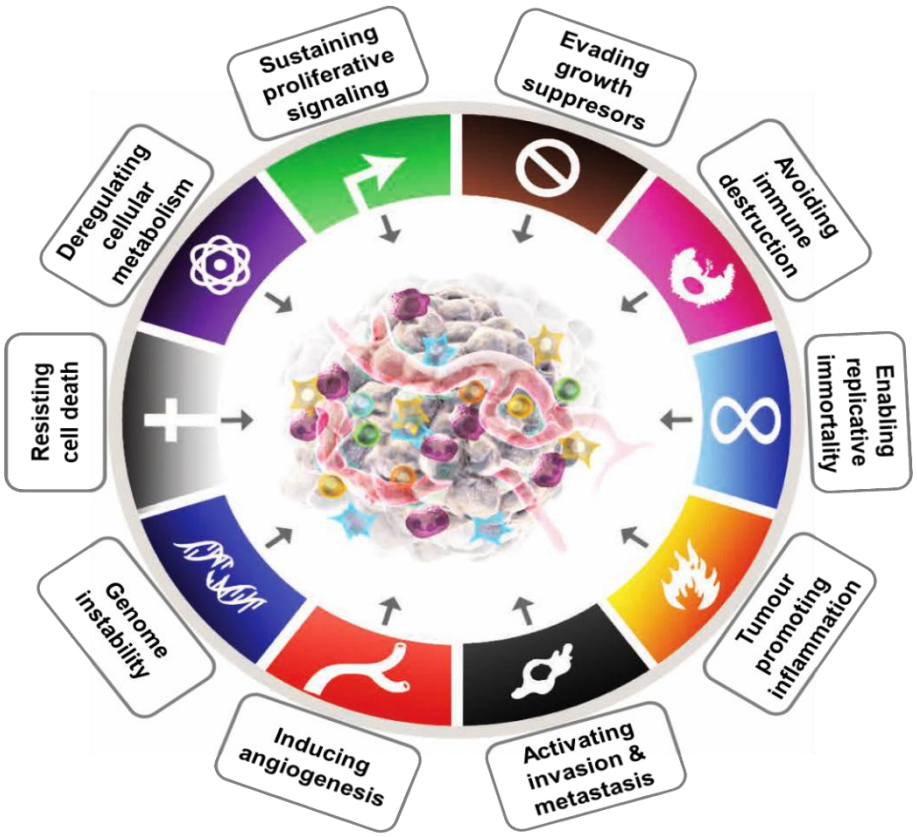

Figure 3: The hallmarks of cancer. Cancer hallmarks provide a solid foundation for understanding the vast complexity of cancer phenotypes and genotypes. The potential biological capabilities that contribute to cancer progression are acquired during the development of tumors. The ten hallmarks include genome instability, inducing angiogenesis, activating invasion and metastasis, tumor promoting inflammation, enabling replicative immortality, avoiding immune destruction, evading growth suppressors, sustained proliferative signaling, resisting cell death and deregulating cellular energetics. The figure was adapted from Hanahan, Douglas 2022.

1.4 E2F1

The family of E2 promoter binding factors (E2F) is divided into four subgroups according to their mechanism of action and potential function. Proteins of the E2F family can either act as

repressors or activators of transcription, depending on their association with Rb (retinoblastoma protein). E2F1, E2F2, and E2F3a (E2F1-3a) are potent transactivators that can transiently bind to and activate E2F target promoters (Attwooll et al. 2004). In contrast, E2F4 and E2F5 possess predominantly repressive activity. E2F1 binds to phosphorylated retinoblastoma protein (pRb), which prevents its interaction with the cell's transcription machinery. Notably, E2F1 is able to transactivates the E2F1 target genes when RB is hypophosphorylated (Manickavinayaham et al. 2020).

E2F1 is a key player in melanoma pathology. Typically, E2F1 expression levels are considerably higher in metastatic melanoma as compared to primary tumors (Alla et al. 2010). In melanoma pathology, metastasis is mainly driven by the E2F1 transcription factor, which orchestrates EMT, neoangiogenesis and extravasation, chemoresistance, and evasion of immune surveillance (Meier et al. 2014; Khan et al. 2017; Engelmann et al. 2013). In addition to its well established biological functions that govern cellular response including cell cycle, DNA synthesis and replication, checkpoint control, DNA damage and repair (Stevens and La Thangue 2004), apoptosis (Ginsberg 2002), autophagy, self-renewal, development and differentiation (Polager et al. 2008) and senescence (Dimri et al. 2000), a high expression of E2F1 is also involved in the activation of downstream prometastatic gene regulatory networks (GRNs), which in turn lead to metastatic transformation in melanoma as well as other types of cancer (Khan et al. 2017). Consistent with that, high E2F1 expression has been associated with poor outcome in many cancers including melanoma (Khan et al. 2017; Richter et al. 2019). Conversely, E2F1 ablation led to a restoration of E-cadherin expression (Alla et al. 2010) and the induction of cell death in melanoma metastatic cells resistant to BRAF inhibitors (Rouaud et al. 2018). Furthermore, E2F1-regulated microRNAs (miRNAs) and long noncoding RNAs (lncRNAs) promote tumor growth, invasion and metastasis by modulating the activation of oncogenic pathways as well as regulating tumor suppressive genes (Niu et al. 2020; Knoll et al. 2014; Logotheti et al. 2020). E2F1's aggressive activity is generally mediated by binding to transcriptional co-regulators which then induce expression of metastasis-related genes in cancer cells (Meier et al. 2014; Wang et al. 2016; Logotheti et al. 2020). For instance, E2F1 forms complexes with metastasis-associated protein 1 (MTA1) thereby potentiating cell motility and expression of hyaluronan synthase 2 (HAS2) and hyaluronic acid (HA) production that in turn modulates the tumor microenvironment by regulating the infiltration of tumor-associated macrophages in TIME (Goody et al. 2019). However, the underlying mechanism by which E2F1 signaling

modulates the immune response in the melanoma microenvironment (TME) remains largely unknown.

1.5 Tumor immune microenvironment (TIME)

The tumor immune microenvironment (TIME) consists of a complex network of multiple cell types including fibroblasts, endothelial cells, infiltrating leukocytes (T cells, B cells, DCs, MDSCs, TAMs), as well as soluble factors e.g. cytokines, chemokines, growth factors and matrix remodeling enzymes as illustrated in Figure 4 (Hassan and Seno 2020). The composition of the tumor microenvironment varies between tumor types. It is believed that the "tumor microenvironment is not just a silent bystander, but rather an active promoter of cancer progression" (Truffi et al. 2020). Within the TIME, tumor cells and non-cancerous cells including immune cells interact with each other either directly (in physical proximity) or indirectly (paracrine signaling). Direct interaction between cancer and immune cells occurs due to adhesion molecules, electrical coupling, and gap junction communication (Dominiak et al. 2020). Secretome and extracellular vesicles are involved in indirect communication between cancer and immune cells. This interaction influences tumor resistance, progression and metastasis. Moreover, it is a critical facilitator of immune escape (Salemme et al. 2021). Depending on the context, immune cells can either suppress or promote tumor growth. The secretome consists of a diverse set of factors including chemokines, cytokines, growth factors, coagulation factors, hormones, enzymes, glycoproteins released by cancer cells and immune cells within TIME ((Ritchie et al. 2021; Nagarsheth et al. 2017). Cytokines are categorized into distinct superfamilies based on their structure and function, including interferons (IFNs), interleukins (ILs), tumor necrosis factors (TNFs), transforming growth factors (TGFs), chemotactic cytokines (chemokines), and colony-stimulating factors (CSFs) (Kartikasari et al. 2021). In general, immune cells change their function and phenotype depending on the stimuli they receive from molecules secreted in the TIME (Da Cunha et al. 2019). Consequently, immune cells also secrete molecules that modulate the activities of neighboring immune and tumor cells (Etxebeste-Mitxeltorena et al. 2021).

Oncogenic signaling pathways such as BRAF/MAPK, Wnt/β-catenin and JAK/STAT can alter the cellular composition of the tumor immune microenvironment in different cancers. For instance, hyper-activation of tumor-intrinsic pathway such as BRAF-MAPK or WNT/β-catenin signaling in melanoma cells, regulates immune cell exclusion from TIME (Kakavand et al. 2017; Sumimoto et al. 2006; Luke et al. 2019). Also, the tumor-derived secretome containing chemokines and cytokines, adenosine, vascular endothelial growth factor (VEGF)

and indolamine 2, 3-dioxygenase (IDO), can modulate the interaction between tumor and immune cells (Truffi et al. 2020; Anderson and Simon 2020; Zhang and Veeramachaneni 2022). A better understanding of the interaction of tumor cells with other cell types in TIME is important for overcoming the limitations of immunotherapy as well as the development of effective therapeutics strategies against cancer.

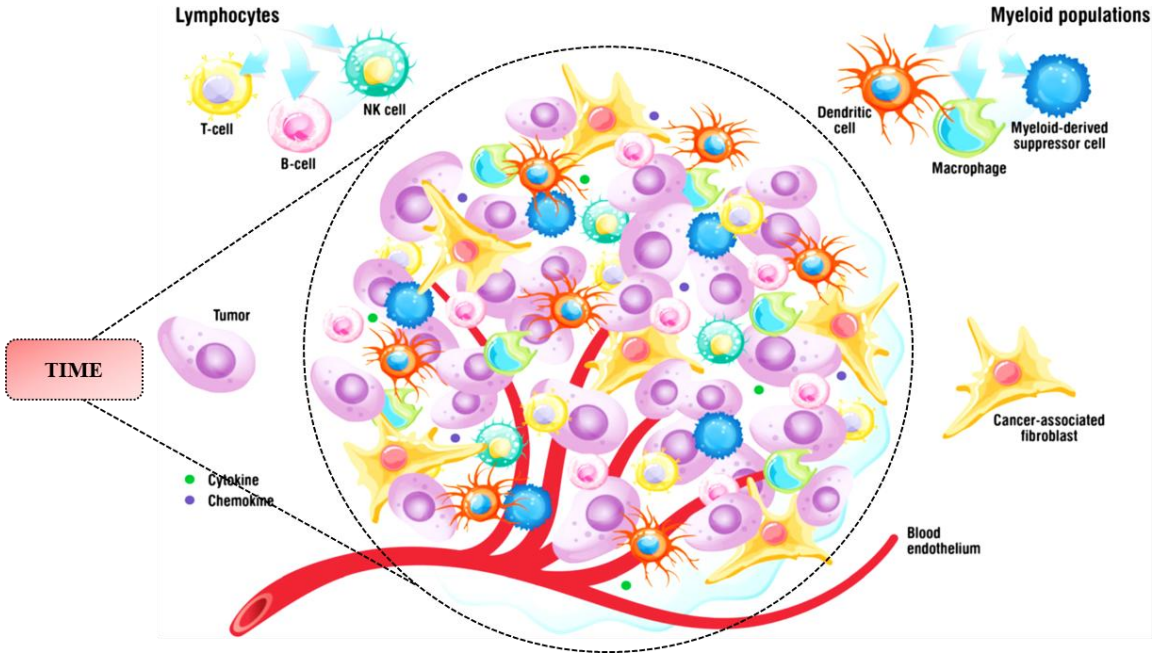

Figure 4: Schematic illustration of the tumor immune microenvironment (TIME). The tumor immune microenvironment comprises cellular and non-cellular components. The cellular component includes cancer cells, endothelial cells, pericytes, carcinoma-associated fibroblasts, and immune cells including B-cells, T-cells and natural killer cells, tumor-associated macrophages, myeloid-derived suppressor cells, and dendritic cells. The secreted factors and extracellular matrix components mainly consist of cytokines, chemokines, growth factors as well as matrix remodeling enzyme. Figure was adapted from (Zhang and Veeramachaneni 2022).

1.6 Role of $CD4^+$ and $CD8^+$ T cells in cancer

T cells are critical for the human immune system to maintain health and to protect against infections with pathogens and the development of tumors. T cells develop from hematopoietic stem cells in the bone marrow in multiple discrete steps, beginning with migration of committed precursors into the thymus, the production of a functional T cell receptor by genetic rearrangement, followed by the exit of naïve T cells from the thymus into the periphery. T cells are divided into two main subsets depending on the expression of the

co-receptors CD4 or CD8. Upon antigen recognition via their T cell receptor (TCR) and provision of co-stimulatory signals on antigen presenting cells, naïve T cells differentiate into effector or memory cells (Sun et al. 2023). Naive $CD4^+$ T cells can differentiated into several subsets including Th1, Th2, Th9, Th17, follicular helper T (TFH) cells, and regulatory T (Treg) cells that produce distinct sets of cytokines and fulfill different functions in the immune system (Speiser et al. 2023). An antitumor immune response can be exerted by $CD4^+$ T cells in several ways; either directly by eliminating tumor cells or indirectly by enhancing antitumoral responses of other immune cells. For example, Th1 cells can directly kill MHC II positive tumor cells by FasL/Fas interactions and/or in a perforin/granzyme B dependent manner (Haabeth et al. 2014). Furthermore, helper T cells (Th) can activate not only other cell types of the adaptive immune system (e.g activate B cells to secrete antibodies) but also activate innate immune cells such as macrophages. In addition, helper T cell-derived cytokines can trigger death receptors on the tumor cells, induce cellular senescence of cancer cells, or affect tumor vasculature. $CD4^+$ T helper cells also improve the efficacy of cytotoxic T lymphocytes (CTLs) responses through the licensing of antigen presenting cells, which in turn increase their antigen-presenting and co-stimulatory capacities to enhance the antitumor immune function of CTLs (Poncette et al. 2022). $CD8^+$ T cells play a central role in cancer immunity through their ability to selectively eradicate malignant cells via multiple mechanisms. For example, $CD8^+$ T cells induce apoptosis by ligation of the Fas receptor with the Fas ligand. In addition, $CD8^+$ T cells kill their targets via the delivery of pro-apoptotic molecules such as granzyme and perforin. Moreover, cytotoxic T cells induce cytotoxicity in cancer cells by releasing cytokines like IFN-γ and TNF-α and exert anti-tumor response by stimulating M1 macrophage (Philip and Schietinger 2022; Huff et al. 2019). Although $CD4^+$ T cells are critical for orchestrating antitumor response, certain $CD4^+$ T subtypes, such as Treg, can contribute to tumor development, persistence, and metastasis.

1.7 Cancer and immunotherapy

Because of the ability of the immune system to recognize and eliminate tumours, many attempts have been made to boost the immune response against cancers. These include nonspecific stimulation with cytokines, active immunization, adoptive immunotherapy and most recently, immune checkpoint inhibitors. Today, immunotherapy is a cornerstone in the treatment of melanoma, capable of reducing the risk of recurrence following conventional treatment modalities such as surgery and chemotherapy (Knight et al. 2023). Checkpoint inhibitors block checkpoint proteins expressed on T cells, such as CD28, CTLA-4 and PD-1

that normally downregulate immune responses, e.g. after an infection has been cleared. Tumor cells often express natural ligands for these checkpoint proteins and thereby actively down-regulate immune response. The most prominent example is PD-L1 that binds PD-1 on activated T cells and inhibits T cell activation and effector functions (Dong et al. 2002). Cytotoxic T-lymphocyte-associated protein 4 (CTLA-4) counteracts the positive signal mediated by CD28 by competing for the same ligands (CD80/86) expressed on APCs with higher affinity, causing T cells exhaustion (Schildberg et al. 2016). By preventing the interaction of checkpoint proteins with their ligands, checkpoint inhibitors re-invigorated exhausted and maintain effector functions of T cells, including T cells directed against tumors, and thereby sustain antitumoral immune control (Franklin et al. 2017; Sanlorenzo et al. 2014). In patients with advanced melanoma, the survival rate is 52% with treatment of anti-PD-1 antibodies (Nivolumab) and 34% when treated with anti CTLA-4 antibodies (Ipilimumab). When both antibodies were combined, long term survival was achieved in 58% of patients with advanced melanoma. Before, the overall survival rate for melanoma patients was 26% at 3 years (Wolchok et al. 2017). Despite the tremendous success in the treatment of cancer patients, the application of checkpoint inhibitors can be limited by autoimmune side effects caused by an over-reactive immune system. Furthermore, a substantial proportion of all tumors are refractory to this type of therapy (Gide et al. 2018). The reasons for this failure are not fully understood, but TIME appears to be a vital factors influencing treatment efficacy (Binnewies et al. 2018).

1.8 Aim of the thesis

The role of E2F1-regulated factors in the T cell response against melanomas is largely unknown. Therefore, the aim of this study was to unveil how E2F1-regulated melanoma immunoregulatory factors modulate the melanoma immune microenvironment.

The specific aims of the studies were:

1) To establish an in vitro co-culture system for studying tumor-immune cell interactions through secreted factors.

2) To investigate whether E2F1 expression in melanoma cells affects the immune microenvironment.

3) To examine the effect of E2F1-regulated melanoma-derived factors on $CD4^+$ and $CD8^+$ T cell response.

4) To assess the mechanism of melanoma-immune cell signaling.

2 Materials and Methods

2.1 Materials

Table 1: Kits

Kits	Manufacturer
CD4 MicroBeads, human	Miltenyi Biotec GmbH, Germany
CD8 MicroBeads, human	Miltenyi Biotec GmbH, Germany
Clariom™ D Array, human	Thermo Scientific Inc., USA
Dual-Luciferase® Reporter Assay System	Promega Inc., USA
ELISA MAX™ Deluxe Set Human IFN- γ	Biolegend Inc., USA
ELISA MAX™ Deluxe Set Human IL6	Biolegend Inc., USA
First Strand cDNA Synthesis Kit	R&D Systems Inc., USA
Human IL10 ELISA	Invitrogen Inc., USA
iQ™ SYBR® Green Supermix	Bio-Rad Laboratories GmbH, Germany
NucleoSpin® Gel and PCR Clean-Up	Macherey-Nagel GmbH & Co. KG, Germany
NucleoSpin® RNA kit	Macherey-Nagel GmbH & Co. KG, Germany
pcDNA™3.1 TOPO® TA Expression Kit	Invitrogen Inc., USA
peqGold Hot Start Mix Y	Peqlab Biotechnologie GmbH,Germany
Pierce™ ECL Western Blotting-Substrat	Thermo Scientific Inc., USA
Plasmid DNA Purification Kit (Nucleo-Bond)	Macherey-Nagel GmbH & Co. KG, Germany
Proteome Profiler Human Cytokine Array Kit	R&D Systems Inc., USA
RNeasy Kits	QIAGEN GmbH, Germany
SuperSignal™ West Femto	Thermo Scientific Inc., USA
TACS® XTT Cell Proliferation Assay	R&D Systems Inc., USA
TuroboFect™ Transfection Reagent	Thermo Scientific Inc., USA
Zombie Green™ Fixable Viability	Biolegend Inc., USA

Table 2: Chemicals and reagents

Chemicals and enzymes	Manufacturer
5x Non-Reducing Sample Buffer	Thermo Scientific Inc., USA
Agar	VWR International GmbH, Germany

Amphotericin B	Thermo Scientific Inc., USA
Aphidicolin	Thermo Scientific Inc., USA
Bio-Rad Protein Assay	Bio-Rad Laboratories GmbH, Germany
Buffy Coat	University Hospital of Rostock, Rostock
Cell Staining Buffer	Biolegend Inc., USA
Corning® Matrigel® Matrix	Corning Inc.,USA
Dimethyl Sulfoxide (DMSO)	Merck & Co., Inc., USA
DMEM	PAN Biotech GmbH, Germany
DNA Loading Dye (6 x)	New England Biolabs GmbH, Germany
Ethidium Bromide	Merck & Co., Inc., USA
FBS	PAN Biotech GmbH, Germany
Ficoll	PAN Biotech GmbH, Germany
Formaldehyde	Sigma-Aldrich GmbH, Germany
GeneRuler 1 kb DNA-Ladder	Thermo Scientific Inc., USA
Isopropanol	Walter-CMP GmbH & Co. KG, Germany
MACS buffer	Miltenyi Biotec GmbH, Germany
Methanol	J.T. Baker, USA
Milk powder	Carl Roth GmbH, Germany
Non-essential amino acid	Thermo Scientific Inc., USA
Penicillin/Streptomycin	PAN Biotech GmbH, Germany
Phytohaemagglutinin (PHA)	Thermo Scientific Inc., USA
Puromycin	Sigma-Aldrich GmbH, Germany
RNeasy Lysis Buffer	QIAGEN GmbH, Germany
Recombinant Human Interleukin 10	Miltenyi Biotec GmbH, Germany
Recombinant Human Interleukin 2	Roche Diagnostics GmbH, Germany
Recombinant Human Interleukin 6	Miltenyi Biotec GmbH, Germany
Restriction Enzyme (KpnI/EcoRV)	New England Biolabs GmbH, Germany
ROTIPHORESE®Gel 40	Carl Roth GmbH, Germany
RPMI-1640	PAN Biotech GmbH, Germany
TEMED	Bio-Rad Laboratories GmbH, Germany
T4 DNA Ligase	New England Biolabs GmbH, Germany
β-Mercaptoethanol	Carl Roth GmbH, Germany

Table 3: Consumables

Consumable supplies	Manufacturer
96-Well PCR Plate	Bio-Rad Laboratories GmbH, Germany
Cell Culture 6-Well Plate	Greiner Bio-One GmbH, Austria
Cell Culture 96-well Plate	Greiner Bio-One GmbH, Austria
Cell Culture Flask (75 cm^2)	Greiner Bio-One GmbH, Austria
Cell Culture Insert	Corning Inc.,USA
Cuvettes (10 x 4 x 45 mm)	SARSTEDT AG & Co. KG, Germany
FACS Tube	STEMCELL Technologies GmbH, Germany
Falcon (15 ml, 50 ml)	Greiner Bio-One GmbH, Austria
Petri Dish	Greiner Bio-One GmbH, Austria
Pipette Tips (10, 20, 100, 200, 1000 µl)	Greiner Bio-One GmbH, Austria
Plastic Cryotubes	Greiner Bio-One GmbH, Austria
Serological Pipette (5-25 ml)	Greiner Bio-One GmbH, Austria

Table 4: Equipment

Devices	Manufacturer
Axiovert 25 and 40 Microscope	Carl Zeiss SMT GmbH,Germany
Bacteria Incubator	Kendro Laboratory GmbH, Germany
BD FACSVerse™ Flow Cytometer	BD Biosciences, Germany
CFX96 Touch™ Real-Time PCR System	Bio-Rad Laboratories GmbH, Germany
ChemiDoc™Touch Imaging System	Bio-Rad Laboratories GmbH, Germany
CO2 Incubator CB150	BINDER GmbH, Germany
Eppendorf Biophotometer	Eppendorf Vertrieb Deutschland GmbH Germany
Gel Doc™ EZ Imager	Bio-Rad Laboratories GmbH, Germany
Hera Cell 240 CO2- Incubator	Heraeus Medical GmbH, Germany
KERN 572-43 Precision Balance	Kern & Sohn GmbH, Germany
Lumat LB9507 Luminometer	Berthold Technologies GmbH, Germany
Multifuge 3L-R Centrifuge	Heraeus Medical GmbH, Germany
Nanodrop ND1000 Spectrophotometer	Peqlab Biotechnologie GmbH, Germany
S@feflow 1.2 Cell Culture Work Cabinet	Nunc GmbH & Co. KG, Germany

SevenExcellence S470-Basic	Mettler Toledo, Switzerland
T100™ Thermal Cycler	Bio-Rad Laboratories GmbH, Germany
Tecan Spark M10 Plate Reader	Tecan Group Ltd., Switzerland
Thermo Mixer 5436	Eppendorf Vertrieb Deutschland GmbH, Germany
Vortex-Genie 2	Scientific Industries Inc.,USA

Table 5: Cell lines

Cell line	Morphology	Medium
SK-Mel147	Human metastatic melanoma cell line derived from dermal lesion (CVCL_3876).	DMEM
SK-Mel147-Ctl	Human melanoma cell clone with stable expression scrambled control shRNA (SHC002), considered as E2F1 control cell line.	DMEM + Puromycin
SK-Mel147-KD	Human melanoma cell clone with stable expression of shRNA against E2F1, considered as E2F1 knockdown cell line.	DMEM + Puromycin
C8161	Human metastatic melanoma cell line derived from abdominal wall (CVCL_0196).	DMEM
C8161-Ctl	Human melanoma cell clone with stable expression scrambled control shRNA (SHC002), considered as E2F1 control cell line.	DMEM + Puromycin
C8161-KD	Human melanoma cell clone with stable expression of shRNA against E2F1, considered as E2F1 knockdown cell line.	DMEM + Puromycin
SK-Mel-103	Human metastatic melanoma cell line isolated from the skin (CVCL_6069).	DMEM
Mel888	Human melanoma cell line derived from hypodermis (CVCL_4632).	DMEM
SK-Mel-19	Human melanoma cell line derived from dermal lesion (CVCL_6031).	DMEM

Table 6: Oligonucleotides

Oligonucleotides	Sequences
β-Actin_Fwd	5′-CGGGAAATCGTGCGTGACATTA-3′
β-Actin_Rev	5′-ACCGCTCATTGCCAATGGTGAT-3′
GAPDH_Fwd	5′-ATCGTGGAAGGACTCATGACCACA-3′
GAPDH_Rev	5′-AAGGCCATG CCA GTGAGCTTC-3′
E2F1_Fwd	5′-TCACGCTATGAGACCTCACT-3′
E2F1_Rev	5′-CTCAAGGACGTTGGTGATGT-3′
IL6_Fwd	5′-ATGAGGAGACTTGCCTGGTG-3
IL6_Rev	5′-CTGGCATTTGTGGTTGGGTC-3′
IL10_Fwd	5′-GGCGCTGTCATCGATTTCTTCC-3′
IL10_Rev	5′-GTAGATGCCTTTCTCTTGGAGC-3′
IL6 promoter_Fwd	5′-CCTGGAGACGCCTTGAAGTA-3′
IL6 promoter_Rev	5′-GGAATCTTCTCCTGGGGGTA-3′
ChIP_A_Fwd	5′-TCCCCCTAGTTGTGTCTTGC-3′
ChIP_A_Rev	5′-ATCTTTGTTGGAGGGTGAGGG-3′
ChIP_B_Fwd	5′-AGGACTGGAGATGTCTGAGG-3′
ChIP_B_Rev	5′-GGGCTAAGGATTTCCTGCAC-3′

Table 7: Antibodies

Target	Species	ID	Conjugate	Manufacturer
E2F1	Rabbit, Polyclonal	#3742	-	Cell Signaling Technology Inc.,USA
IL6	Rabbit, Monoclonal	D3K2N, #12153	-	Cell Signaling Technology Inc.,USA
Stat3	Mouse, Monoclonal	124H6, #9139	-	Cell Signaling Technology Inc.,USA
Phospho-Stat3 (Tyr705)	Rabbit, Monoclonal	D3A7, #9145	-	Cell Signaling Technology Inc.,USA
β-Actin	Mouse Monoclonal	AC-15, #A1978	-	Sigma-Aldrich GmbH, Germany
SNAI	Rabbit, Polyclonal	H-130, #sc-28199	-	Santa Cruz Biotechnology Inc.,

				USA
Vimentin	Mouse Monoclonal	V9, #sc-6260	-	Santa Cruz Biotechnology Inc., USA
E-cadherin	Rabbit, Monoclonal	#3195	-	Cell Signaling Technology Inc.,USA
N-cadherin	Mouse, Monoclonal	#610921	-	BD Biosciences, Germany
Slug	Rabbit, Monoclonal	C19G7, #9585	-	Cell Signaling Technology Inc.,USA
IL10RA	Rabbit, Polyclonal	#PA5-119895	-	Invitrogen Inc., USA
Control IgG Rabbit	Rabbit	#sc-2027	-	Santa Cruz Biotechnology Inc., USA
Anti-Mouse IgG-HRP	Horse	#7076	HRP	Cell Signaling Technology Inc.,USA
Anti-Rabbit IgG-HRP	Goat	#7074	HRP	Cell Signaling Technology Inc.,USA
Anti-hIL6-IgG	Mouse, Neutralizing monoclonal	#mabg-hil6-3	-	InvivoGen Inc.,USA
Human CD3	Mouse, Monoclonal	HIT3a, #300318	APC-Cy7	Biolegend Inc., USA
Human PD-1	Mouse, Monoclonal	EH12.2H7, #329906	PE	Biolegend Inc., USA
Human CD4	Mouse, Monoclonal	RPA-T4, #300514	APC	Biolegend Inc., USA
Human CD8	Mouse, Monoclonal	SK1#344722	APC	Biolegend Inc., USA
Isotype Control	Mouse IgG1,k	MOPC-21 #329906		Biolegend Inc., USA

Table 8: Plasmids

Name	Description
pcDNA3.1(+)	Vector with a CMV promoter for expression in mammalian cells (Addgene).
pcDNA3.1-E2F1	An E2F1 expressed plasmid with CMV promoter generated by Alla et al., 2010.
pcDNA3.1-E2F1-E132	E2F1 DNA binding defective mutant generated by Alla et al., 2010.
pcDNA3.1-E2F1-TA	E2F1 transactivation- defective vector generated by Alla et al., 2010.
pGL4-IL6-promoter	Reporter plasmid encoding the luciferase reporter gene (firefly luciferase) with upstream IL6 promoter.
pGL4.75(hRLuc-CMV)	Reporter plasmid encoding the luciferase reporter gene (renilla luciferase) with upstream CMV promoter (Promega).
pLKO.1-puro-sh.E2F1	Lentiviral based vector with stable expression of shRNA against E2F1 (Sigma-Aldrich).
pLKO.1-puro-sh.control	Lentiviral based vector with stable expression of a scramble shRNA (Sigma-Aldrich).

Plasmids maps are shown in appendix.

Table 9: Software and online databases

Name	Manufacturer/Link
Image lab 6.0	Bio-Rad Laboratories GmbH, Germany
Image J 1.53t	NIH, USA
BD FACSSuite™ V1.0.6.5230	BD Biosciences, Germany
FlowJo™ v10	BD Biosciences, Germany
Affymetrix Transcriptome Analysis Console (TAC)	Thermo Scientific Inc., USA
Enrichr	https://maayanlab.cloud/Enrichr/
SRPLOT	https://www.bioinformatics.com.cn/srplot

UCSC Genome Browser	https://genome.ucsc.edu/
JASPAR	https://jaspar2020.genereg.net/
UCSC XENA	https://xena.ucsc.edu/
OligoCalc	http://biotools.nubic.northwestern.edu/OligoCalc.html
NCBI	https://www.ncbi.nlm.nih.gov/
Venndiagram	https://bioinformatics.psb.ugent.be/webtools/Venn/

2.2 Methods

2.2.1 Cell culture

Melanoma cell lines were cultivated at 37°C with 5% CO2 in DMEM culture medium supplemented with 10% FBS, 1x MEM non-essential amino acids, 100 µg/mL Penicillin, 100 U/mL Streptomycin, 1,25 µg/mL Amphotericin B, (optional, 2 µg/mL Puromycin, only for stable cell lines).

T cells were grown in RPMI 1640 culture medium containing 10% FBS, 2 mM L-Glutamine, 1 mM Sodium pyruvate, 4.5 g/L Glucose, 10 mM HEPES, 1.5 g/L NaHCO3, 1x MEM non-essential amino acids, 100 µg/mL Penicillin, 100 U/mL Streptomycin, 1,25 µg/mL Amphotericin B at 37°C with 5% CO2.

2.2.2 Cell thawing and cryopreservation

For thawing cells, cryovials were retrieved from liquid nitrogen storage or -80°C, transferred to the cell culture laboratory on ice and thawed by placing the lower half of the vial into a 37°C water bath for 1-3 minutes. The cell suspension was transferred into a 15 mL falcon tube containing 5 mL of pre-warmed medium followed by centrifugation for 5 minutes at 1500 rpm to pellet the cells. Finally, the cell pellet was re-suspended in fresh, pre-warmed culture media.

For cell cryopreservation, cells were washed with PBS and detached from petri dish by trypsinization. The cells were then centrifuged and the pellet resuspended in fresh media. Following cell counting, the cells were resuspended in freezing media (90% FBS + 10% DMSO) prior to placing cells (1-2 x 10^6 cells/mL) in a cryovial. The cryovials were put in a cell freezing container and transferred immediately to -80°C for at least 24 hours before permanent storage in liquid nitrogen.

2.2.3 Cell counting and viability assessment

For cell counting, 10 µL of a cell culture aliquot was mixed with 90 µL of trypan blue solution (Thermo Scientific), and 10 µL the mixture was introduced into a Neubauer cell counting chamber. Cells (living and dead), in the 4 big squares, were counted under the microscope and the mean was calculated. The number of cells was determined using following formula.

Cell number (cell/mL) = Mean of cell counting × Dilution factor×10^4

To assess the percentage the viable cells, living and dead cells (unable to exclude Trypan blue) were counted using the following formula.

$$\text{Cell viability}(\%) = \frac{\text{The number of live cells}}{\text{Total number of cells}} \times 100$$

2.2.4 Generation of stable cell lines by lentiviral transduction

Stable E2F1 knockdown melanoma cell lines were generated using lentiviruses kindly provided by the Institute for Experimental Gene Therapy. For this purpose, 1×10^5 SK-Mel-147 and C8161 melanoma cell lines were resuspended into 9 mL media containing control and targeted lentiviral particles and subsequently transferred into 10 cm plates and incubated for 1 hour at 37°C with 5% CO_2. Afterwards, 3 mL of fresh culture medium was added to each plate and the cells incubated for 72 hours at 37°C with 5% CO_2. Next, medium was removed and cells were harvested by trypsinization and centrifuged at 1500 rpm for 5 min. The cells were then resuspended in selective medium containing puromycin (2 µg/mL). Successful knockdown of E2F1 was verified by Western blot.

2.2.5 PBMCs isolation from buffy coat

To isolate plasma and peripheral blood mononuclear cells (PBMCs) from buffy coats, Ficoll (PAN Biotech GmbH, Germany) density gradient centrifugation was performed for 30 minutes at 1000 × *g* without using the break. Following centrifugation, the interphase between plasma and Ficoll was carefully harvested. PBMCs were then washed two times with PBS and then resuspended in culture medium.

2.2.6 Isolation of T cells

For the purification of $CD4^+$ or $CD8^+$ T cells, 20 µL of microbeads for either CD4 or CD8 (Miltenyi Biotec) were added to 10^7 PBMCs and incubated for 15 minutes at 2-8°C. After washing the cells with MACS™ buffer (Miltenyi Biotec), cells were placed in LS columns in the magnetic field of a QuadroMACS™ (Miltenyi Biotec). Subsequently, the LS column was rinsed three times with MACS™ buffer followed by flushing out the magnetically labeled

cells by firmly pushing a plunger into column, and $CD4^+$ or $CD8^+$ T cells were collected in a tube for further processing.

2.2.7 Co-culture system

On day 1, melanoma cells expressing high or low levels of E2F were seeded in a 6-well plate (Corning) at a density of 1×10^5 cells per well. After 24 hours, $CD4^+$ or $CD8^+$ T cells isolated from healthy human buffy coats were co-cultured with the melanoma cells in the insert of trans-well plates (Corning) in the presence of 20 U/mL IL2 and 0.25 µg/mL PHA (Phytohemagglutinin) for 72 hours in a 5% CO2 humidified atmosphere. After 72 hours, cell culture supernatant, as well as melanoma and immune cells were collected for further analyses.

2.2.8 Flow cytometry

After culture for 72 hours, $CD4^+$ or $CD8^+$ T cells were harvested and centrifuged at 300 × g for 9 minutes. The cells were then washed with cell staining buffer (Biolegend) and subsequently stained with Zombie Green™ Fixable Viability Kit (Biolegend) according to manufacturer's instructions and incubated for 10-15 minutes at room temperature. Afterwards, cells were stained with the following antibodies (all from Biolegend): APC-Cy7-coupled anti-human CD3, APC-coupled anti-human CD4, APC-coupled anti-human CD8, PE-coupled anti-human PD-1 and Isotope control (Mouse IgG, k) followed by incubation for 15-20 minutes at RT (room temperature). Cells were analyzed by flow cytometry (BD FACSVerse™) and FlowJo software (FlowJo, LLC).

2.2.9 Enzyme-linked immunosorbent assay (ELISA)

The concentration of cytokines in the supernatant of cells were measured using the human IFN-γ (Biolegend), IL6 (Biolegend), and IL10 (Invitrogen) ELISA kits following the instructions of the manufacturers. Briefly, 96-well plates were coated with capture antibodies diluted in coating buffer and incubated overnight at 4°C. On the following day, the plates were washed thrice with ELISA washing buffer and blocked with ELISA blocking buffer for 1 hour at room temperature. Subsequently, plates were washed three times with washing buffer. Next, cell culture supernatant (100 µL) as well as standard were added to plates and incubated overnight at 4°C. The following day, the plates were washed and the detection antibodies were added and incubated for two hours at room temperature followed by three washes with ELISA washing buffer. Streptavidin-horseradish peroxidase was then added and incubated for 30 min in the dark followed again by a washing step, before TMB substrate

solution was added. The reaction was stopped by adding stop solution (2N H2SO4). Subsequently, the plates were read on a Tecan ELISA reader, using a test wavelength of 450 nm and a reference wavelength of 570 nm. The standard curve was generated by 2-fold serial dilution of the standard for a total 8 values.

2.2.10 Proteome Profiler-Human Cytokine Array

The human cytokine array (R&D system) allows assessment of 36 soluble factors including cytokines, chemokines and growth factors, and was performed according to the manufacturer's instructions. In brief, immune cells ($CD4^+$ and $CD8^+$ T cells) were treated with or without IL6 for 72 hours. Supernatants from monocultured (cultivation of melanoma, $CD4^+$ or $CD8^+$ T cells alone) and melanoma cell co-cultured with T cells was then subjected to cytokine array analysis. To this end, membranes containing 36 different capture antibodies were blocked with array buffer for 1 hour. Subsequently, cell culture supernatant and a cocktail of cytokine, chemokine and growth factor detection antibodies was added and incubated overnight at 4°C with gentle shaking. After carefully washing with wash buffer, the membranes were incubated for 30 min with streptavidin-HRP (1:2000) diluted in assay diluent A. After, another washing step, the membranes were developed using ECL (Thermo Scientific) and the membranes exposed using the ChemiDoc™ Touch Imaging System (BioRad) to detect the signal. The spots were quantified by Image lab software (BioRad) and the signal intensity was normalized against the internal standards.

2.2.11 Western blotting (Immunoblotting)

Western Blotting, also known as immunoblotting, was used to identify specific proteins resolved by SDS polyacrylamide gel electrophoresis according to their molecular mass.

2.2.11.1 Cell lysis and protein extraction

To prepare cellular extracts, cells were washed in PBS and then lysed in NP 40 buffer (50 mM TRIS-HCl pH7.5, 150 mM NaCl, 1% NP-40, 0,5% sodium deoxycholate) supplemented with 1% protease and phosphatase inhibitor cocktail (Roche) and incubated for 30 min on ice. Debris was removed by centrifugation at 4°C for 15 min and 14,000 rpm and the cleared cell lysates stored at -20°C.

2.2.11.2 Bradford assay for determining protein concentration

Total concentration of protein was quantified using protein assay dye reagent concentrate (BioRad). In the Bradford assay, Coomassie Brilliant Blue G-250 binds to proteins in solution, which confers the proteins a blue color with an absorbance maximum at 595 nm.

The intensity of the color is directly related to the amount of protein in the sample. To prepare the sample for protein measurement, 1 µL of protein extract was diluted into 999 µL master mix (700 µL of water, 99 µL of PBS, and 200 µL of protein assay dye reagent concentrate). The mixture was then incubated for five minutes at room temperature and the concentration of the protein was measured using a BioPhotometer (Eppendorf) at 595 nm. A pre-programmed BSA calibration curve was used to determine the protein concentration.

2.2.11.3 SDS-PAGE and Western blotting

SDS-PAGE, one-dimensional polyacrylamide (PAA) gel electrophoresis, separates polypeptide chains according to their molecular weight. The binding of sodium dodecyl sulfate (SDS) to polypeptide chains causes them to have a negative charge proportional to their molecular weight. The PAA gel is usually composed of a stacking gel in the upper layer (125 mM TRIS-HCl pH6.8, 0.1% SDS, 4% polyacrylamide, 0.11% TEMED, 0.051% ammonium persulfate) and a separating gel (375 mM TRIS-HCl pH8.8, 0.1% SDS, 10% polyacrylamide, 0.06% TEMED, 0.051%ammonium persulfate) in the lower layer. For 20 µL sample preparation, 40-50 µg protein extract was mixed with 4 µL of 5x non-reducing sample buffer (Pierce Biotechnology), 2 µL of 10x DTT (1 M), and the remaining volume filled with water and the mixture heated at 95°C for 5 minutes to convert the secondary and tertiary structure of proteins into denatured polypeptides. Prepared samples and prestained PageRuler (Thermo scientific) were then loaded into a stacking gel. The gel was run at 80 V for 2-3 hours. The proteins separated by SDS-PAGE were transferred to a nitrocellulose membrane (Hybond ECL) in a transfer unit (BioRad). The membrane was first activated by incubation for 5 min in 100% methanol. The blotting sandwich was composed of one sponge, 2 pieces of Whatman paper, then the gel, and over the gel the activated nitrocellulose membrane, then 2 pieces of Whatman paper and finally one more sponges and the transfer blot chamber filled with transfer buffer (40 mM TRIS, 25 mM glycine, 20% methanol). The transfer was carried out at 130 V for 1.5 hours. After transfer, the membrane was blocked with blocking buffer (5% nonfat dry milk powder or 5% BSA + 0.1% Tween 20 + TBS: 20 mM TRIS, 140 mM NaCl) for 1 hour at room temperature (RT), and then incubated overnight at 4°C with the primary antibody with gentle shaking. Next day, membranes were washed 3 times for 5 min with TBST (20 mM TRIS, 140 mM NaCl, 0.1% Tween 20) and then incubated with a horseradish peroxidase-conjugated (HRP) secondary antibody for 1 hour at RT and subsequently washed twice with TBST for 5 min and once with TBS (20 mM TRIS, 140 mM NaCl). Specific signals were detected by using ECL Plus Western Blotting Detection Kits

(Thermo Scientific) or SuperSignal™ West Femto (Thermo Scientific) and the membranes exposed to ChemiDoc™ Touch Imaging System (BioRad). The signal intensity of bands was quantified using Image lab software (BioRad).

2.2.12 Cloning of recombinant plasmids

Recombinant plasmids were generated using restriction enzymes and the digested insert and vector DNA fragments covalently linked using T4 ligase.

2.2.12.1 Polymerase chain reaction (PCR)

To amplify the IL6 promoter region, PCR was performed using genomic DNA as a template. PCR reaction mixture consisted of 25 µL peqGOLD hot start master mix, 2 µL forward and 2 µL reverse primers, 1 ng template genomic DNA and water to make up 50 µL. The DNA was amplified in a thermal cycler with the following program: initial denaturation at 95˚C for 5 min, followed by 35 cycles of denaturation at 95˚C for 10 sec, annealing at 57°C for 30 sec, extension for 30 sec at 72°C and followed by cooling to 4°C. The PCR products were separated by electrophoresis at 120 V in 1% agarose gels in 1 x TAE buffer containing 2 µL ethidium bromide (per 100 mL agarose gel) and visualized by UV light.

2.2.12.2 Restriction enzyme digestion of PCR product (insert) and vector

The insert (PCR product) and vector DNA were digested with restriction enzymes to create compatible ends for cloning. For the generation of the pGL4[luc2]-IL6 promoter plasmids, the respective PCR products and respective DNA vectors were digest with EcoRV and KpnI restriction enzymes (New England Biolabs) in the corresponding reaction buffers according to the manufacturer's instructions. The size of PCR products and vector were separated by electrophoresis at 120 V for 45-60 min in 1% agarose gels with EtBr (2 µL /100mL) in 1 x TAE buffer and examined in the UV-Gel-documentation-system.

2.2.12.3 DNA purification from agarose gels

Following gel electrophoresis, DNA band was excised from the agarose gel and purified using NucleoSpin® Gel and PCR Clean-Up (Macherey-Nagel) according to the manufacturer's instructions. 200 µL NT1 buffer for each 100 mg of agarose gel was added to the excised agarose gel. The mixture was incubated for 10 min at 50°C to solubilize the agarose gel followed by transferring the sample to NucleoSpin® Gel and PCR Clean/up column and centrifugation for 30 sec at 11,000 x g. Subsequently, the supernatant was carefully removed and the pellet washed once with 700 µL NT3 buffer. After removing the NT3 buffer completely by centrifugation, the pellets was air-dried for 10-15 min, and then re-

suspended in 15-30 µL of water to elute DNA. The supernatant containing DNA was collected after centrifugation at 11,000 x g for 1 min.

2.2.12.4 Ligation

The digested insert and vector products were mixed at 3:1 molar ratio, and ligated with 1 µL 10x T4 buffer and 1 µL T4 ligase in a final volume of 10µL for overnight at 16° C.

2.2.12.5 Transformation

For the heat-shock transformation, 5 µL of the ligation reaction was incubated with 50 µL of chemically competent E. coli cells (XL-10) on ice for 30 minutes followed by heat-shock at 42°C for 45 seconds and then placed back on ice for 2 minutes. The whole mixture was then quickly transferred into 1 mL of S.O.C (super optimal broth with catabolite repression) medium and incubated in an incubator at 37°C for 1 hour. The cell suspensions were then centrifuged at 8000 rpm for 2 min and 800 µL supernatant were discarded. The bacteria pellet was resuspended in the remaining S.O.C medium and plated on LB agar plates containing 50 µg/mL ampicillin and incubated at 37°C overnight. Next day, several single colonies were picked and cultured in 2 mL LB media (ampicillin 50 µg/mL) in a bacterial shaker at 37°C overnight.

2.2.12.6 Minipreps

For mini prep, 1.5 mL of overnight bacterial culture was centrifuged at 14000 rpm for 3 min. The supernatant was discarded and the pellet re-suspended in 300 µL RES buffer (50 mM Tris/HCl pH8, 10 mM EDTA, 100 µg/mL RNase A). Bacterial cells lysis was performed by adding 300 µL LYS buffer (200 mM NaOH, 1% SDS) for 5 minutes at room temperature followed by addition of 300 µL NEU buffer (2.6 M potassium acetate pH 7.2) for 10 minutes on ice. The resulting viscous solution was centrifuged at 14000 rpm for 10 minutes and 4°C. The supernatant was mixed with 630 µL isopropanol in a new tube and centrifuged the same way for 20 minutes. The resulting DNA pellet was washed once with 70% ethanol and centrifuged again for 5 minutes. The DNA pellet was dried and dissolved in 30 µL of water. To test the plasmid DNA, 1 µL of DNA was digested with restriction enzymes and separated in an agarose gel.

2.2.12.7 Maxipreps

Plasmid maxi-preparations were carried out using the NucleoBond AX 500 kit (Macherey-Nagel) according to the manufacturer's instructions. In brief, 400 mL of bacteria culture were centrifuged at 4600 rpm for 15 min at 4°C and the supernatant was discarded. Subsequently,

12 mL resuspension buffer (50 mM Tris-HCl, 10 mM EDTA, 100 µg/mL RNase A, pH 8.0) was added to the bacterial pellet and resuspended until homogenous, followed by the addition of 12 mL lysing buffer (200 mM NaOH, 1 % SDS) and a 5 min incubation at room temperature. Next, 12 mL neutralization buffer (2.8 M KAc, pH 5.1) was added and the mix centrifuged at 4600 rpm for 10 min. In the meantime, the maxi column was rinsed with equilibration buffer (100 mM Tris, 15 % ethanol, 900 mM KCl, 0.15 % Triton X-100, adjusted to pH 6.3 with H3PO4) and the supernatant was then loaded onto the column and allowed to drain by gravity flow. The bound DNA was washed three times with wash buffer (100 mM Tris, 15 % ethanol, 1.15 M KCl, adjusted to pH 6.3 with H3PO4) and then eluted from the column using elution buffer (100 mM Tris, 15 % ethanol, 1 M KCl, adjusted to pH 8.5 with H3PO4). The DNA was pelleted using isopropanol, the DNA pellet washed with 70% ethanol and then resuspended in 1 mL of TE buffer. Identity of the plasmid DNA was confirmed by sequencing at Microsynth Seqlab.

2.2.13 Transient transfection

Transient Transfection of melanoma cells was carried out using TurboFect™ Transfection Reagent (Thermo Scientific) according to the manufacturer's instructions. In brief, cells ($1.5x10^6$) were seeded in 10 cm plates one day prior to transfection. Next day, the transfection cocktail consisting of 200 µL FBS free medium, 1µg DNA and 2 µL of 1x TurboFect™ reagent was prepared and incubated at room temperature for 20 minutes. Then, the mixture was added to each well by droppings. 48 hours later, cells were harvested for immunoblotting.

2.2.14 RNA isolation

Isolation of total RNA from different melanoma cell lines, $CD4^+$ and $CD8^+$ T cells was carried out using the NucleoSpin® RNA isolation kit (Macherey-Nagel). Purity and concentration of RNA were determined using a NanoDrop ND1000 Spectrophotometer (Peqlab Biotechnologie). The RNA samples were immediately stored at -80 °C until further use.

2.2.15 Reverse transcription

The isolated RNA was subjected to reverse transcription using the first strand cDNA synthesis kit (Thermo Scientific) according to the manufacturer’s instructions. To reverse transcribe 1 µg of RNA into complementary DNA (cDNA), oligo(dT)18 primer was used and

reverse transcription was performed for 60 min at 37°C followed by 5 min at 95°C to inactivate the enzyme and cooling to 4°C. The sample was stored at -20°C for future use.

2.2.16 Quantitative real-time polymerase chain reaction (qPCR)

qPCR was performed to quantify the mRNA expression levels using SYBR premix iQ™ SYBR® Green Supermix (Bio-Rad Laboratories) on CFX96 Touch real-time PCR detection system (Bio-Rad Laboratories) according to manufacturer's instructions. SYBR Green fluorescent dye binds to double-stranded DNA molecules by intercalating between the DNA bases. Upon binding to double-stranded DNA, SYBR green increased the fluorescence signal which is directly proportional to the amount of double-stranded DNA present in the samples. All experiments were performed in triplicate for each condition. Relative mRNA expression levels were calculated using the $2^{-\Delta\Delta CT}$ method, with GAPDH and actin as the internal controls. The thermo-cycling conditions were as follows: initial denaturation at 95˚C for 30 sec, followed by 40 cycles of denaturation at 95˚C for 10 sec, annealing at between 58˚C and 60˚C (depending on oligonucleotides) for 30 sec, extension at 72˚C for 30 sec.

2.2.17 Chromatin immunoprecipitation (ChIP)

Chromatin immunoprecipitation (ChIP) was used to evaluate the interaction of protein with DNA in cells. These experiments were performed according to the (Nelson et al. 2006) protocol, but with an optimized ChIP buffer (50 mM TRIS-HCL pH7.5, 120 mM NaCl, 10 mM KCl, 2 mM MgCl2, 1 mM EDTA, 1 mM EGTA, 0.5% sodium deoxycholate, 0.5% NP-40, 0.5% Triton-X 100). One day prior to the ChIP assay, melanoma cells were seeded at $5x10^6$ cells per 150 mm dish. On the following day, cells were incubated with formaldehyde (40 µL/1 mL cell culture medium) for 15 min at room temperature to cross link proteins with DNA, followed by addition of glycine to stop the crosslinking reaction. Subsequently, melanoma cells were lysed using the ChIP buffer supplemented with phosphatase protease inhibitor cocktail (Roche). Chromatin was then sheared by sonification (15 sec on, 15 sec off pulse for 4 times at 50% amplitude) and the sample placed on ice for two minutes between pulses. Subsequently, an aliquot of each sample was collected and the DNA was pelleted by ethanol precipitation and stored at -20°C for future use as input. The samples were then immunoprecipitated by adding 2 µg of anti-E2F1 antibody (Cell Signaling Technology) for 1 mg of cell lysate, or an unconjugated anti-rabbit IgG antibody (Cell Signaling Technology) as mock-IP. The protein-protein complexes were then pulled down by binding the antibodies to protein G-coupled Sepharose beads (GE Healthcare). After washing the samples with ChIP buffer, both sample and input DNA samples were isolated using Chelex 100 solution

followed by boiling for 10 min at 95°C, in order to reverse cross-links and to extract DNA. Sample and input were then centrifuged to remove the Chelex and Chelex bounded proteins and the extracted DNA carefully collected from the supernatant. The immunoprecipitated DNA fragments were amplified and quantified using PCR-based methods or stored upto 1 month at -20°C for future use.

2.2.18 Luciferase reporter assay

To analyze the transcriptional regulation of the IL6 promoter by E2F1, the dual-luciferase reporter assay (Promega) was performed according to manufacturer's instructions. On day 1, melanoma cells with high or low E2F1 levels, were seeded in 48-well plates. On the following day, E2F1 knockdown cells or their scrambled shRNA-expressing control cells were transiently co-transfected with pGL4.10 [luc2]-IL6-promoter (firefly luciferase) plasmid and pGL4.75 [hRLuc/CMV] (renilla luciferase). In addition, SK-Mel-147 E2F1 knockdown cells were transiently co-transfected with pGL4.10 [luc2]-IL6 promoter plasmid and pGL4.75 [hRLuc/CMV] along with or without pcDNA3.1 (control plasmid), pcDNA3.1-E2F1 (E2F1expression plasmid), pcDNA3.1-E2F1-E132 (E2F1 mutant expression plasmid), and pcDNA3.1-E2F1-TA (E2F1 mutant expression plasmid). After 24 hours, cells were washed with PBS followed by the incubation of the cells with 1X passive lysis buffer for 15 min at room temperature with gentle shaking. To measure dual (firefly and renilla) luciferase activity, 20 µL of lysate was transferred to the luminometer (Berthold Technologie) that automatically dispense 50 µL of LARII, substrate for firefly luciferase, and measured immediately firefly luciferase activity with a luminometer. Subsequent automated addition of 50 µL Stop & Glo reagent, substrate for renilla luciferase, rapidly quenched firefly luminescence, with simultaneous activation of the renilla luciferase luminescent reaction and quantitated the renilla luciferase activity. The firefly RLU were normalized using the renilla RLU.

2.2.19 Invasion assay (Boyden chamber assay)

To study the invading capability of melanoma cells, invasion assay also known as Boyden chamber assay was performed. For this purpose, melanoma cells (1×10^5) were seeded in serum-free medium in a cell culture insert (pore size: 8.0 µm) on a Matrigel-coated membrane and suspended in 6-well plates with 15% FBS medium. Cell culture inserts were coated with Matrigel (Corning) which was thawed on ice, mixed with an FBS-free medium and adjusted to 3 mg/mL in concentration. Matrigel coated inserts were then incubated for 20-30 minutes at 37°C until the gel solidified. After incubation, the cells were placed on the

Matrigel-coated inserts in 1% FBS medium and the inserts were suspended in the lower chamber containing medium with 15% FBS as chemoattractant. Matrigel and non-migrated cells were removed with cotton swabs after 24 hours of incubation of cells in the incubator at 37°C with 5% CO2. The inserts were then washed with PBS and cells were stained with the fluorescent dye DAPI. Images of the underside of the membrane were taken with a fluorescence microscope and the number of invaded cells was counted with ImageJ software (NIH, USA).

2.2.20 Migration assay (wound healing assay)

Migration assay, also known as wound healing assay, was carried out to determine migration patterns of cancer cells. For migration assay, cells were seeded into 2-well silicone cell inserts (IBIDI) at a density of 1×10^5 cells/per 100 µL cell culture medium. Inserts were carefully removed, and cells were then washed with PBS, once the cells reached about 90% confluency. Afterwards, fresh culture medium containing cell proliferation inhibitor aphidicolin (5µg/mL) was added and the size of wound area measured under a light microscope. After 24 hours, the measurement was repeated. Cell migration was measured by assessing the wound area in each photograph. The images were analyzed with ImageJ software (NIH, USA).

2.2.21 Cell proliferation assay (XTT assay)

For cell proliferation and viability assay, cells were seeded at a density of 2500 cells/well in a total volume of 100 µL in 96-well plates with or without IL10 (2 ng/mL). XTT assay was performed according to manufacturer's instruction using TACS® XTT cell proliferation assay kit (R&D Systems). The cell supernatant was removed and the cells were incubated for 2 hours with 150 µL TACS XTT labeling mixture (100 µL fresh growth medium, 50 µL XTT reagent and 1 µL XTT activator). Afterwards, the absorbance was measured at 490 nm using a microplate reader (Tecan Spark M10, Tecan). Cell proliferation kinetics was determined by performing the XTT assay after different time intervals.

2.2.22 Micro-array analysis

For micro-array analysis, cells were lysed using chaotropic lysis buffer (RNeasy Lysis Buffer, RTL) and RNA extraction and purification was carried out using the RNeasy Kits (Qiagen), including a DNase I digestion step on the chromatography spin column. Finally, purity and concentration of RNA samples were determined with a NanoDrop 1000 spectrophotometer (Thermo Fisher Scientific). The gene expression profiling was performed

using Applied Biosystem TM ClariomTM D arrays (formerly Affymetrix, Thermo Fisher Scientific) according to previously described protocol (Koczan et al. 2018)). Clariom D arrays analysis was carried out by Dr. Dirk Koczan at Institute for Immunology, Core Facility Genomics, University of Rostock. Briefly, total RNA (70 ng) from each sample was subjected to reverse-transcription and subsequent polymerase chain reaction to synthesize T7 promoter-tagged double-stranded DNA (cDNA). The cDNA was then incubated overnight with T7 RNA polymerase for in vitro transcription, resulting in the synthesis of complementary RNA (cRNA). Following this, the cRNA was reverse-transcribed using random primers and dNTPs to synthesize single-stranded sense cDNA. Following the removal of template RNA using RNase H, the sense-strand cDNA was enzymatically fragmented using uracil-DNA glycosidase and apurinic/apyrimidinic endonuclease 1. Subsequently, the 3′ ends of the single-stranded DNA fragments were labelled with biotin using terminal deoxynucleotidyl transferase. Hybridization on Clariom D microarrays was performed at 45°C overnight using a GeneChip Hybridization Oven 645 (Affymetrix). Following hybridization, the microarrays were washed and stained on an Affymetrix Fluidics Station 450 and then scanned at a resolution of 0.7 µm using the GeneChip Scanner 3000 7G (Affymetrix). To visually inspect the scanned array images as well as to generate raw data i.e., CEL files, containing processed pixel intensity values for each probe on the Clariom D microarrays, Affymetrix GeneChip Command Console Software was employed. For data processing, the CEL files were analyzed using Affymetrix Transcriptome Analysis Console (TAC) software, with the following parameters (Analysis Type: Expression (Gene), Array Type: Clariom_D_Human, Summarization: Gene Level – SST-RMA, Gene-Level Fold Change < -1 or > 1, Condition Type: Comparison, Algorithm settings: default), performing normalization of signal intensity, quality control and statistical analysis. Significantly differentially regulated genes (p-value < 0.05) in test samples versus corresponding controls were determined. Gene lists were processed to obtain only relevant official gene names. Differential gene expression analyses (DGE) and in silico analyses were done by Dr. Krishna Pal Singh at the Department of Systems Biology and Bioinformatics, University of Rostock.

2.2.23 Enrichment and functional network analysis

For gene set enrichment analysis and functional network analysis, down-regulated genes (E2F1-KD vs control) in SK-Mel-147 were mapped to the E2F1_Chip_Seq_target genes (14906). E2F1_Chip_Seq_target genes were extracted from the transfac database (https://genexplain.com/transfac/) Next, to identify immune related genes involved in immune modulation, cytokine production, and regulators of secretion were retrieved from the

AmiGO database (http://amigo.geneontology.org). The immune-related gene list was compiled by Dr. Stephan Marquardt. For enrichment analysis, genes were analyzed using the Enrichr tool (https://maayanlab.cloud/Enrichr/) with the MSigDB Hallmark 2020 database. To explore the interaction between the genes and their functional networks, differentially expressed genes were uploaded to the STRING database (https://string-db.org/). A cut-off standard of a comprehensive score greater than 0.4 was applied to construct the networks. Nodes represent genes and edges represent interactions.

2.2.24 Patient survival analysis

Overall survival curves were analyzed using the Kaplan-Meier method, with statistical significance evaluated by the log-rank test. Data from melanoma patients were obtained from the Cancer Genome Atlas (TCGA) database, specifically the TCGA Skin Cutaneous Melanoma (SKCM) study cohort. Patients were separated according to the median expression levels of E2F1, IL10, and IL6 mRNA, individually or in combination thereof, using the Xena browser (https://xena.ucsc.edu/).

2.2.25 Statistical analysis

All experiments were performed at least in triplicate, if not stated otherwise. Statistical significance was calculated by paired Student's t-test (two-sided). P values less than 0.05 were considered as significant (* $P < 0.05$, ** $P < 0.01$, *** $P < 0.001$), and $P > 0.05$ as not significant (n.s.). All data are presented as mean ± standard deviation (SD).

3. Results

3.1. Evaluating the correlation between E2F1 expression and melanoma invasiveness

E2F1 is playing a pivotal role in melanoma pathology, impacting multiple cancer hallmarks, including regulation of cell cycle, survival, apoptosis, and metabolism. In addition, E2F1 induces metastasis by orchestrating epithelial–mesenchymal transition (EMT), neoangiogenesis, extravasation, and chemoresistance (Alla et al. 2010; Engelmann et al. 2013; Logotheti et al. 2020; Rosenfeldt et al. 2014). To determine whether E2F1 expression levels are associated with invasiveness, E2F1 expression levels in the melanoma cell lines SK-Mel-29 and Mel888 (low invasiveness and low metastatic potential) and SK-Mel-147, C8161, SK-Mel-103, (high invasiveness and high metastatic potential) (Alla et al. 2010) was analyzed by Western blot (Figure 5B) and invasiveness assessed using Boyden chamber assay (Figure 5A). The least invasive melanoma cell lines SK-Mel-29 and Mel888 showed low E2F1 expression levels compared to the highly invasive cell lines SK-Mel-147, SK-Mel-103 and C8161. These results suggested that E2F1 expression in melanoma cell lines positively correlates with the invasive potential.

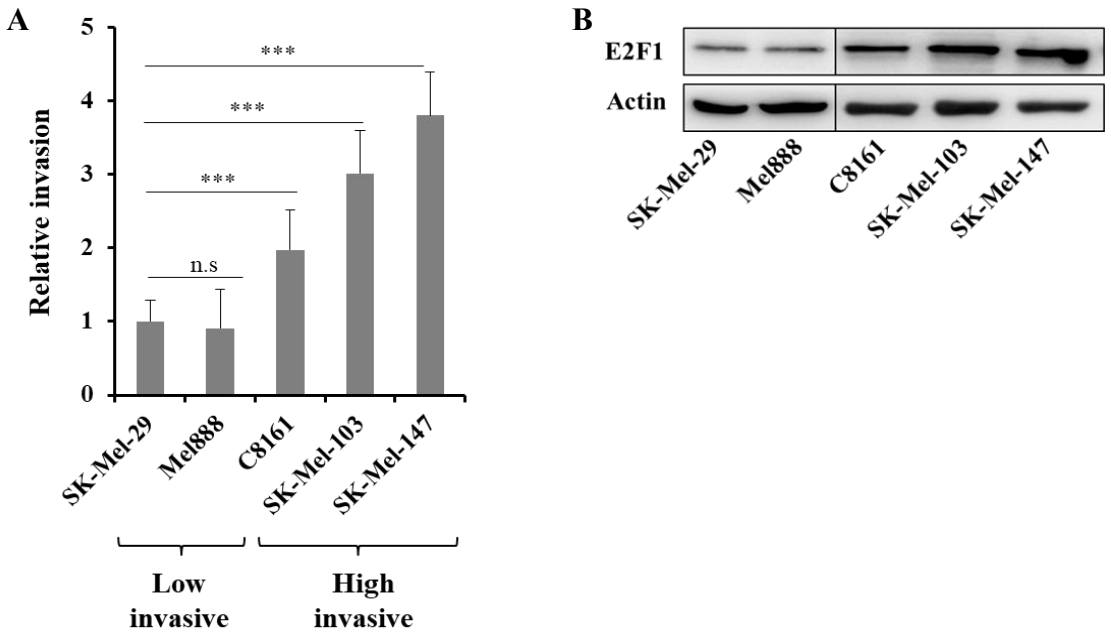

Figure 5: Invasive potential of indicated melanoma cell lines positively correlated with E2F1 expression. (A) Boyden chamber assay was used to measure invasiveness of different low and high invasive melanoma cell lines. **(B)** E2F1 expression in different melanoma cell lines was determined by Western blot. Actin served as gel loading control. All experiments were performed in triplicate. Data were analyzed using Student's t-test (two sided) and considered significant if *P<0.05, **P<0.01, ***P<0.001 and not significant (n.s.) if P>0.05.

3.2 Development of a co-culture system for studying the tumor microenvironment

E2F1 is considered a key cancer biomarker and tumor promoter in different malignancies (Li et al. 2023). However, the impact of E2F1 on immunoregulatory genes and their roles in the tumor immune microenvironment (TIME) is not entirely understood. To study the effect of the E2F1-induced melanoma secretome on phenotype and transcriptional program of immune cells, a trans-well co-culture system was established where different melanoma cell lines were cultivated with $CD4^+$ or $CD8^+$ T cells isolated from PBMCs of different healthy donors. The outline of the co-culture setup is presented in Figure 6A. To directly assess the effect of E2F1 on the melanoma secretome, pairs of melanoma cell lines with high and reduced levels of E2F1 expression (designated E2F1-high and E2F1-low) were used. These pairs were generated by shRNA-mediated knockdown of E2F1 in the E2F1-high melanoma cell lines SK-Mel-147 and C8161. Successful knockdown of E2F1 was verified by Western blot as shown in Figure 6A. The different melanoma cell lines were co-cultured with $CD4^+$ or $CD8^+$ T cells that had been activated using low dose of the T cell mitogen phytohemagglutinin (PHA) and IL2 to facilitate detection of activating and inhibitory effects of the secretome on immune cells and of immune cells on the tumor cells. In parallel, the melanoma cell lines as well as $CD4^+$ and $CD8^+$ T cells were cultured alone (designated monoculture).

In monoculture, $CD4^+$ and $CD8^+$ T cells were stimulated with or without PHA for 72 hours to induce activated and nonactivated T cell states. T cells activation status was tested by measuring typical activation markers, namely IFN-γ secretion and PD-1 expression (Brenchley et al. 2002; Castro et al. 2018; Simon and Labarriere 2018). IFN-γ secretion was quantified by ELISA, while PD-1 expression level was measured using flow cytometry. The corresponding data for $CD4^+$ T cells are depicted in Figures 6B and 6C, while those for $CD8^+$ T cells are presented in Figures 6D and 6E. The findings demonstrated that activated T cells exhibited significantly elevated IFN-γ secretion and PD-1 expression compared to nonactivated T cells. The gating strategies for PD-1 expression are shown in appendix (Figure 18).

To evaluate potential toxicity in both coculture and monoculture conditions, the viability of $CD4^+$ and $CD8^+$ T cells was monitored using flow cytometry (Figure 6D, 6E), while melanoma cell viability was tested by trypan blue exclusion (Figure 6F, 6G). Collectively, the results showed no significant differences in cell viability between coculture and monoculture conditions, demonstrating that the established coculture system does not induce cytotoxic effects.

Results

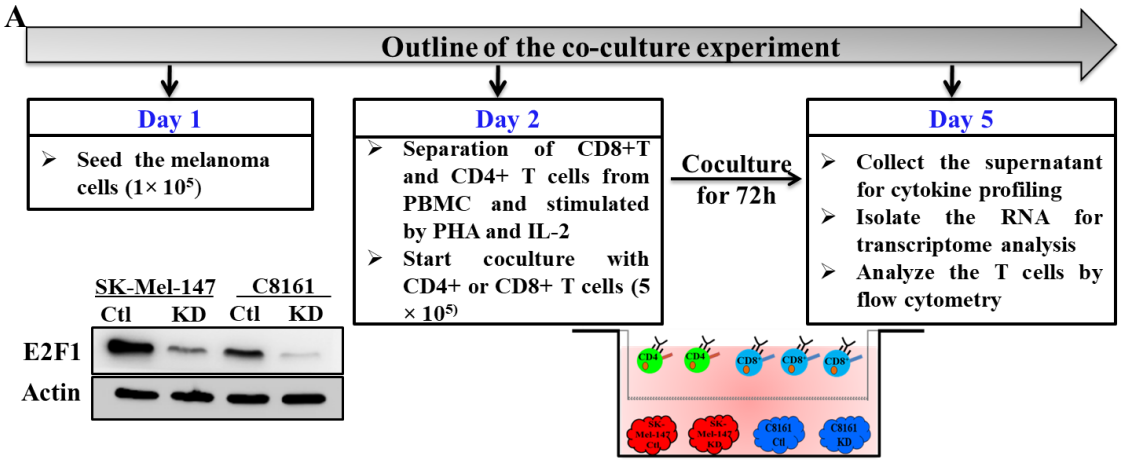
A
Outline of the co-culture experiment
Day 1
Seed the melanoma cells (1× 10^5)
Day 2
Separation of CD8+T and CD4+ T cells from PBMC and stimulated by PHA and IL-2
Start coculture with CD4+ or CD8+ T cells (5 × 10^5)
Coculture for 72h
Day 5
Collect the supernatant for cytokine profiling
Isolate the RNA for transcriptome analysis
Analyze the T cells by flow cytometry
SK-Mel-147
C8161
Ctl
KD
Ctl
KD
E2F1
Actin

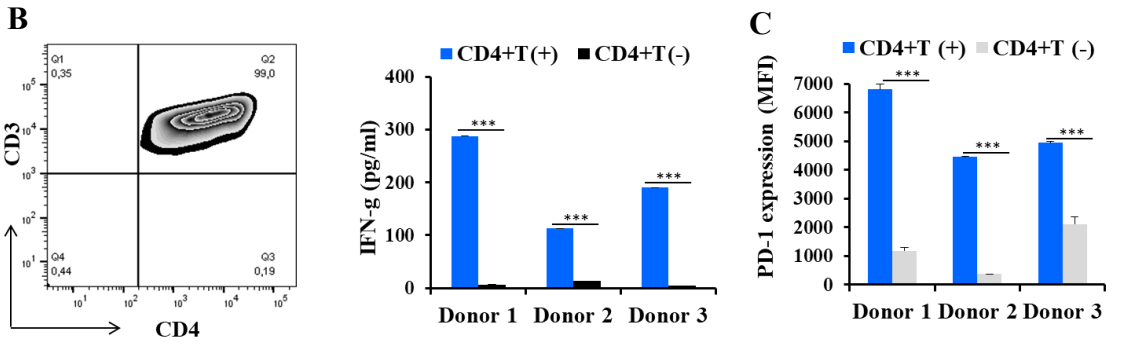
B
CD3
CD4
Q1 0,35
Q2 99,0
Q4 0,44
Q3 0,19
CD4+T(+)
CD4+T(-)
IFN-g (pg/ml)
Donor 1
Donor 2
Donor 3
C
CD4+T (+)
CD4+T (-)
PD-1 expression (MFI)
Donor 1 Donor 2 Donor 3

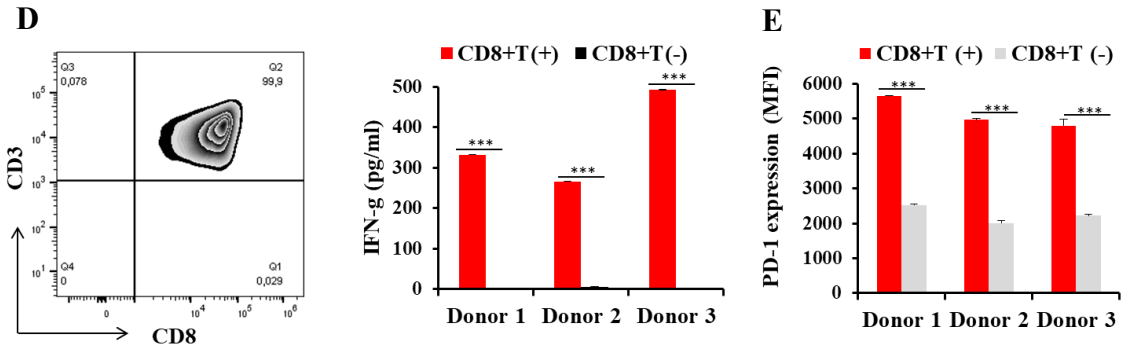
D
CD3
CD8
Q3 0,078
Q2 99,9
Q4 0
Q1 0,029
CD8+T(+)
CD8+T(-)
IFN-g (pg/ml)
Donor 1
Donor 2
Donor 3
E
CD8+T (+)
CD8+T (-)
PD-1 expression (MFI)
Donor 1 Donor 2 Donor 3

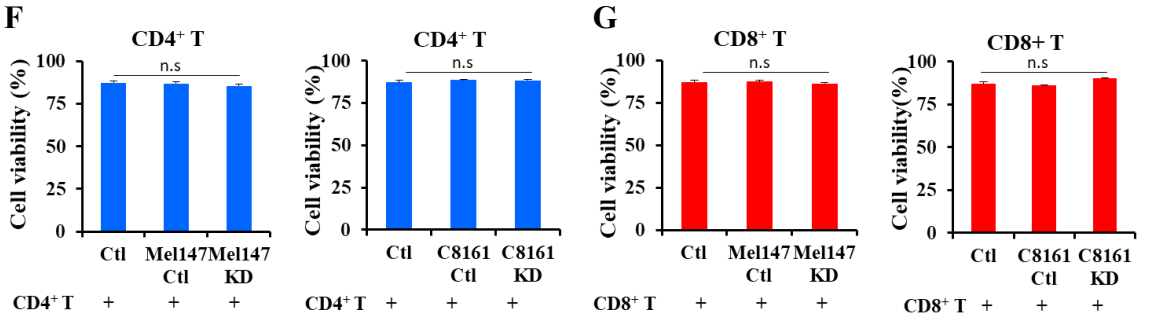
F
CD4+ T
Cell viability (%)
n.s
Ctl
Mel147 Ctl
Mel147 KD
C8161 Ctl
C8161 KD
CD4+ T
G
CD8+ T
CD8+T
CD8+ T

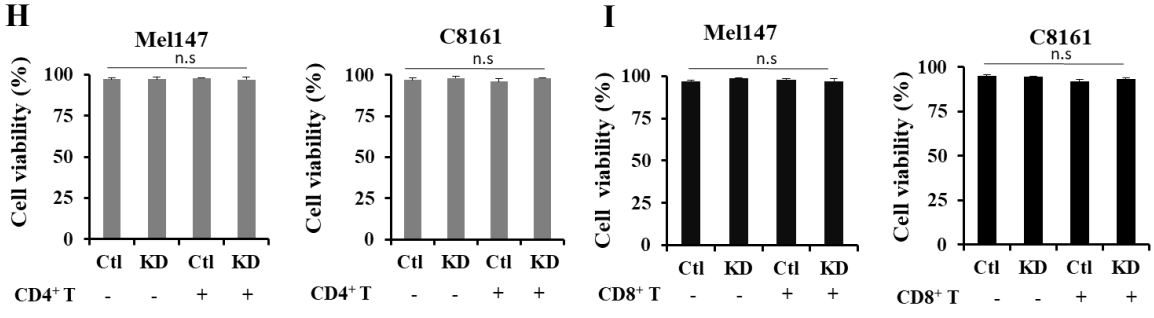
H
Mel147
C8161
Cell viability (%)
n.s
Ctl
KD
CD4+ T
I
CD8+ T

Figure 6: Co-culture system for studying tumor/immune cell interactions. (A) Outline of the experimental setup of the co-culture system. Successful E2F1 knockdown (KD) in melanoma cell lines (SK-Mel-147 and C8161) was confirmed by Western blot and purity of isolated $CD4^+$ and $CD8^+$ T cells was verified by flow cytometry. **(B, C, D, E)** IFN-γ secretion and PD-1 expression of $CD4^+$ (**B, C**) and $CD8^+$ T cells (**D, E**) after incubation with (+) or without (-) PHA. IFN-γ secretion and PD-1 expression were detected by ELISA and flow cytometry, respectively. PD-1 expression on T cells was measured as mean fluorescence intensity (MFI). **(F, G)** Viability analysis of $CD4^+$ **(F)** and $CD8^+$ T cells **(G)** after cultivation with or without melanoma cells was assessed by flow cytometry (data are representative of three healthy donors). **(H, I)** Viability analysis of melanoma cells was assessed by trypan blue staining after monoculture or co-culture with $CD4^+$ **(H)** or $CD8^+$ T cells **(I) (**data are representative of three healthy donors). All experiments were performed in triplicate. The data were analyzed using Student's t-test (two sided) and considered significant if *P<0.05, **P<0.01, ***P<0.001 and not significant (n.s.) if P>0.05.

Following monoculture of T cells and co-culture of SK-Mel-147 Ctl (high-E2F1) and SK-Mel-147 KD (E2F1-knockdown) melanoma cell lines with $CD4^+$ or $CD8^+$ T cells for 72 hours, the cell culture supernatant was subjected to cytokine and proteome profiling using an array containing 36 factors including cytokines, chemokines, growth factors and other soluble proteins. The secretion of different molecules under the influence of E2F1 in various co-cultured conditions is shown as heat map (Figure 7). In comparison to $CD4^+$ T monoculture, co-culturing of SK-Mel-147 Ctl cells with $CD4^+$ T cells resulted in increased levels of most secreted proteins (cytokines and chemokines). Moreover, co-cultivation of SK-Mel-147 Ctl cells with $CD4^+$ T cells resulted in increased secretion of various factors, including CCL1, CCL2, C5/C5a, CXCL10, CXCL11, IL1a, IL4, IL10, IL13, IL17E, IL12p70, IL27, and IL32a, compared to both $CD4^+$ T cell monoculture and co-culture with SK-Mel-147 KD cells. Conversely, co-culture of SK-Mel-147 KD cells with $CD4^+$ T cells led to increased secretion of CXCL12, IFN-γ, IL2, IL8, IL21, and TNF-α compared to both $CD4^+$ T cell monoculture and co-culture with SK-Mel-147 Ctl cells.

On the other hand, co-culture of $CD8^+$ T cells with SK-Mel-147 Ctl, compared to both $CD8^+$ T cell monoculture and co-culture with SK-Mel-147 KD cells, resulted in decreased levels of IL1β, IL12p70, IL32a and TREM-1. Conversely, co-culture of $CD8^+$ T cells with SK-Mel-147 KD led to an increased secretion of multiple chemokines and cytokines, such as CCL1, CCL2, C5/C5a, CXCL1, CXCL11, CXCL12, IFN-γ, IL1α, IL1ra, IL18, and IL21, and IL27 compared to both $CD8^+$ T cell monoculture and co-culture with SK-Mel-147 Ctl. Overall,

these findings indicated that the established in vitro co-culture system is an effective model for studying the effects of the tumor-derived secretome on immune cells and vice versa.

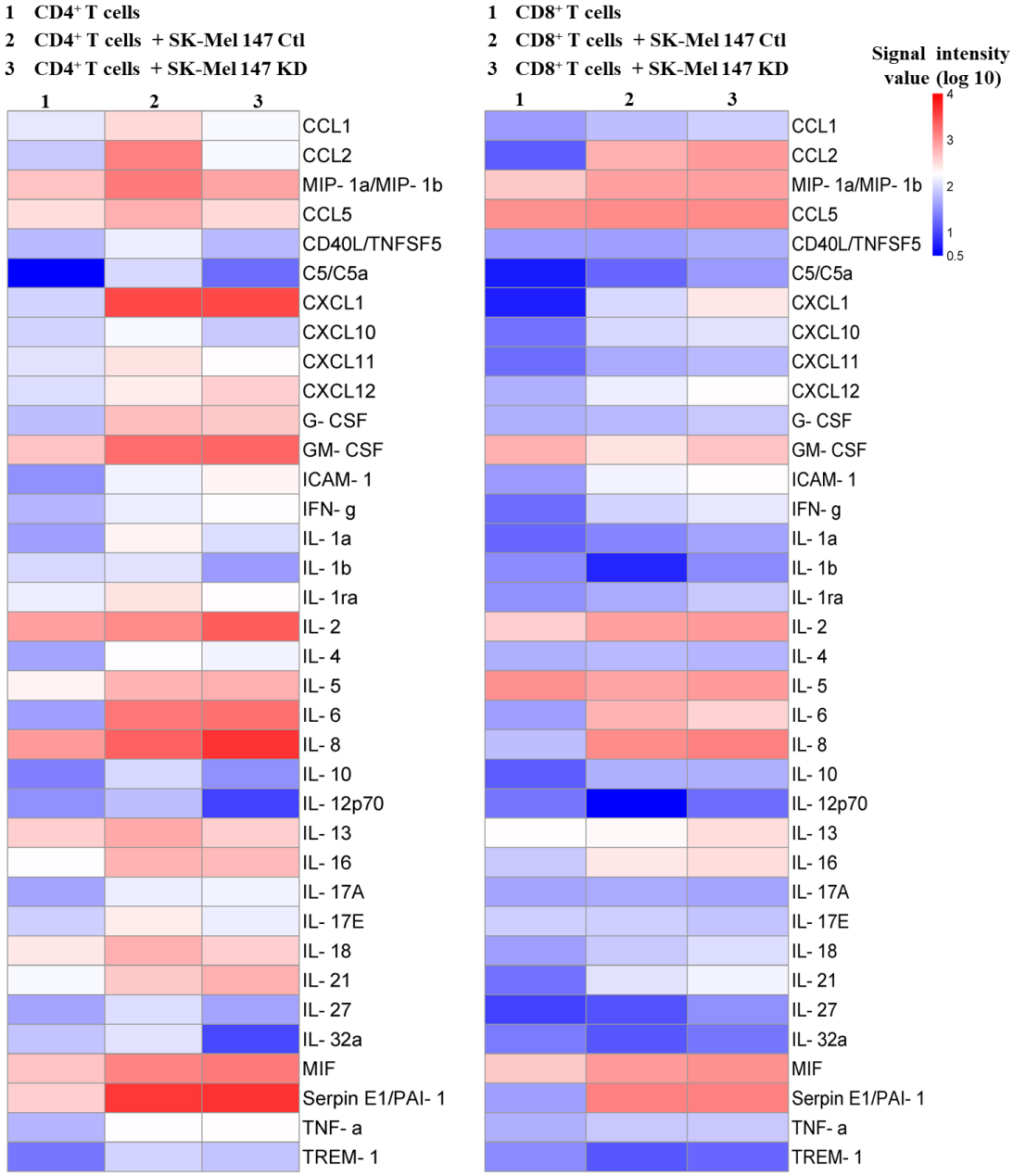

Figure 7: Proteomic profiling of secreted factors. Heat map of secreted proteins following co-culture of SK-Mel-147 Ctl (E2F1 high) and SK-Mel-147 KD (E2F1 low) cells with $CD4^+$ or $CD8^+$ T cells as well as monoculture of $CD4^+$ or $CD8^+$ T cells. Cell culture supernatants were analyzed by protein array (data are representative of one healthy donor). The signal intensity value of the cytokine array was normalized against the internal standards and subsequently converted into log10 values for heat map generation.

3.3 Identification of E2F1-regulated immunomodulatory factors in melanoma

The role of E2F1 in EMT and resistance to tumor therapy is well accepted (Knoll et al. 2014; Rosenfeldt et al. 2014; Yan et al. 2014; Khan et al. 2017). Furthermore, increased levels of E2F1 have been reported in invasive and metastatic tumors and are associated with poor patient survival (Alla et al. 2010; Vera et al. 2013). However, little is known about the role of E2F1 in shaping the tumor-immune microenvironment. The detection of differentially secreted immunomodulatory proteins depending on E2F1 expression levels in the co-culture experiments suggested that E2F1-regulated factors impact on immune cells. To identify E2F1-regulated immunomodulatory genes in melanoma cells, RNA was isolated from SK-Mel-147 Ctl and SK-Mel-147 KD cells. These cell lines were selected because the parental cell line had shown the highest invasive potential and high E2F1 expression (Figure 5A). After quality control, RNA samples were subjected to microarray analysis. Differential gene expression analyses (DGE) and in silico analysis were carried out by Dr. Krishna Pal Singh, Department of Systems Biology and Bioinformatics, University of Rostock. The data obtained from the Transcription Analysis Console (TAC) was utilized to generate gene lists. Differential gene expression analysis (p value ≤ 0.05) of E2F1-depleted cells revealed 865 upregulated and 1258 downregulated transcripts (Figure 8A).

Next, to search for putative targets of E2F1, a list of genes harboring E2F1 binding sites (14906) was retrieved from the transfac database. This list of genes was then integrated with downregulated genes (1258) of the melanoma cell lines with the earlier generated list of potential E2F1 target genes (14906). This analysis identified 512 genes contain potential E2F1 binding sites indicating that E2F1 may regulates these targets. Next, to identify E2F1-dependent immune functional genes, an additional list of immune modulating genes (2138) involved in immune modulation, cytokine production, and regulation of secretion, which was extracted from AmiGO database. This list of immune modulatory genes was then integrated with the 512 predicted E2F1 targets. Finally, the analysis identified 54 significantly downregulated putative E2F1-targets with an impact on immune regulation in melanoma cells. The outline of the in silico analysis is shown in Figure 8B. The list of 54 identified genes is provided in the appendix (Table-10).

Next, Gene Set Enrichment Analysis (GSEA) was performed to investigate whether the predicted E2F1 target genes (54) mediate both immune modulation and metastatic activity. The GSEA analysis revealed enrichment of several hallmarks emphasizing genes not only associated with cancer, for example mTORC1 signalling, angiogenesis, PI3K/AKT/mTOR signaling and EMT, but also unleashed immunomodulation signatures such as inflammatory

response, TNF-α and IL6 signalling pathways. The list of genes involved in these hallmarks are shown in Figure 8C. Notably, IL6 gene involved in multiple hallmarks, including apoptosis, inflammatory response, UV response, TNF-α and IL6 signalling pathways, epithelial-mesenchymal transition (EMT), and hypoxia, alongside with other genes. The other genes associated with these pathways are also presented in Figure 8C. E2F1 is known to drive metastasis and progression in various cancers through mechanisms mediated by the PI3K/AKT/mTOR and mTORC1 signalling pathways (Qiao et al. 2021; Xu et al. 2020; Real et al. 2011). Additionally, the E2F1-targets show strong enrichment of immune regulatory pathways such as TNF-α and IL6 that are critically involved in the pathogenesis of several immunological disorders like Rheumatoid arthritis (RA) and multiple sclerosis (MS) (Hirano 2021; Jang et al. 2021).

To gain a deeper understanding of the underlying functional connections in the E2F1 regulated 54 identified genes, functional network analysis was conducted using STRING (https://string-db.org/). Functional and network analysis demonstrated that E2F1-regulated factors are highly interconnected. More importantly, IL6 occupied a central network hub position (Figure 8D) indicating that E2F1 regulates an immunomodulatory network via IL6. More importantly, IL6 showed the highest differential expression after E2F1 knockdown in melanoma cells. Thus, IL6 emerged as a promising candidate that could be associated with common pathways underlying melanoma progression as well as key mediator of immune regulatory function orchestrated by E2F1.

Results

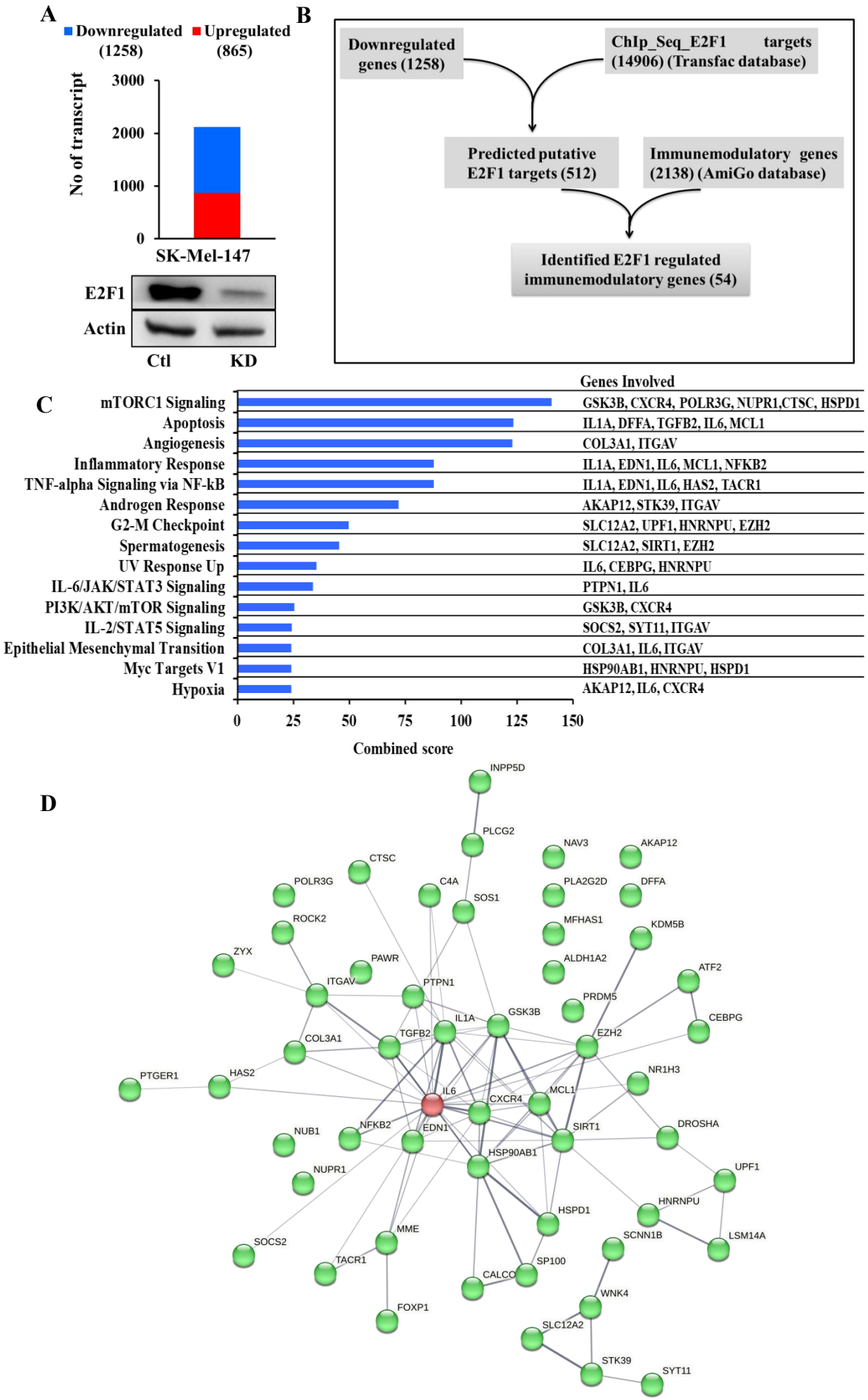
A
Downregulated (1258)
Upregulated (865)
No of transcript
3000
2000
1000
0
SK-Mel-147
E2F1
Actin
Ctl
KD
B
Downregulated genes (1258)
ChIp_Seq_E2F1 targets (14906) (Transfac database)
Predicted putative E2F1 targets (512)
Immunemodulatory genes (2138) (AmiGo database)
Identified E2F1 regulated immunemodulatory genes (54)
C
Genes Involved
mTORC1 Signaling
GSK3B, CXCR4, POLR3G, NUPR1,CTSC, HSPD1
Apoptosis
IL1A, DFFA, TGFB2, IL6, MCL1
Angiogenesis
COL3A1, ITGAV
Inflammatory Response
IL1A, EDN1, IL6, MCL1, NFKB2
TNF-alpha Signaling via NF-kB
IL1A, EDN1, IL6, HAS2, TACR1
Androgen Response
AKAP12, STK39, ITGAV
G2-M Checkpoint
SLC12A2, UPF1, HNRNPU, EZH2
Spermatogenesis
SLC12A2, SIRT1, EZH2
UV Response Up
IL6, CEBPG, HNRNPU
IL-6/JAK/STAT3 Signaling
PTPN1, IL6
PI3K/AKT/mTOR Signaling
GSK3B, CXCR4
IL-2/STAT5 Signaling
SOCS2, SYT11, ITGAV
Epithelial Mesenchymal Transition
COL3A1, IL6, ITGAV
Myc Targets V1
HSP90AB1, HNRNPU, HSPD1
Hypoxia
AKAP12, IL6, CXCR4
0
25
50
75
100
125
150
Combined score
D
INPP5D
PLCG2
CTSC
NAV3
AKAP12
POLR3G
C4A
SOS1
PLA2G2D
DFFA
ROCK2
MFHAS1
KDM5B
ZYX
PAWR
ALDH1A2
ATF2
ITGAV
PTPN1
PRDM5
GSK3B
IL1A
CEBPG
TGFB2
EZH2
COL3A1
PTGER1
HAS2
NR1H3
IL6
CXCR4
MCL1
NUB1
NFKB2
EDN1
SIRT1
DROSHA
HSP90AB1
NUPR1
UPF1
HSPD1
HNRNPU
SCNN1B
LSM14A
SOCS2
MME
TACR1
SP100
CALCO
WNK4
FOXP1
SLC12A2
STK39
SYT11

Figure 8: Identification of E2F1-induced immunomodulatory factors. (A) Total number of differentially expressed genes (DGE) identified between SK-Mel1-47 Ctl and SK-Mel-147 E2F1 KD cells, with number of up and down regulated genes indicated. **(B)** Workflow of in silico pipeline for the prediction of E2F1-regulated genes in melanoma cells. **(C)** GSEA analysis of the identified E2F1-regulated factors in the transcriptome of melanoma cell lines showed a strong enrichment for prometastatic and immunomodulatory functions. Enrichment analysis was performed using the Enrichr tool (https://maayanlab.cloud/Enrichr/enrich/) with the MSigDB Hallmark 2020 database. **(D)** Functional network analysis and network visualization using string software illustrated a highly interconnected network with IL6 positioned as the hub. All microarray experiments were performed in triplicate for each sample.

3.4 Correlation between E2F1 and IL6 expression in melanoma cell lines

To understand the molecular mechanistic relationship between E2F1 and IL6, a pair of E2F1 knockdown melanoma cell lines were generated. These pairs were generated by shRNA-mediated knockdown of E2F1 in the E2F1-high melanoma cell lines SK-Mel-147 and C8161. The protein expression of E2F1 and IL6 was confirmed by Western blot, as shown in Figure 9A. Next, the mRNA expression levels of E2F1 and IL6 were examined by qPCR in these melanoma cell lines (high-E2F1/invasive and low E2F1/non-invasive). These experiments showed that mRNA expression of IL6 is markedly decreased in the E2F1-low melanoma cell lines compared to the E2F-high melanoma cell lines (Figure 9B). Furthermore, secretion of IL6 from E2F1-high and E2F1-low melanoma cell lines were determined by ELISA. A significant reduction in the levels of IL6 in the cell culture supernatant was noticed in E2F1-low cell lines as compared with E2F1-high cell lines (Figure 9C). The results collectively suggest that the expression and secretion of IL6 positively correlate with E2F1 expression in melanoma cell lines.

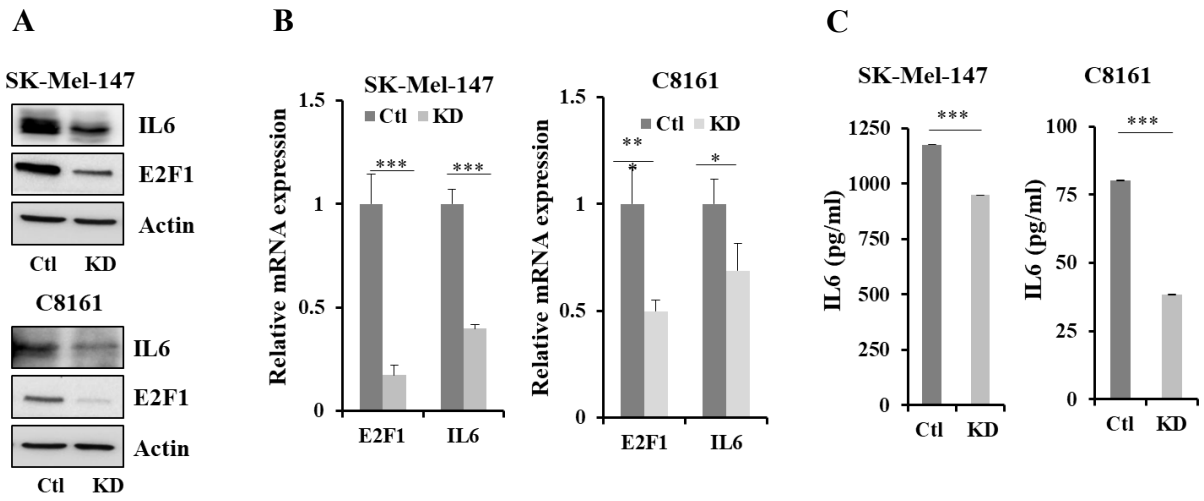

Figure 9: Functional correlation between E2F1 and IL6 expression in different melanoma cell lines. (A) intracellular protein levels by Western blot. **(B)** E2F1 and IL6 mRNA expression was analyzed by qPCR and **(C)** Levels of secreted IL6 were determined by ELISA. All experiments were performed in triplicate. The data were analyzed using Student's t-test (two sided) and considered significant if *P<0.05, **P<0.01, ***P<0.001.

3.5 IL6 contributes to E2F1-regulated EMT and invasiveness of melanoma cells

IL6 is a critical mediator of tumor metastasis, playing a significant role in promoting both invasiveness and epithelial-to-mesenchymal transition (EMT) (Zhang et al. 2021). To investigate the functional contribution of IL6 in melanoma cell metastasis further, SK-Mel-147 E2F1-KD cells were treated with recombinant IL6 and expression of genes involved in EMT analysed by Western blot. Knockdown of E2F1 resulted in decreased levels of N-cadherin and Vimentin, and an increased level of E-cadherin. In contrast, IL6 treatment reduced E-cadherin levels in E2F1-KD cells and restored N-cadherin and Vimentin levels (Figure 10A). Boyden chamber assays demonstrated that invasive potential of E2F1 low melanoma cells (SK-Mel-147 KD) was significantly impaired as compared to control SK-Mel-147 cells, highlighting the role of E2F1 in melanoma cell invasion. Interestingly, treatment with IL6 (5ng/mL) restored the invasive capacity of SK-Mel-147 KD cells, suggesting that IL6 can compensate for the loss of E2F1 in promoting cell motility. Conversely, the addition of an IL6 inhibitor (neutralizing mAb, 30 ng/mL) led to the strong reduction in cell motility, emphasizing the critical role of IL6 in melanoma cell invasion (Figure 10B). Neither IL6 nor IL6 inhibitor affected the viability of melanoma cells, excluding toxic effects as cause for the observed results (Figure 10C). Collectively, these findings suggested that IL6 contributes to E2F1-induced melanoma metastasis by inducing genes involved in EMT and thereby promoting invasiveness of melanoma cells.

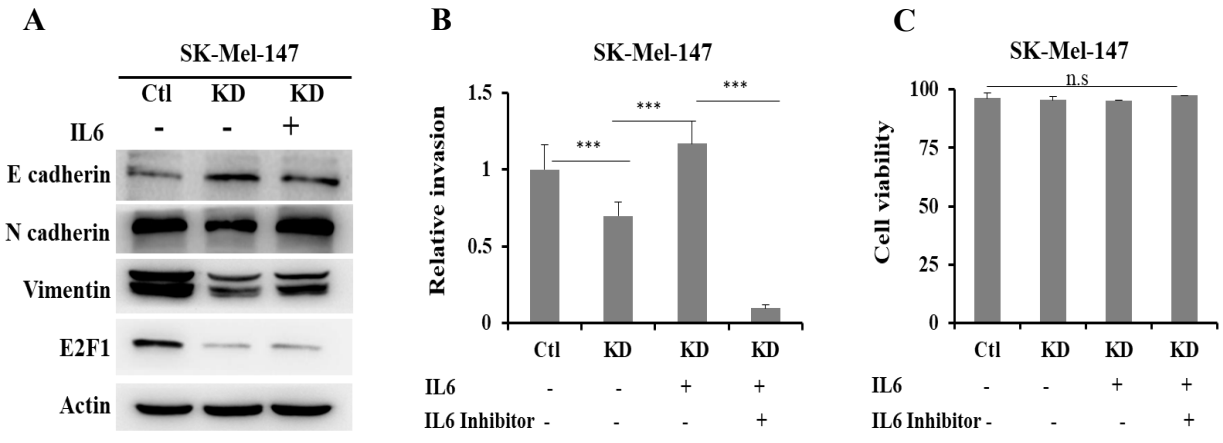

Figure 10: Contribution of IL6 to E2F1-induced melanoma invasiveness and EMT. **(A)** Western blot analysis of the expression of EMT markers in SK-Mel-147 Ctl, SK-Mel-147 KD cells, and SK-Mel-147 KD treated with IL6. **(C)** Invasive potential of E2F1 Ctl and KD cells was analyzed using Boyder chamber assay. E2F1 KD cells were also treated with recombinant IL6 alone, or IL6 plus an IL6 neutralizing mAb (IL6 inhibitor). **(D)** Cell viability of E2F1 Ctl and KD melanoma cells untreated or treated with IL6 alone, or with IL6 and an IL6 neutralizing mAb, was measured by trypan blue staining. All experiments were performed in triplicate. The data were analyzed using Student's t-test (two sided) and considered significant if *P<0.05, **P<0.01, ***P<0.001 and not significant (n.s.) if P>0.05.

3.6 IL6 is a direct transcriptional target of E2F1

To analyze transcriptional regulation of the IL6 promoter, E2F1 binding sites were mapped within the 10 kbp region upstream of the IL6 transcription start site. To this end, the ENCODE Transcription Factor ChIP-seq data of the UCSC genome browser was utilized. A major E2F1 binding cluster of 701 bp proximal to the translational start site was identified. Next, to identify the exact binding positions of E2F1 in the IL6 promoter region, the JASPAR database was analyzed. This analysis revealed two E2F1-responsive binding motifs (BS1: -112 bp and BS2: +7 bp) as schematically illustrated in figure 11A. To validate whether newly predicted E2F1 binding motifs (BS1: -112 bp and BS2: +7 bp) are subject to binding on the IL6 promoter, two ChIP assays (ChIP A and ChIP B) were performed in the SK-Mel-147 Ctl (E2F1 high) and SK-Mel-147 KD (E2F1 depleted) cell lines. ChIP A and ChIP B were performed to confirm the E2F1 binding site 1 at -112 bp and E2F1 binding site 2 at +7 bp respectively. These experiments showed that E2F1 binding was drastically reduced in E2F1-knockdown cells compared to the Ctl cell line indicating the binding of E2F1 sites to the IL6 promoter (Figure 11B).

Next, to confirm IL6 transcriptional activity by E2F1, a luciferase construct comprising the predicted E2F1 binding sites (969 bp fragment) was cloned into a pGL4.10 [luc2]- reporter plasmid and transiently transfected in E2F1-high and E2F1-low melanoma cell lines. The outline of the cloning strategies is provided in appendix (Figure 19). Knockdown of E2F1 in SK-Mel-147 (E2F1-low cell lines) resulted in a greatly reduced (approximately 40% lower) luciferase activity compared to E2F1 control cells (SK-Mel-147) (Figure 11C). To assess whether E2F1 transactivates IL6 directly, empty vector (pCMV_Ctl), or E2F1 wildtype, or E2F1 mutants deficient in DNA binding (E132), or transactivation (ΔTA), were co-transfected with pGL4.10[luc2]- reporter plasmid into the SK-Mel-147 E2F1-low cell line. Compared to the empty vector and E2F1 mutants (E132 or ΔTA), E2F1 expression resulted

in the reactivation of IL6 promoter activity (Figure 11D). In contrast, overexpression of either E2F1 mutant did not induce promoter activity, indicating that both the DNA-binding domain and the transactivation domain of E2F1 are essential for the transcriptional regulation of IL6. The expression of E2F1 and its mutants was confirmed by Western blot analysis (Figure 10E). Altogether, the results suggested that E2F1 regulates the transcriptional activity of the IL6 promoter.

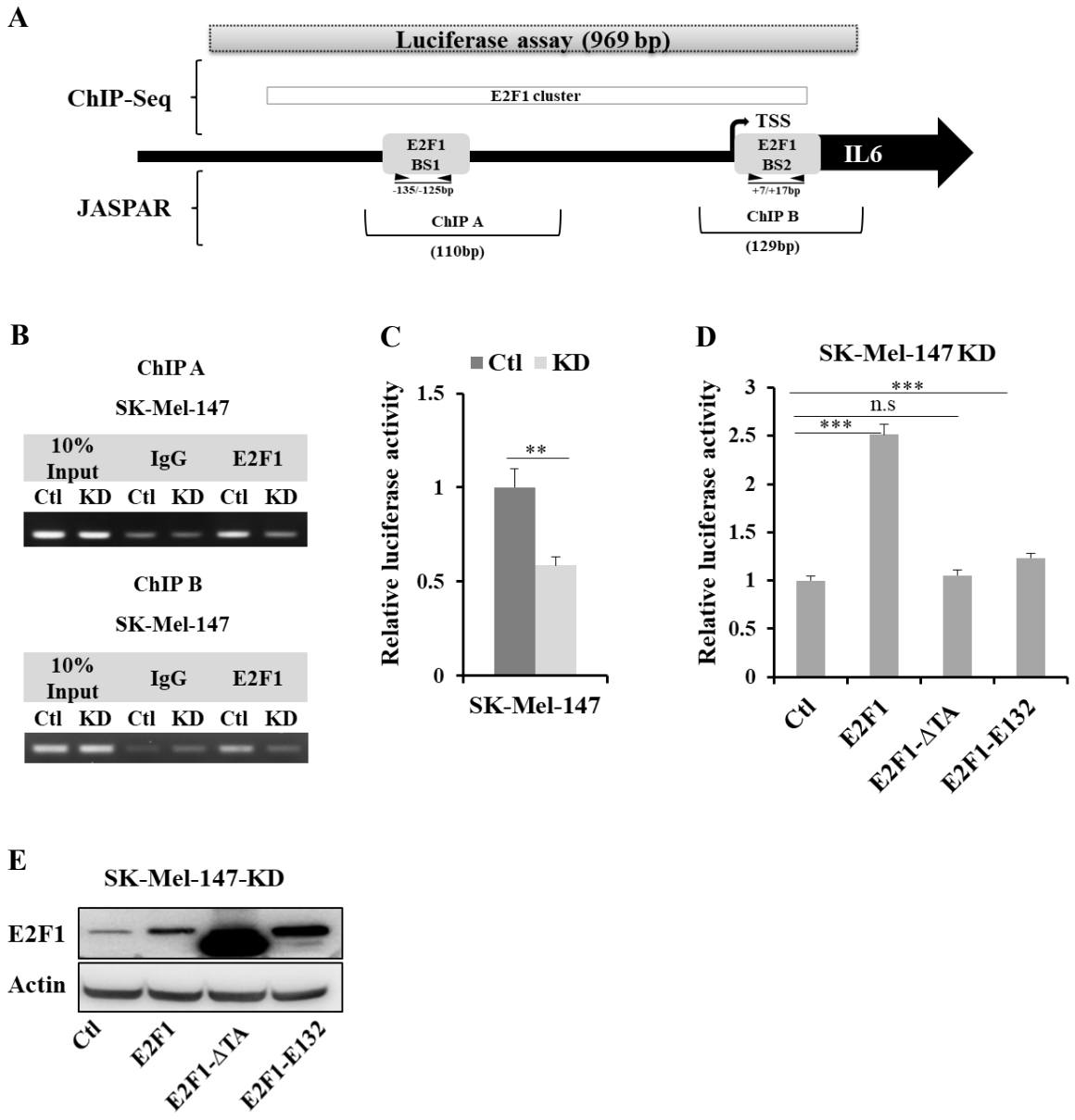

Figure 11: E2F1 transcriptionally regulates IL6 expression. (A) Schematic illustration of the newly predicted binding site for E2F1 as well as E2F1 ChIP seq clusters (https://genome.ucsc.edu) on the IL6 promoter. E2F1 binding sites (BS) were predicted by JASPAR (https://jaspar.elixir.no/). The ChIP fragments utilized for analysis, along with their respective sizes are also illustrated. All positions are annotated relative to the transcription start site (TSS) **(B)** ChIP assay in E2F1-high and low

melanoma cells. Input represents 10% of sheared chromatin, IgG served as mock control. **(C)** Luciferase activity of an IL6 promoter construct was measured after transfection in E2F1-high melanoma cells versus their KD counterparts **(D)** Relative luciferase activities after co-transfection of IL6 promoter construct together with expression plasmid for wild type E2F1, a DNA binding deficient E2F1 mutant (E132) or transactivation- defective E2F1 mutant (ΔTA) in Sk-Mel-147 E2F1 KD cells. **(E)** Expression levels of these E2F1 proteins were analyzed by Western blot. All experiments were performed in triplicate. The data were analyzed using Student's t-test (two sided) and considered significant if *P<0.05, **P<0.01, ***P<0.001 and not significant (n.s.) if P>0.05.

3.7 Impact of T cells on E2F1-regulated IL6 secretion in melanoma cells

Given that E2F1 regulates an immunomodulatory network via IL6 (Figure 7D), experiments were designed to investigate whether $CD4^+$ or $CD8^+$ T influence E2F1-regulated IL6 secretion in two E2F1-high (SK-Mel147 Ctl and C8161 Ctl) and two E2F1 low melanoma cell lines (SK-Mel147 KD and C8161 KD). In parallel, the melanoma cell lines as well as $CD4^+$ and $CD8^+$ T cells were cultured alone (monoculture). The concentration of IL6 in the supernatants was quantified by ELISA under both monoculture and co-culture conditions. As expected, monoculture of E2F1-high melanoma cell lines produced significantly higher levels of IL6 compared to E2F1-knockdown melanoma cell lines. Surprisingly, the level of IL6 was significantly elevated when melanoma cells (E2F1 high/low) were co-cultured with $CD4^+$ T cells (Figure 12A). A similar pattern was observed when melanoma cells (E2F1 high/low) were co-cultured with $CD8^+$ T cells (Figure 12B). These results demonstrated that IL6 was predominantly produced by the melanoma cells, with minimal secretion by $CD4^+$ or $CD8^+$ T cells, but in the presence $CD4^+$ or $CD8^+$ T cells IL6 levels were significantly increased. This are true for both cell lines even though Mel147 cells produced significantly higher levels of IL6 than C8161 cells.

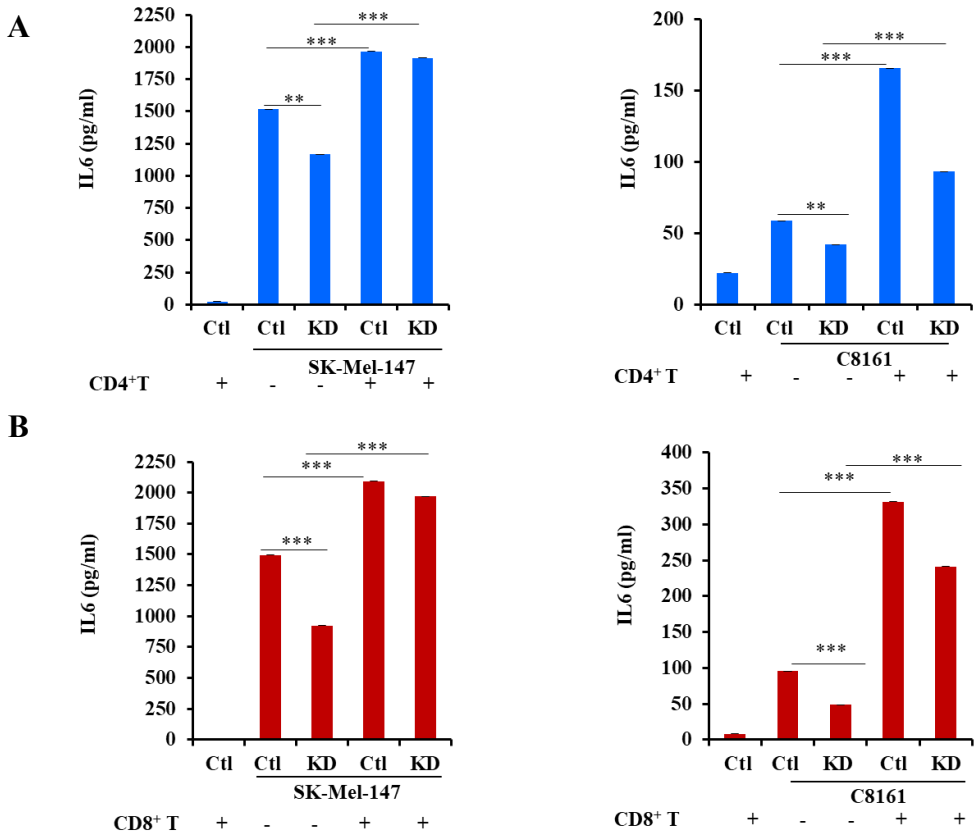

Figure 12: Effect of T cells on E2F1-regulated IL6 secretion by melanoma cells. (A) CD4+ T cells and (B) CD8+ T cells were co-cultivated with SK-Mel-147 Ctl and SK-Mel-147 KD, as well as C8161 Ctl and C8161 KD cells. In parallel, $CD4^+$ and CD8+ T cells, as well as melanoma cell lines were cultured alone. IL6 in the cell culture supernatants was measured by ELISA. Data are representative of T cells from three healthy donors. All experiments were performed in triplicate. The data were analyzed using Student's t-test (two sided) and considered significant if *P<0.05, **P<0.01, ***P<0.001.

3.8 Melanoma-derived IL6 influences the secretion of immunomodulatory factors by T cells

To evaluate the impact of IL6 on the secretion of immunomodulatory factors by T cells, supernatant of co-cultures from SK-Mel-147 Ctl and $CD4^+$ T cell was subjected to cytokine array profiling. In parallel, supernatant from $CD4^+$ T cells treated with recombinant IL6 for 72 hours was analyzed to better differentiate between the immunomodulatory effect of IL6 alone and the IL6-containing melanoma secretome. IL6 treatment of $CD4^+$ T cells resulted in an increased release of many cytokines, most notably IL10. By contrast, IL17A, IL4, IL5, and CXCL1 levels were slightly reduced with the strongest reduction observed for GMCSF. These factors, however, were upregulated in the SK-Mel-147 Ctl and $CD4^+$ T cells co-

cultures. Moreover, three factors i.e IL6, CXCL1, and C5/C5a were dramatically elevated in the supernatant of co-cultures. Importantly, comparable levels of IL10 were detected in the supernatants of both, $CD4^+$ T cells co-cultured with tumor cells and $CD4^+$ T cells treated with IL6 (Figure 13A). On the other hand, IL6 treatment of CD8+ T cells led to an increased release of several cytokines, including C5/C5a, ICAM-1, and IL10. In contrast, the levels of IL8, CXCL1, IL17A, IL1β, IL5, IL12p70, and CXCL10 were slightly reduced. Furthermore, co-culturing E2F1-high melanoma cells with CD8+ T cells resulted in enhanced secretion of numerous cytokines, including IL10, CCL2, SerpinE1/PAI-1, and IFN-γ, alongside with a decreased expression of TREM-1, IL-32a, GM-CSF, and IL1β, with the most significant reduction observed for IL12p70 (Figure 13B). Collectively, these experiments indicated that melanoma cells exert an immunomodulatory effect in modulating the production of cytokines and chemokines by T cells, and many of these effects are also mediated by IL6. To understand the immunomodulatory effect of the tumor derived IL6 in more detail, $CD4^+$ T and $CD8^+$ T cells were treated with different concentrations of recombinant IL6. The ELISA results revealed that IL6 increased the secretion of IL10 by $CD4^+$ and $CD8^+$ T cells in a dose-dependent manner (Figure 13C, 13D). Interestingly, the production of IL10, as determined by ELISA, and mRNA expression by qPCR, was significantly diminished when $CD4^+$ (Figure 13E-F) and $CD8^+$ T (Figure 13G-H) cells were treated with an IL6 neutralizing mAb. The viability of $CD4^+$ and $CD8^+$ T cells was not affected by modulation of IL6 signaling (Figure 13I, 13J). Overall, these results indicated that IL6 modulates the $CD4^+$ and $CD8^+$ T cell response in terms of IL10 secretion.

Results

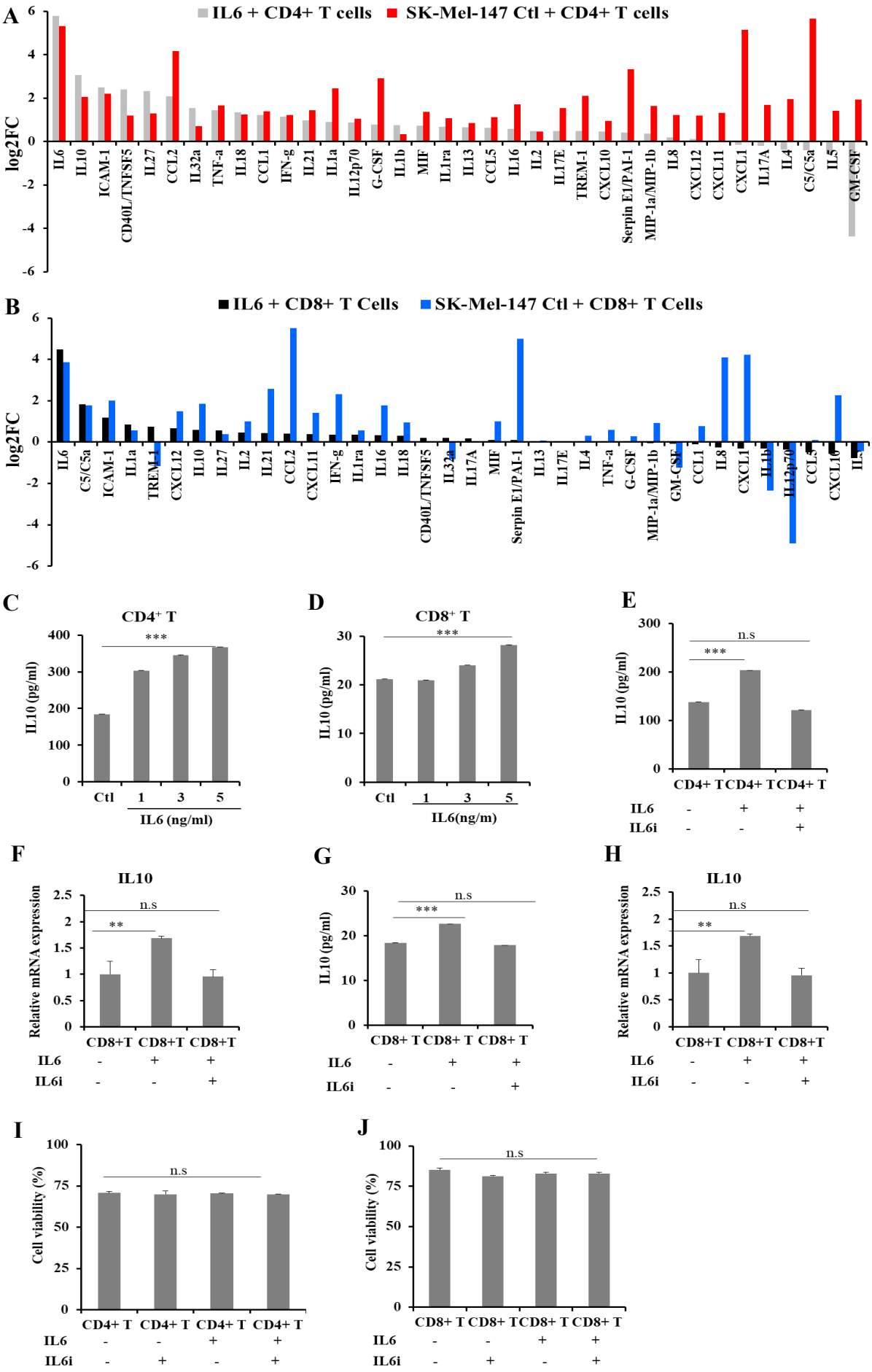
A
IL6 + CD4+ T cells
SK-Mel-147 Ctl + CD4+ T cells
log2FC
IL6
IL10
ICAM-1
CD40L/TNFSF5
IL27
CCL2
IL32a
TNF-a
IL18
CCL1
IFN-g
IL21
IL1a
IL12p70
G-CSF
IL1b
MIF
IL1ra
IL13
CCL5
IL16
IL2
IL17E
TREM-1
CXCL10
Serpin E1/PAI-1
MIP-1a/MIP-1b
IL8
CXCL12
CXCL11
CXCL1
IL17A
IL4
C5/C5a
IL5
GM-CSF
B
IL6 + CD8+ T Cells
SK-Mel-147 Ctl + CD8+ T Cells
log2FC
IL6
C5/C5a
ICAM-1
IL1a
TREM-1
CXCL12
IL10
IL27
IL2
IL21
CCL2
CXCL11
IFN-g
IL1ra
IL16
IL18
CD40L/TNFSF5
IL32a
IL17A
MIF
Serpin E1/PAI-1
IL13
IL17E
IL4
TNF-a
G-CSF
MIP-1a/MIP-1b
GM-CSF
CCL1
IL8
CXCL1
IL1b
IL12p70
CCL5
CXCL10
IL5
C
CD4+ T
IL10 (pg/ml)
***
Ctl
1
3
5
IL6 (ng/ml)
D
CD8+ T
IL10 (pg/ml)
***
Ctl
1
3
5
IL6(ng/m)
E
IL10 (pg/ml)
n.s
***
CD4+ T
CD4+ T
CD4+ T
IL6
IL6i
F
IL10
Relative mRNA expression
n.s
**
CD8+T
CD8+T
CD8+T
IL6
IL6i
G
IL10 (pg/ml)
n.s
***
CD8+ T
CD8+ T
CD8+ T
IL6
IL6i
H
IL10
Relative mRNA expression
n.s
**
CD8+T
CD8+T
CD8+T
IL6
IL6i
I
Cell viability (%)
n.s
CD4+ T
CD4+ T
CD4+ T
CD4+ T
IL6
IL6i
J
Cell viability (%)
n.s
CD8+ T
CD8+ T
CD8+ T
CD8+ T
IL6
IL6i

Figure 13: Impact of E2F1-induced IL6 melanoma secretome on $CD4^+$ and $CD8^+$ T cells. (A) $CD4^+$ and **(B)** $CD8^+$ T cells were stimulated with PHA in the presence or absence of IL6 (5 ng/mL) for 72 hours. Subsequently, cell culture supernatant was collected for cytokine expression profiling (data are representative of one donor). **(C)** $CD4^+$ and **(D)** $CD8^+$ T cells were stimulated as in **A** for 72 hours with increasing concentrations of IL6. Subsequently, IL10 production was determined by ELISA. IL10 mRNA and protein secretion in $CD4^+$ **(E, F)** and $CD8^+$ T cells **(G, H)** was measured upon treatment with recombinant IL6 and/or IL6 inhibitor (IL6i) by qPCR and ELISA, respectively. Effect of IL6 and IL6 inhibitor on $CD4^+$ **(I)** and $CD8^+$ **(J)** T cell viability as determined by flow cytometry. Data are representative of three healthy donors. All experiments were performed in triplicate. The data were analyzed using Student's t-test (two sided) and considered significant if *P<0.05, **P<0.01, ***P<0.001 and not significant (n.s.) if P>0.05.

3.9 Melanoma-immune cell communication via the E2F1-IL6/IL10 axis

To gain further insight into the potential E2F1-IL6/IL10 axis, the effect of IL6 neutralizing mAb was tested in the co-culture system of T cells with different melanoma E2F1-high and low cell lines. These experiments demonstrated that IL6 levels were significantly reduced upon treatment with the IL6 neutralizing antibody, indicating that IL6 production follows an autocrine loop (Figure 14A). Moreover, IL10 production was significantly reduced upon addition of the IL6 neutralizing monoclonal Ab (Figure 14B). These experiments confirmed that IL10 was mostly released by $CD4^+$ T cells. Taken together, these results suggested that the E2F1-IL6 axis regulates IL10 secretion by $CD4^+$ T cells and thereby modulates melanoma-immune cell communication. To investigate whether $CD8^+$ T cells also participated in this melanoma-immune cell crosstalk, $CD8^+$ T cells were co-cultivated with pairs of melanoma wild type and E2F1 KD cell lines in the presence or absence of an IL6 neutralizing mAB. As with $CD4^+$ T cells, addition of an IL6 neutralizing antibody reduced IL6 and IL10 levels (Figure 14C, 14D), suggesting that E2F1-induced IL6 also regulates IL10 expression in $CD8^+$ T cells. Of note, the concentration of IL10 produced $CD8^+$ T cells as compared to $CD4^+$ T cells upon co-culture with melanoma cells was significantly lower, which may reflect a possible difference in the immune response between the two subtypes of T cells. Nevertheless, these results clearly demonstrated that E2F1-induced IL6 modulates cytokine production by neighboring immune cells.

Results

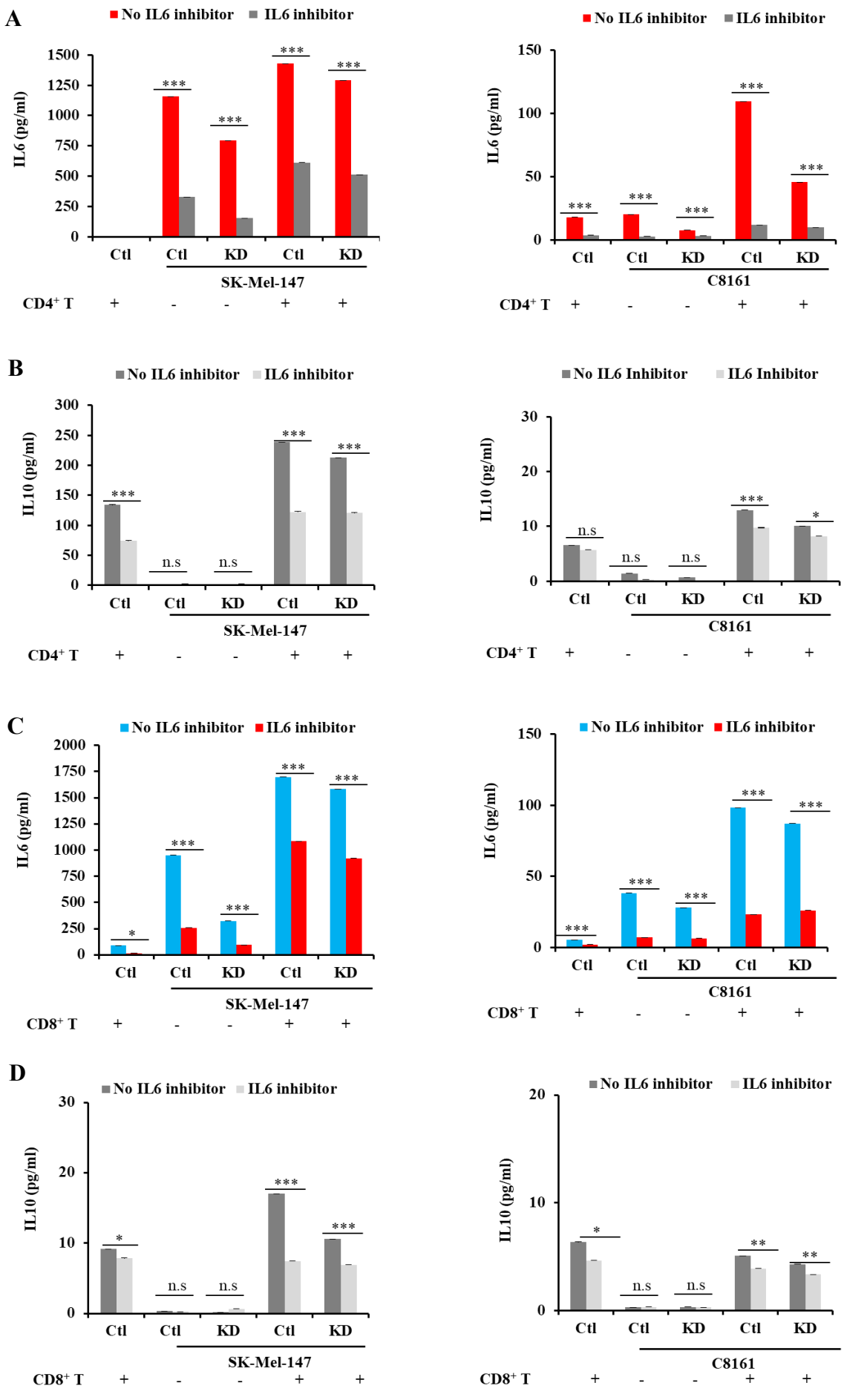
A
No IL6 inhibitor
IL6 inhibitor
IL6 (pg/ml)
Ctl
Ctl
KD
Ctl
KD
SK-Mel-147
CD4+ T
+
-
-
+
+
C8161
B
No IL6 Inhibitor
IL6 Inhibitor
IL10 (pg/ml)
n.s
C
CD8+ T
D

Figure 14: Melanoma-immune cell communication via the E2F1/IL6/IL10 axis. IL6 and IL10 secretion by high and low E2F1-expressing SK-Mel-147 and C8161 melanoma cell lines was analyzed following monoculture or co-culture with $CD4^+$ **(A-B)** or $CD8^+$ **(C-D)** T cells in the presence or absence of an IL6 neutralizing antibody (IL6 inhibitor). IL6 and IL10 concentrations were determined by ELISA. Data are representative of three healthy donors. All experiments were performed in triplicate. The data were analyzed using Student's t-test (two sided) and considered significant if *P<0.05, **P<0.01, ***P<0.001 and not significant (n.s.) if P>0.05.

3.10 IL10 exerts anti-metastasis effects on melanoma cells

IL10 is a pleotropic cytokine but its biological role in the melanoma microenvironment is still obscure (Wang et al. 2019). Since the E2F1-induced melanoma secretome modulated IL10 gene expression in neighbouring T cells, this study sought to investigate whether IL10 exerts a feedback effect on melanoma cells. To address this possibility, pairs of E2F1-high and low melanoma cell lines (SK-Mel-147 Ctl and KD, C8161 Ctl and KD) were treated with IL10 (2 ng/mL) for 24 hours. Subsequently, Boyden chambers assay was performed to test the effect of IL10 on the invasiveness of melanoma cells. Interestingly, E2F1 knockdown and IL10 treatment both reduced invasiveness of melanoma cells and together exerted an additive effect (Figure 15A). Furthermore, IL10 treatment had a significant inhibitory effect on the migratory activity of E2F1-low cell lines in the wound healing assay (Figure 15B). To determine the effect of IL10 on the expression of EMT markers, E2F1-high and low melanoma cell lines (SK-Mel-147 Ctl and KD, C8161 Ctl and KD) were treated with IL10 (2 ng/mL) for 3 days before EMT marker expression was analyzed. These experiments showed that IL10 treatment caused a significant reduction in the expression of EMT markers such as Vimentin, Slug and SNAI l as detected by Western blot in E2F1-low cell lines (Figure 15C). Importantly, no detectable difference in IL10 receptor expression, as measured by WB, was observed between E2F1 high and low melanoma cell lines (Figure 15D). In order to determine whether IL10 affected melanoma cell proliferation, two E2F1 high and E2F1 knockdown melanoma cell lines (SK-Mel-147 Ctl and KD, C8161 Ctl and KD) were treated with IL10 for different time periods. The results of XTT cell proliferation assay showed that IL10 had no inhibitory effect on melanoma cell viability and did not inhibit proliferation of tumor cells (Figure 15E). Taken together the results suggested that IL10 has a negative effect on invasiveness and migratory capacity of melanoma cells, especially in cells with low E2F1 levels.

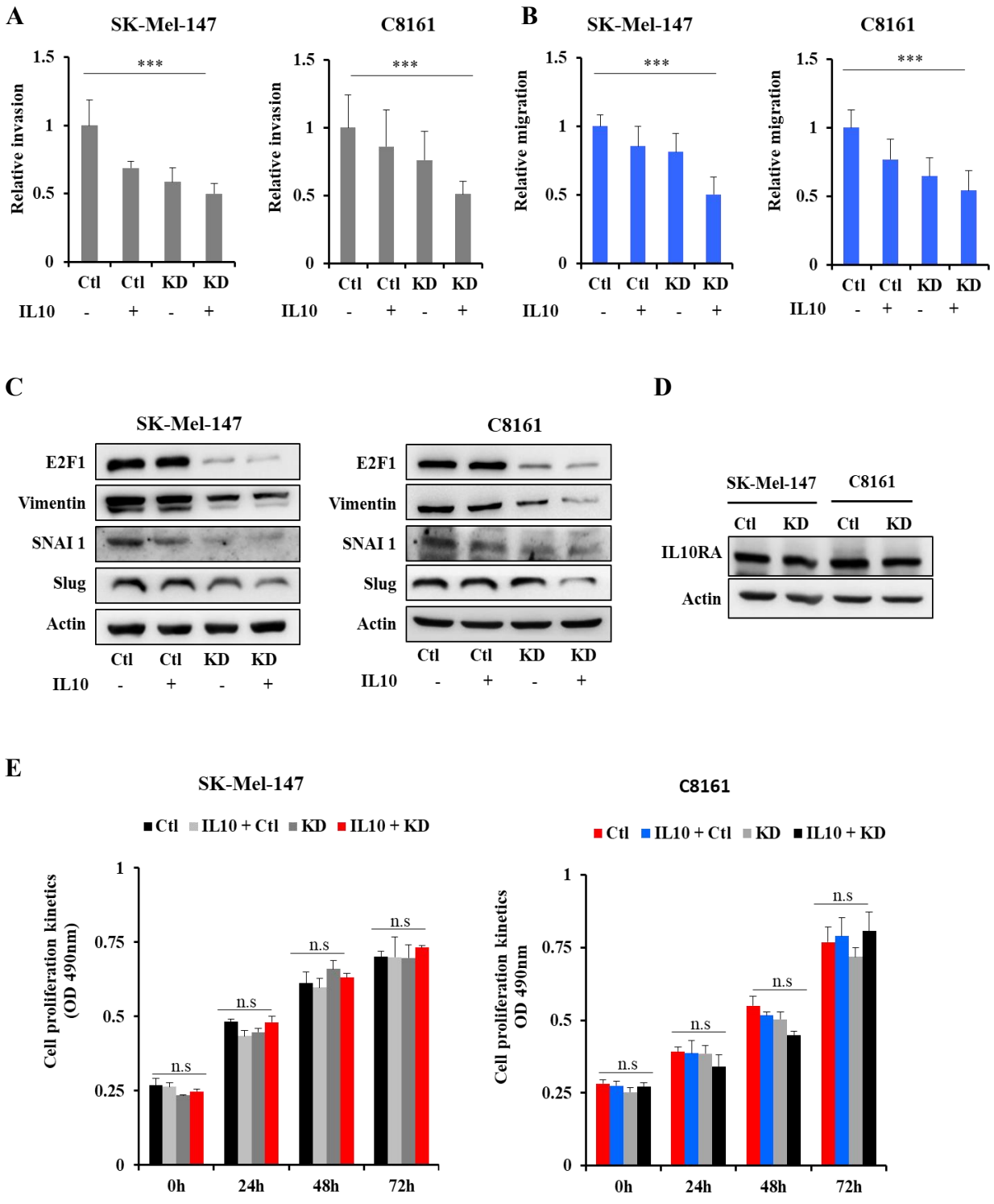

Figure 15: **IL10 reduces the invasiveness and migratory capacity of melanoma cells**. Invasiveness **(A)** and migratory activity **(B)** of E2F1-high and E2F1-low melanoma cell lines in the absence or presence of IL10 was assessed using the Boyder chamber and wound healing assays. **(C-D)** Western blot analysis of EMT marker and IL10 receptor expression in response to IL10 treatment. **(E)** Effect of IL10 on melanoma cell proliferation examined by XTT assay. All experiments were performed in triplicate. Data were analyzed using Student's t-test (two sided) and considered significant if *P<0.05, **P<0.01, ***P<0.001 and not significant (n.s.) if P>0.05.

3.11 Impact of different E2F1/IL6/IL10 signatures on melanoma patient survival

IL6 has been demonstrated to promote E2F1-driven metastatic activity in melanoma cells, as depicted in Figure 10. Conversely, IL10 inhibits the metastatic properties of melanoma cells, with its anti-metastatic effects being notably pronounced under conditions of low E2F1 expression (Figure 15). To evaluate the potential clinical relevance of these findings, Kaplan-Meier analyses of RNA-Seq data from TCGA datasets in SKCM (human skin cutaneous melanoma) patients were performed based on the calculated median value. As shown in figure 16A, high E2F1 levels alone were consistently associated with poor outcome, while high IL10 levels alone were associated with longer survival (Figure 16B). Neither high nor low expression levels of IL6 had a significant impact on the overall survival rates of melanoma patients (Figure 16C). The antagonizing effects of IL10 and E2F1 on patients survival became evident when expression levels of both were analyzed (Figure 16D). When IL6 expression was added as third variable, patient overall survival (OS) negatively correlated with IL6 levels (Figure 16E). These findings suggest that patients achieve most significant benefits from elevated levels of IL10 and low levels of E2F1 and IL6. Combined low expression of E2F1, IL10, and IL6 correlates with better OS (Figure 16E, pink line) than combined high expression of E2F1, IL10, and IL6 (Figure 16E, violet line). There is no significant difference in overall survival between patients with high E2F1/low IL10/low IL6 expression (Figure 16E, maroon line) compared to patients with low expression of E2F1 and IL10 along with high expression of IL6 (Figure 16E, red line). Moreover, patients with low E2F1/high IL10/high IL6 profile (orange line) have better OS than patients with high E2F1 and increased level of either IL10 or IL6 (Figure 16E, green and blue line). Finally, TGCA data analysis identified a subgroup of melanoma patients with low E2F1/high IL10/low IL6 molecular signatures with a striking survival advantage, which are supported by the in vitro experiments of this study.

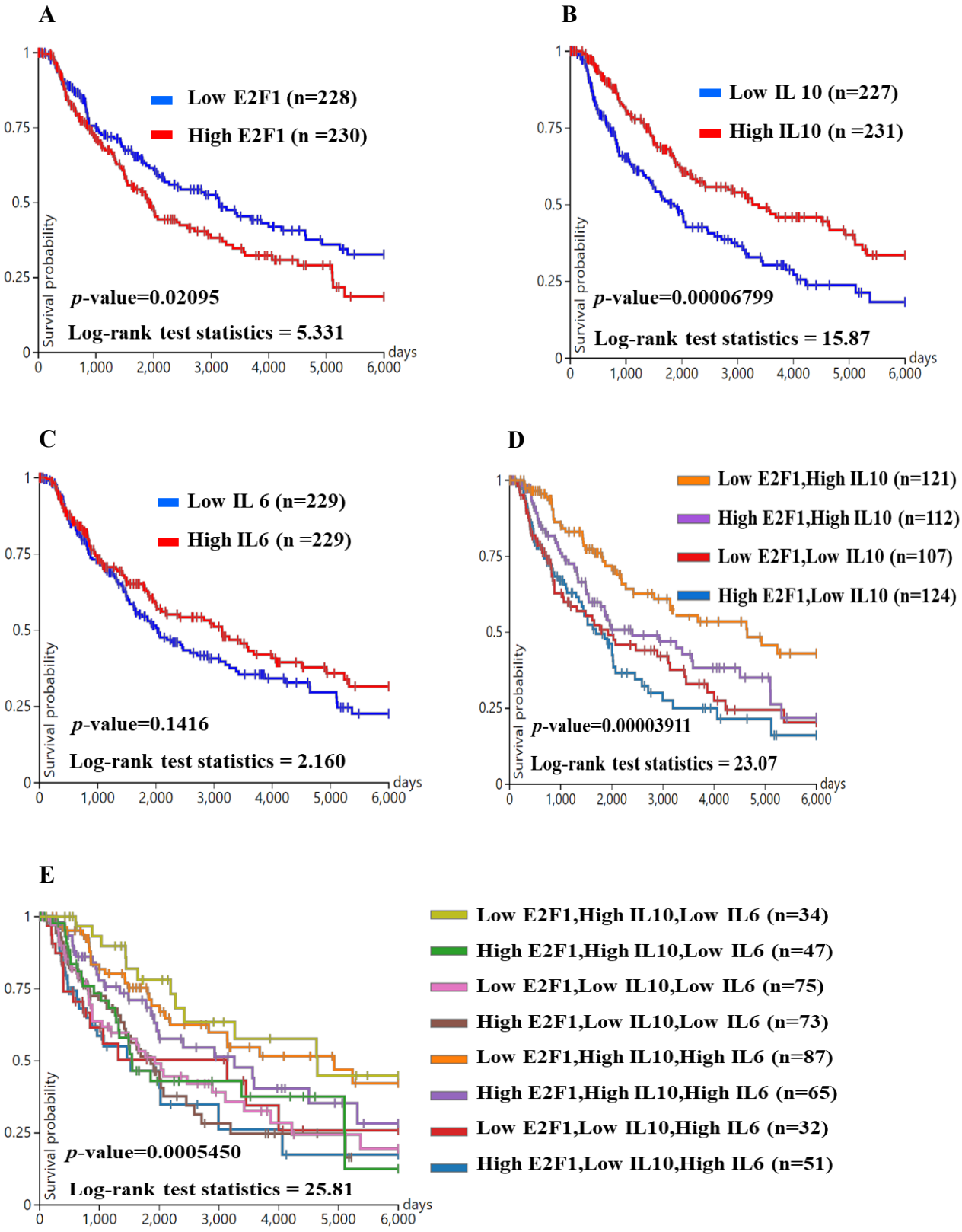

Figure 16: IL10 correlates with patient survival. Kaplan-Meier plots for overall survival probability based on RNA-Seq data of SKCM (human skin cutaneous melanoma) patients from TCGA datasets performed using UCSC Xena browser. **(A)** E2F1-low (blue) versus E2F1-high (red) mRNA levels. **(B)** Low IL10 (blue) versus high IL10 levels (red). **(C)** Low IL6 (blue) versus high IL6

levels (red). **(D)** Patients co-expressing low levels of E2F1 and high levels of IL10 (low E2F1/high IL10, yellow) in their tumors have a significant better survival rate than tumors with high E2F1 and low IL10 expression (high E2F1/low IL10, blue) but their survival time is shorter than in patients with high E2F1/high IL10, (violet) or low E2F1/lowIL10 (red) expression patterns. **(E)** Patients with tumors that express low E2F1, high IL10 and low IL6 (low E2F1/high IL10/low IL6, yellow) survive significant longer than all other patients groups. Log-rank test p-values are depicted on the survival curves.

4. Discussion

Melanoma is still a significant health problem, especially among fair-skinned people of European descent (Arnold et al. 2022). Although new drugs and treatment regimens have been approved in the recent decade that have revolutionized melanoma treatment, most notably checkpoints inhibitors, some patients are refractory or resistant of these therapies (Buder-Bakhaya and Hassel 2018; Seliger and Massa 2021). Emerging evidence suggests that the interaction between immune cells and tumor cells in the TIME significantly influences therapeutic responses and clinical outcome (Wu and Dai 2017). Tumors have been implicated in creating an immunosuppressive microenvironment that inhibits immune recognition and elimination via several mechanisms, including the recruitment of immunosuppressive cells, activation of immune checkpoint pathways, and exclusion of immune cells. Gaining a better understanding of these immunosuppressive mechanisms will allow developing novel strategies to improve efficacy of cancer immunotherapies. Here, this study investigated the immunomodulatory properties of the E2F1-induced melanoma secretome and to which extent it influences the immune response by modulating TIME.

4.1 A co-culture system to study the tumor immune microenvironment

To mimic the interaction between immune ($CD4^+$ or $CD8^+$ T) and melanoma cells through secreted factors in the tumor immune microenvironment, an in vitro trans-well co-culture system was established which allows analysing viability, and the secretory and transcriptional profile of tumor and immune cells. The suboptimal activation of the T cells by low dose of the T cell mitogen phytohemagglutinin (PHA) and IL2 in this system allows studying positive and negative effects of the tumor secretome on the co-cultured T cells. No drastic fluctuations in IFN-γ secretion were observed among different donors, verifying the robustness of the experimental setup. Special attention was given to the number of melanoma and immune cells to ensure that neither cell type was facing nutrient shortage. The high degree of cell viability at the end of the incubation period indicated that this was indeed not the case. However, due to media exhaustion, the co-culture system had to be limited to 72 hours, which is too short for studying T cell differentiation (Cousins et al. 2002; Ford et al. 2023). Also, no cell contact mediated immune modulation could be studied in this co-culture setting because homogeneous cell populations were required for the intended transcriptome analyses. Recently, a similar approach was used to investigate the effect of T cell-derived secreted factors on colon cancer cell proliferation in the immune microenvironment. In these experiments, the cancer cells were co-cultivated with immune cells for 48 hours only (Che et

al. 2024). A recent study suggests that an established co-culture model is a suitable tool for studying the influence of E2F1 on the communication between melanoma and T cells ($CD4^+$ or $CD8^+$) in tumor immune microenvironment (Spitschak et al. 2024). Taken together, these findings demonstrate that the co-culture system established in this study is an effective tool for studying the effect of tumor cell derived secretme on immune cells or vice versa, the effect of immune cell-derived factors on melanoma cells.

4.2 Identification of E2F1-regulated immunomodulatory factors in melanoma cells

E2F1 is an indispensable component of the DNA damage response and repair (Stevens and La Thangue 2004). However, it is not known whether E2F1 influences immune functions within TIME. By using an in silico pipeline that is based on combined transcriptomic approaches with bioinformatics and structural modeling, 54 E2F1-dependent immunomodulatory genes were identified. Gene set enrichment analyses revealed several cancer-related hallmarks, such as mTORC1 signaling, PI3K/ Akt /mTOR signaling and epithelial-mesenchymal transition. These signaling pathways are well known mediators of E2F1-driven epithelial-to-mesenchymal transition (EMT) and therapy resistance in melanoma (Qiao et al. 2021; Xu et al. 2020; Real et al. 2011).The results are consistent with previous studies showing that E2F1-induced tumor progression activates downstream pathways such as Ras/MAPK/ERK pathway and the PI3K/Akt pathway, as well as metastasis (Alla et al. 2010). Furthermore, the study identified several immune-related hallmarks such as inflammatory response, TNF-α signal via NF-kB, IL6/JAK/STAT3 and IL2/STAT5 signaling pathways. Within the complex tumor microenvironment, cancer cells are known to hijack inflammatory mechanisms to promote their own growth and survival. Several factors secreted by surrounding cells, including immune cells, have been described to promote tumor growth, angiogenesis, invasion, metastasis, and drug resistance (Greten and Grivennikov 2019; Kitamura et al. 2015). The inflammatory response is primarily regulated by three pathways, NF-kB, MAPK, and JAK-STAT (Chen et al. 2018). These finding suggested that E2F1 modulates the tumor immune microenvironment (TIME) by shaping the inflammatory microenvironment.

4.3 IL6 is a direct transcriptional target of E2F1

Up to now, four different transcription factors have been reported to regulate transcription of the IL6 gene, namely NF-κB, activation protein (AP)-1, CCAAT/enhancer binding protein (C/EBP), and cAMP response element (CRE)-binding protein (CREB) (Hershko et al. 2002; Xiao et al. 2004). In a recent study, Yoon et al. reported that E2F1 and STAT3 synergistically

activate H2AZ transcription in glioma stem cells (Yoon et al. 2022). But, the present study demonstrated that E2F1 directly regulates the transcription of IL6 in melanoma cells.

Two new E2F1 binding sites were identified in the IL6 promoter. Although IL6 was described to be produced by different cell types including immune cells (T cells, B cells, macrophage, DC, NK cells) as well as different types of cancers (Murakami et al. 2019; Hoejberg et al. 2012b; Xu et al. 2022), our experiments demonstrated that melanoma, but not immune cells, were the primary if not exclusive source of IL6. However, IL6 secretion by melanoma cells was exacerbated in the presence of $CD4^+$ or $CD8^+$ T cells, thereby creating an immunosuppressive TIME by promoting pro-metastatic properties such as invasiveness and EMT. What factors produced by T cells caused this increase in IL6 production and which transcription factors and signaling pathways were involved in this enhanced expression, remain to be determined. No changes in the transcriptional regulation of the IL6 receptor were detected in these co-culture experiments, indicating that melanoma-derived IL6 has a primarily paracrine function in TIME. It is noteworthy that there is a marked difference in the secretion and expression of the IL6 cytokine between the SK-Mel-147 and C8161 melanoma cell lines, which may be attributed to variations in E2F1 expression levels and genetic backgrounds that affect cytokine production. For example, differences in the mutational landscape or genetic alterations in signaling pathways may influence expression and secretion of IL6.

Liu et al. reported that E2F1 plays an important role in promoting inflammatory pathways by transactivating the IL6 promoter in nasopharyngeal carcinoma (Liu et al. 2020). Although the authors used the same bioinformatics tool (JASPAR and UCSC), the present study identified two different new E2F1 binding sites upstream of BS1 and BS2 in a region that was not investigated in their study. Why BS1 and BS2 remained unidentified in their study is not known. However, the identification of additional new binding sites in the promoter region suggests that expression of the IL6 gene is tightly regulated by E2F1. In further difference to the present study, Liu et al. assessed regulation of IL6 expression only at the transcriptional level and investigated the immunomodulatory effect of IL6 on macrophages but not T cells. Taken together, both studies suggest an important role of IL6 as immune modulator in the tumor microenvironment in different tumor entities. Moreover, this study demonstrated that $CD4^+$ or $CD8^+$ T enhanced the secretion of IL6 by melanoma. Which T cell-derived factor(s) induced this IL6 production by melanoma cells remains to be investigated.

4.4 Cytokine profiling and role of E2F1 induced secretome in tumor immune microenvironment

One has to keep in mind that cytokines and chemokines can have opposing effects depending on the immune context and that the expression of certain immune modulatory factors may have unpredictable effects. Cytokine profiling experiments revealed increased expression of several cytokines, including IL4, IL10, IL13 and IL17E when $CD4^+$ T cells were co-cultured with E2F1 high-expressing melanoma cells (SK-Mel-147 Ctl) compared to co-culture with E2F1-low cells (SK-Mel-147 KD). These cytokines are characteristic of T helper type 2 (Th2) cells, suggesting that high expression of E2F1 favours Th2 polarization via Th2-type cytokine production. Moreover, IL6 has been demonstrated to facilitate Th2 differentiation by inducing IL4 production (Diehl and Rincón 2002). These observations suggest that elevated IL6 expression also plays a potential role in triggering Th2 cell development. Th2 cells play a key role in tumorigenesis and metastasis as well as immune escape of tumors due to the down-regulation of antitumoral immune responses (Li et al. 2021; Wan 2010).

On the other hand, co-cultivation of E2F1-low melanoma cells with $CD4^+$ T cells resulted in enhanced secretion of IL2, IFN-γ, and TNF-α as compared to co-culture with E2F1 high-expressing melanoma cells. Notably, the loss of E2F1 led to a significant reduction in IL6 levels. IL6 inhibits Th1 differentiation by cytokine mediated signalling pathways (Diehl and Rincón 2002). IL2, IFN-γ, and TNF-α are typically produced by T helper type 1 (Th1) cells. These findings suggest that knockdown of E2F1 as well as down-regulation of IL6 promote a shift towards Th1 polarization by modulating cytokine profiles. Th1 cells mediate antitumor immunity, either by killing tumor cells directly or indirectly by activating innate and adaptive immune cells, by reducing angiogenesis, or by inducing cancer cell apoptosis (Andreu-Sanz and Kobold 2023). Chemokines play important roles in recruiting immune cells to the tumor. For example, CCL1 is considered one of the major regulatory T cell attracting factors that create an immunosuppressive environment (Kuehnemuth et al. 2018). NK cells, Th1 and $CD8^+$ cytotoxic T cells are recruited by the CXCL10/CXCL11 axis (Ozga et al. 2021). These finding strongly indicated that E2F1 plays a pivotal role in immune regulation in TIME, possibly by modulating immune cell recruitment, polarization, or activity. A shift from Th1 to Th2 is commonly observed in patients with advanced cancer (Shang et al. 2024). These findings suggest that E2F1 expression could be a critical factor in regulating the balance between Th1 and Th2 responses, potentially influencing cancer progression.

Cytokine profiling experiments revealed increased levels of several cytokines such as IFN-γ, IL1, IL12 and IL27 when CD8+ T cells were co-cultured with E2F1 knockdown melanoma

cells (SK-Mel-147 KD) compared to co-culture with E2F1 high-expressing melanoma cells (SK-Mel-147 Ctl). The expression of IFN-γ is a functional surrogate marker for cytotoxic $CD8^+$ T cells, also known as Tc1 cells (Ghanekar et al. 2001). IL1, IL12 and IL27 not only contribute to $CD8^+$ T cell expansion and differentiation, but also enhance the antitumor effector function of $CD8^+$ T cells by increasing expression of granzyme B and IFN-γ (Gerhardt et al. 2023; Ben-Sasson et al. 2013; van den Eeckhout et al. 2021). Thus, low E2F1 levels may enhance the effector functions of cytotoxic $CD8^+$ T cells by regulating the release of cytokines.

Interestingly, the co-culturing of E2F1-high melanoma cells (SK-Mel-147 Ctl) with $CD8^+$ T cells increased IL6 and IL17A levels. IL6 has been shown to potently inhibit $CD8^+$ T cell activation and cytokine production (Tsukamoto et al. 2018), and to confer therapeutic resistance, such as multidrug resistance (MDR) and resistance to immunotherapy (Huseni et al. 2023b; Ghandadi and Sahebkar 2016). Furthermore, it has been demonstrated that cancer cells expressing IL17 reduce the infiltration of $CD8^+$ T cells and promote exhaustion of $CD8^+$ T cells within TIME (Wang et al. 2020; Kim et al. 2021). Collectively, these findings highlight the role of E2F1 in promoting an immunosuppressive tumour microenvironment, most likely by modulating the secretion of cytokines.

Cytokine profiling of monocultures of immune cells ($CD4^+$ and $CD8^+$ T cells) revealed that all proteins were secreted by both T cell types, albeit to differing extents. However, when immune cells and melanoma cells were co-cultured, the cytokine secretion patterns shifted. This change suggests that the interaction between immune cells and melanoma cells influenced their respective cytokine production. Such alterations indicate a bidirectional crosstalk, where immune cells affect the tumor microenvironment, and in turn, melanoma cells modulate the immune response. Shifts in the cytokine patterns depending on E2F1 expression levels are difficult to interpret. Moreover, the difference in the cytokine patterns observed after co-culturing T cells with E2F1-high and low melanoma cells are based on cytokine arrays. Unlike ELISA, cytokine arrays have a relatively low sensitivity and are not well suited for detecting low concentrations of cytokines (Anloague and Lowery 2019) and several exposures are needed when expression levels of different cytokines vary strongly. Nevertheless, cytokine arrays can provide first information on possible changes in the expression of a large set of cytokines, which then needs to be verified using other detection methods like ELISA. In addition, modifying the co-culture system to allow for T cell differentiation might provide direct functional insights into the role of E2F1 in immunomodulation.

4.5 E2F1-IL6-IL10 melanoma-immune cell crosstalk

In addition to the well-established proinflammatory effects of IL6, the IL6/JAK/STAT3 signalling pathway has been implicated in promoting tumorigenesis, invasiveness, and metastasis in many cancers including melanoma (Johnson et al. 2018; Murakami et al. 2019; Na et al. 2013). Elevated IL6 serum levels have been associated with poor outcome in melanoma patients (Hoejberg et al. 2012a) and most recently, was reported to impair anti-PDL1 and anti-CTLA4 checkpoint inhibition (Huseni et al. 2023b). Consistent with this, blockade of IL6 enhanced the anti-tumor cytotoxic T lymphocyte response and tumor control following immune checkpoint inhibition as compared with ICI alone (Delyon and Lebbe 2022). Thus, IL6 levels may predict immune checkpoint therapy response and strategies to reduce IL6 levels may enhance efficacy of immune checkpoint therapy (Bent et al. 2021). Overall, IL6 inhibition may enhance antitumor immunity by decreasing Th17 and increasing Th1 and $CD8^+$ T cells density in tumours, and alleviate ICB-induced autoimmunity (Hailemichael et al. 2022).

E2F1-regulted secretion of the pro-inflammatory cytokine IL6 melanoma cells exerted an immunomodulatory effect on $CD4^+$ and $CD8^+$ T cells and induced the release of the anti-inflammatory cytokine IL10. IL6 expression has been linked to IL10 production within melanomas in a previous study (Terai et al. 2012), but the producing cell population and the immunological consequences have not been defined. IL10 has been reported to be produced by immune cells such as activated T cells and dendritic cells (Naing et al. 2018). Additional cell types, such as melanoma cells, especially primary melanoma tumours, are also capable of producing IL10 (Itakura et al. 2011). The present study demonstrated that melanoma cell-derived IL6 causes IL10 production in T cells and delineated a previously unknown E2F1-IL6-IL10 axis where E2F1 expression in melanoma cells induces IL6 secretion, which in turn enhances the production of IL10 in $CD4^+$ and $CD8^+$ T cells through intercellular cytokine signalling.

Although having pro and anti-inflammatory functions, IL6 and IL10 both signal through the signal transducer and activation of transcription 3 (STAT3) (Braun et al. 2013). How these opposing effects are achieved is not fully understood. Both, IL6 and IL10, activate STAT3 which induces expression of suppressor of cytokine signalling 3 (SOCS3) in immune cells. SOCS3 in turn inhibits IL6 signalling via binding to gp130, thereby terminating STAT3 activation. However, SOCS3 does not block activation of STAT3 by IL10, which results in prolonged STAT3 activity. Most likely, transient STAT3 activation causes a pro-

inflammatory, while prolonged STAT3 activation causes an anti-inflammatory response (Yasukawa et al. 2003; Wang et al. 2011).

Anti-inflammatory interleukins such as IL10 are critical immune regulators that counterbalance pro-inflammatory signals and facilitate the resolution of inflammation (Iyer and Cheng 2012). However, IL10 is known to have pleiotropic effects and the function of cytokines is often context-dependent (Atwell et al. 1998). Although classically considered as an immunosuppressive cytokine IL10, can inhibit macrophage function, thereby causing tumour cell proliferation and angiogenesis in an in vivo melanoma model (Saraiva et al. 2019;Garcia-Hernandez et al. 2002). Furthermore, IL10 suppresses the activation and effector function of $CD4^+$ and $CD8^+$ T cells and tumor-infiltrating $CD8^+$ IFN-γ^+ T cells in patients with different tumors including breast (Chang et al. 2021), ovarian (Li et al. 2019) and esopharyngeal cancer (Li and Zuo 2019). Moreover, tumor-associated macrophage (TAM) secreted IL10 drives immune evasion in the tumor microenvironment, resulting in poor prognosis and low therapeutic responsiveness to adjuvant chemotherapy in gastric cancer patients (Zhang et al. 2022). On the other hand, it has been shown by Naing et al. that PEGylated IL10 induces $CD8^+$ T cell-mediated immunity in cancer patients through its ability to stimulate proliferation, tumor infiltration, and the production of IFN-γ and granzyme B (Naing et al. 2018). In addition, a combination of PEGylated IL10 with immune checkpoint blockade enhanced intratumoral expansion of antigen-specific $CD8^+$ T cells (Tannir et al. 2021; Tannir et al. 2018). Qiao, et al. demonstrated that IL10 combined with immune checkpoint blockade (ICB) significantly prolonged antitumoral effects by regulating IFN-γ production by dendritic cells, by enhancing $CD8^+$ T cell-dependent antitumoral responses and by reducing adverse effects caused by immune checkpoint therapy (Qiao et al. 2019). This study adds another facet to the function of this cytokine by showing that IL10 exerts significant anti-metastatic effects on E2F1-low melanoma cell lines by reducing invasiveness in an in vitro model. E2F1 is known to regulate a wide range of metastatic pathways that result in promoting migratory activity, invasiveness, and EMT (Alla et al. 2010; Khan et al. 2017). Furthermore, IL6 significantly enhances the E2F1-driven metastatic activity. This study revealed that IL10 can counter these effects, as long as E2F1 expression and IL6 expression levels are low. How IL10 suppresses EMT and the development of mesenchymal phenotypes is not known yet, but a better understanding of its antimetastatic mechanisms could lead to the design of improved adjuvant therapies.

To date, TCGA is providing the largest publicly available tumor tissue RNA-seq data with real clinical applicability that includes samples collected at different institutes (Rehan Akbani

et al. 2015). Here, TCGA data from malignant melanoma patients was utilized to determine the prognostic values of hub genes (E2F1, IL6 and IL10) with respect to overall survival. Kaplan-Meier analyses revealed that E2F1 is an important prognostic biomarker and high levels are associated with poor survival of melanoma patients. Also in other tumor types such as lung, ovarian, and breast cancer, E2F1 overexpression has been found to be associated with unfavorable overall survival (Li et al. 2023). Surprisingly, high expression of IL10 in the melanoma tumor microenvironment was associated with improved overall survival. However, opposite results were described in other tumor entities such as breast (Chu et al. 2020), thyroid (Cunha et al. 2017), and cervical cancer (Liu et al. 2021), where patients with high IL10 mRNA expression had a worse prognosis. Also, high IL6 expression is associated with significantly shortened overall survival in different tumors types, including breast cancer (Tawara et al. 2019), and lung adenocarcinoma (Dong et al. 2019). Moreover, recent studies have demonstrated that elevated IL6 levels attenuate the therapeutic efficacy of anti-PD-L1 checkpoint inhibitors and suppress the anti-tumor cytotoxic T lymphocyte (CTL) response (Huseni et al. 2023). However, prognostic markers for melanoma have not been fully elucidated. In this regard, the finding that low expression of IL6 had a favorable effect on overall survival when combined with low E2F1 and high IL10 expression suggested that combinations of different prognostic factors need to be evaluated in melanoma patients. Thus, the finding that patients with low-E2F1/high-IL10/low-IL6 expression show significantly longer survival may indicate that patients can be sub-grouped according to their individual prognostic patterns and antitumoral therapies tailored accordingly.

Discussion

In summary, the main points of this work are illustrated in a simplified graphical overview (Figure 17).

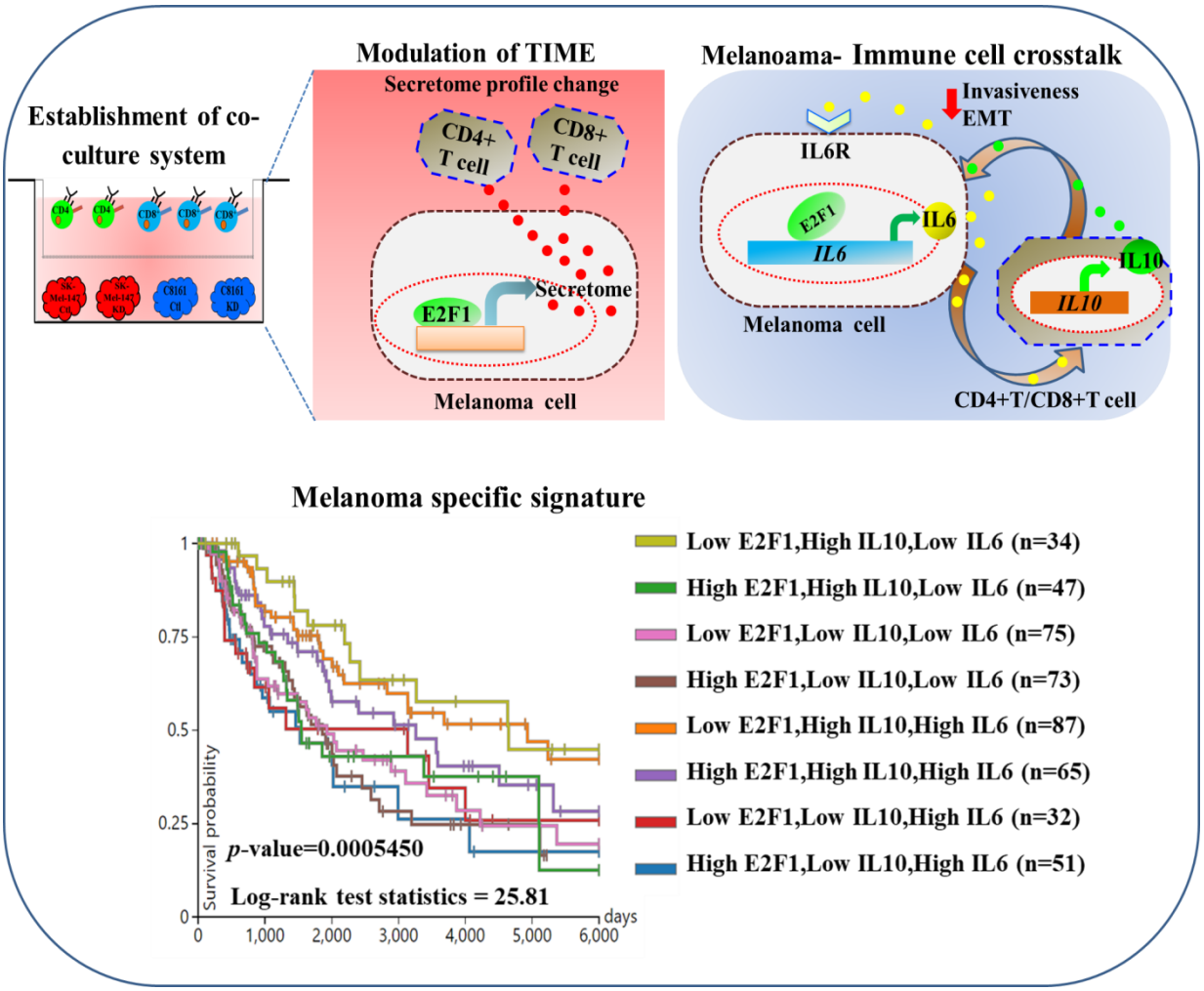

Figure 17: Overview of the main findings of this work. A trans-well co-culture system was established to study the effect of the E2F1-induced melanoma secretome on $CD4^+$ and $CD8^+$ T cells and of T cell secreted factors on melanoma cells. These experiments revealed that a tumor-intrinsic E2F1 directly transactivates the expression of IL6 in melanoma cells, and that tumor-derived IL6 induces the expression of IL10 in $CD4^+$ and $CD8^+$ T cells (E2F1-IL6-IL10 axis). IL10 exerts antimetastatic effects on tumor cells by reducing invasiveness and EMT. The analysis of TCGA data from Melanoma patients corroborated these findings by showing that survival is prolonged in melanoma patients with low-E2F1/high-IL10/low-IL6 signatures. TIME; tumor immune microenvironment, EMT; epithelial-mesenchymal transition.

5. References

Akira, Shizuo; Uematsu, Satoshi; Takeuchi, Osamu (2006): Pathogen recognition and innate immunity. In *Cell* 124 (4), pp. 783–801.

Alla, Vijay; Engelmann, David; Niemetz, Annett; Pahnke, Jens; Schmidt, Anke; Kunz, Manfred et al. (2010): E2F1 in melanoma progression and metastasis. In *Journal of the National Cancer Institute* 102 (2), pp. 127–133. DOI: 10.1093/jnci/djp458.

Anderson, Nicole M.; Simon, M. Celeste (2020): The tumor microenvironment. In *Current biology : CB* 30 (16), R921-R925. DOI: 10.1016/j.cub.2020.06.081.

Andreu-Sanz, David; Kobold, Sebastian (2023): Role and potential of different T helper cell subsets in adoptive cell therapy. In *Cancers* 15 (6), p. 1650.

Anloague, Aric; Lowery, Jonathan W. (2019): Comparison of Human Cytokine Array, Cytokine Bead Arrays, and Protein ELISA in determining cytokine production in media supernatant from in vitro strain of human dermal fibroblasts. In *Capstone Final Project*.

Arnold, Melina; Singh, Deependra; Laversanne, Mathieu; Vignat, Jerome; Vaccarella, Salvatore; Meheus, Filip et al. (2022): Global burden of cutaneous melanoma in 2020 and projections to 2040. In *JAMA dermatology* 158 (5), pp. 495–503.

Attwooll, Claire; Denchi, Eros Lazzerini; Helin, Kristian (2004): The E2F family: specific functions and overlapping interests. In *The EMBO journal* 23 (24), pp. 4709–4716.

Atwell, Darryl M.; Grichnik, Katherine P.; Newman, Mark F.; Reves, Joseph G.; McBride, William T. (1998): Balance of proinflammatory and antiinflammatory cytokines at thoracic cancer operation. In *The Annals of thoracic surgery* 66 (4), pp. 1145–1150.

Basset, Christelle; Holton, John; O'Mahony, Rachel; Roitt, Ivan (2003): Innate immunity and pathogen–host interaction. In *Vaccine* 21, S12-S23.

Ben-Sasson, Shlomo Z.; Hogg, Alison; Hu-Li, Jane; Wingfield, Paul; Chen, Xi; Crank, Michelle et al. (2013): IL-1 enhances expansion, effector function, tissue localization, and memory response of antigen-specific CD8 T cells. In *Journal of Experimental Medicine* 210 (3), pp. 491–502.

Bent, Eric H.; Millán-Barea, Luis R.; Zhuang, Iris; Goulet, Daniel R.; Fröse, Julia; Hemann, Michael T. (2021): Microenvironmental IL-6 inhibits anti-cancer immune responses generated by cytotoxic chemotherapy. In *Nat Commun* 12 (1), p. 6218.

Binnewies, Mikhail; Roberts, Edward W.; Kersten, Kelly; Chan, Vincent; Fearon, Douglas F.; Merad, Miriam et al. (2018): Understanding the tumor immune microenvironment (TIME) for effective therapy. In *Nature medicine* 24 (5), pp. 541–550.

Braun, David A.; Fribourg, Miguel; Sealfon, Stuart C. (2013): Cytokine response is determined by duration of receptor and signal transducers and activators of transcription 3 (STAT3) activation. In *Journal of Biological Chemistry* 288 (5), pp. 2986–2993.

Broertjes, J. (2015): The Ten Hallmarks of Cancer in Cutaneous Malignant Melanoma [REVIEW]. In *2444-2593*. Available online at https://dadun.unav.edu/handle/10171/39289.

References

Brown, Joel S.; Amend, Sarah R.; Austin, Robert H.; Gatenby, Robert A.; Hammarlund, Emma U.; Pienta, Kenneth J. (2023): Updating the Definition of Cancer. In *Molecular cancer research : MCR* 21 (11), pp. 1142–1147. DOI: 10.1158/1541-7786.MCR-23-0411.

Buder-Bakhaya, Kristina; Hassel, Jessica C. (2018): Biomarkers for clinical benefit of immune checkpoint inhibitor treatment—a review from the melanoma perspective and beyond. In *Front. Immunol.* 9, p. 379459.

Cancer (2024). Available online at https://www.who.int/health-topics/cancer#tab=tab_1, updated on 6/12/2024, checked on 6/12/2024.

Chang, Chun-Ming; Lam, Ho Yin Pekkle; Hsu, Hao-Jen; Jiang, Shinn-Jong (2021): Interleukin-10: A double-edged sword in breast cancer. In *Tzu chi medical journal* 33 (3), pp. 203–211.

Che, Rui; Wang, Qingsong; Li, Minzhe; Shen, Jian; Ji, Jianguo (2024): Quantitative Proteomics of Tissue-Infiltrating T Cells From CRC Patients Identified Lipocalin-2 Induces T-Cell Apoptosis and Promotes Tumor Cell Proliferation by Iron Efflux. In *Molecular & Cellular Proteomics* 23 (1).

Chen, Linlin; Deng, Huidan; Cui, Hengmin; Fang, Jing; Zuo, Zhicai; Deng, Junliang et al. (2018): Inflammatory responses and inflammation-associated diseases in organs. In *Oncotarget* 9 (6), p. 7204.

Chi, Hongbo; Pepper, Marion; Thomas, Paul G. (2024): Principles and therapeutic applications of adaptive immunity. In *Cell* 187 (9), pp. 2052–2078.

Chu, Pei-Yi; Wang, Shin-Mae; Chen, Po-Ming; Tang, Feng-Yao; Chiang, En-Pei Isabel (2020): Expression of MTDH and IL-10 Is an Independent Predictor of Worse Prognosis in ER-Negative or PR-Negative Breast Cancer Patients. In *Journal of Clinical Medicine* 9 (10), p. 3153. DOI: 10.3390/jcm9103153.

Cooper, Geoffrey M.; Adams, Kenneth W. (2023): The cell. A molecular approach. Ninth edition. New York, NY: Oxford University Press.

Cousins, David J.; Lee, Tak H.; Staynov, Dontcho Z. (2002): Cytokine coexpression during human Th1/Th2 cell differentiation: direct evidence for coordinated expression of Th2 cytokines. In *The Journal of Immunology* 169 (5), pp. 2498–2506.

Cunha, Lucas Leite; Morari, Elaine Cristina; Nonogaki, Sueli; Marcello, Marjory Alana; Soares, Fernando Augusto; Vassallo, José; Ward, Laura Sterian (2017): Interleukin 10 expression is related to aggressiveness and poor prognosis of patients with thyroid cancer. In *Cancer Immunol Immunother* 66 (2), pp. 141–148. DOI: 10.1007/s00262-016-1924-4.

Da Cunha, Bianca Rodrigues; Domingos, Célia; Stefanini, Ana Carolina Buzzo; Henrique, Tiago; Polachini, Giovana Mussi; Castelo-Branco, Pedro; Tajara, Eloiza Helena (2019): Cellular interactions in the tumor microenvironment: the role of secretome. In *Journal of Cancer* 10 (19), p. 4574.

Delyon, Julie; Lebbe, Celeste (2022): IL-6 blockade in cancer patients treated with immune checkpoint blockade: a win-win strategy. In *Cancer Cell* 40 (5), pp. 450–451.

References

Diehl, Sean; Rincón, Mercedes (2002): The two faces of IL-6 on Th1/Th2 differentiation. In *Molecular immunology* 39 (9), pp. 531–536.

Dimri, G. P.; Itahana, K.; Acosta, M.; Campisi, J. (2000): Regulation of a senescence checkpoint response by the E2F1 transcription factor and p14(ARF) tumor suppressor. In *Molecular and Cellular Biology* 20 (1), pp. 273–285. DOI: 10.1128/MCB.20.1.273-285.2000.

Dominiak, Agnieszka; Chełstowska, Beata; Olejarz, Wioletta; Nowicka, Grażyna (2020): Communication in the cancer microenvironment as a target for therapeutic interventions. In *Cancers* 12 (5), p. 1232.

Dong, Haidong; Strome, Scott E.; Salomao, Diva R.; Tamura, Hideto; Hirano, Fumiya; Flies, Dallas B. et al. (2002): Tumor-associated B7-H1 promotes T-cell apoptosis: a potential mechanism of immune evasion. In *Nature medicine* 8 (8), pp. 793–800.

Dong, Yuanmei; Liu, Yang; Bai, Hui; Jiao, Shunchang (2019): Systematic assessment of the clinicopathological prognostic significance of tissue cytokine expression for lung adenocarcinoma based on integrative analysis of TCGA data. In *Scientific Reports* 9 (1), p. 6301.

Dratwa, Marta; Wysoczańska, Barbara; Łacina, Piotr; Kubik, Tomasz; Bogunia-Kubik, Katarzyna (2020): TERT-Regulation and Roles in Cancer Formation. In *Front. Immunol.* 11, p. 589929. DOI: 10.3389/fimmu.2020.589929.

Engelmann, David; Mayoli-Nüssle, Deborah; Mayrhofer, Christian; Fürst, Katharina; Alla, Vijay; Stoll, Anja et al. (2013): E2F1 promotes angiogenesis through the VEGF-C/VEGFR-3 axis in a feedback loop for cooperative induction of PDGF-B. In *Journal of molecular cell biology* 5 (6), pp. 391–403.

Etxebeste-Mitxeltorena, Mikel; Del Rincón-Loza, Inés; Martín-Antonio, Beatriz (2021): Tumor Secretome to Adoptive Cellular Immunotherapy: Reduce Me Before I Make You My Partner. In *Frontiers in immunology* 12, p. 717850. DOI: 10.3389/fimmu.2021.717850.

Feitelson, Mark A.; Arzumanyan, Alla; Kulathinal, Rob J.; Blain, Stacy W.; Holcombe, Randall F.; Mahajna, Jamal et al. (2015): Sustained proliferation in cancer: Mechanisms and novel therapeutic targets. In *Seminars in cancer biology* 35 Suppl (Suppl), S25-S54. DOI: 10.1016/j.semcancer.2015.02.006.

Ford, Shayne Lavondua; Buus, Terkild Brink; Nastasi, Claudia; Geisler, Carsten; Bonefeld, Charlotte Menné; Ødum, Niels; Woetmann, Anders (2023): In vitro differentiated human CD4+ T cells produce hepatocyte growth factor. In *Front. Immunol.* 14, p. 1210836.

Franklin, C.; Livingstone, E.; Roesch, A.; Schilling, B.; Schadendorf, D. (2017): Immunotherapy in melanoma: recent advances and future directions. In *European Journal of Surgical Oncology (EJSO)* 43 (3), pp. 604–611.

Garcia-Hernandez, M. L.; Hernández-Pando, Rogelio; Gariglio, Patricio; Berumen, Jaime (2002): Interleukin-10 promotes B16-melanoma growth by inhibition of macrophage

functions and induction of tumour and vascular cell proliferation. In *Immunology* 105 (2), pp. 231–243.

Gerhardt, Lara; Hong, Megan M. Y.; Yousefi, Yeganeh; Figueredo, Rene; Maleki Vareki, Saman (2023): IL-12 and IL-27 promote CD39 expression on CD8+ T cells and differentially regulate the CD39+ CD8+ T cell phenotype. In *The Journal of Immunology* 210 (10), pp. 1598–1606.

Ghandadi, Morteza; Sahebkar, Amirhossein (2016): Interleukin-6: a critical cytokine in cancer multidrug resistance. In *Current pharmaceutical design* 22 (5), pp. 518–526.

Ghanekar, S. A.; Nomura, L. E.; Suni, M. A.; Picker, L. J.; Maecker, H. T.; Maino, V. C. (2001): Gamma interferon expression in CD8(+) T cells is a marker for circulating cytotoxic T lymphocytes that recognize an HLA A2-restricted epitope of human cytomegalovirus phosphoprotein pp65. In *Clinical and diagnostic laboratory immunology* 8 (3), pp. 628–631. DOI: 10.1128/cdli.8.3.628-631.2001.

Gide, Tuba N.; Wilmott, James S.; Scolyer, Richard A.; Long, Georgina V. (2018): Primary and acquired resistance to immune checkpoint inhibitors in metastatic melanoma. In *Clinical Cancer Research* 24 (6), pp. 1260–1270.

Ginsberg, Doron (2002): E2F1 pathways to apoptosis. In *0014-5793* 529 (1), pp. 122–125. DOI: 10.1016/S0014-5793(02)03270-2.

Goody, D.; Gupta, S. K.; Engelmann, D.; Spitschak, A.; Marquardt, S.; Mikkat, S. et al. (2019): Drug Repositioning Inferred from E2F1-Coregulator Interactions Studies for the Prevention and Treatment of Metastatic Cancers. In *Theranostics* 9 (5), pp. 1490–1509.

Greten, Florian R.; Grivennikov, Sergei I. (2019): Inflammation and cancer: triggers, mechanisms, and consequences. In *Immunity* 51 (1), pp. 27–41.

Gutschner, Tony; Diederichs, Sven (2012): The hallmarks of cancer: a long non-coding RNA point of view. In *RNA biology* 9 (6), pp. 703–719. DOI: 10.4161/rna.20481.

Haabeth, Ole Audun Werner; Tveita, Anders Aune; Fauskanger, Marte; Schjesvold, Fredrik; Lorvik, Kristina Berg; Hofgaard, Peter O. et al. (2014): How do CD4+ T cells detect and eliminate tumor cells that either lack or express MHC class II molecules? In *Front. Immunol.* 5, p. 174.

Hailemichael, Yared; Johnson, Daniel H.; Abdel-Wahab, Noha; Foo, Wai Chin; Bentebibel, Salah-Eddine; Daher, May et al. (2022): Interleukin-6 blockade abrogates immunotherapy toxicity and promotes tumor immunity. In *Cancer Cell* 40 (5), pp. 509–523.

Hanahan, Douglas (2022): Hallmarks of Cancer: New Dimensions. In *Cancer discovery* 12 (1), pp. 31–46. DOI: 10.1158/2159-8290.CD-21-1059.

Hassan, Ghmkin; Seno, Masaharu (2020): Blood and cancer: cancer stem cells as origin of hematopoietic cells in solid tumor microenvironments. In *Cells* 9 (5), p. 1293.

Hershko, Dan D.; Robb, Bruce W.; Luo, Guangju; Hasselgren, Per-Olof (2002): Multiple transcription factors regulating the IL-6 gene are activated by cAMP in cultured Caco-2 cells.

References

In *American Journal of Physiology-Regulatory, Integrative and Comparative Physiology* 283 (5), R1140-R1148.

Hoejberg, Lise; Bastholt, Lars; Johansen, Julia S.; Christensen, Ib Jarle; Gehl, Julie; Schmidt, Henrik (2012a): Serum interleukin-6 as a prognostic biomarker in patients with metastatic melanoma. In *Melanoma research* 22 (4), pp. 287–293.

Hoejberg, Lise; Bastholt, Lars; Schmidt, Henrik (2012b): Interleukin-6 and melanoma. In *Melanoma research* 22 (5), pp. 327–333.

Huff, Wei X.; Kwon, Jae Hyun; Henriquez, Mario; Fetcko, Kaleigh; Dey, Mahua (2019): The evolving role of CD8+ CD28− immunosenescent T cells in cancer immunology. In *International Journal of Molecular Sciences* 20 (11), p. 2810.

Huseni, Mahrukh A.; Wang, Lifen; Klementowicz, Joanna E.; Yuen, Kobe; Breart, Beatrice; Orr, Christine et al. (2023b): CD8+ T cell-intrinsic IL-6 signaling promotes resistance to anti-PD-L1 immunotherapy. In *Cell Reports Medicine* 4 (1).

Itakura, Eijun; Huang, Rong-Rong; Wen, Duan-Ren; Paul, Eberhard; Wünsch, Peter H.; Cochran, Alistair J. (2011): IL-10 expression by primary tumor cells correlates with melanoma progression from radial to vertical growth phase and development of metastatic competence. In *Modern Pathology* 24 (6), pp. 801–809.

Iyer, Shankar Subramanian; Cheng, Gehong (2012): Role of interleukin 10 transcriptional regulation in inflammation and autoimmune disease. In *Critical Reviews™ in Immunology* 32 (1).

Johnson, Daniel E.; O'Keefe, Rachel A.; Grandis, Jennifer R. (2018): Targeting the IL-6/JAK/STAT3 signalling axis in cancer. In *Nature reviews Clinical oncology* 15 (4), pp. 234–248.

Kakavand, Hojabr; Rawson, Robert V.; Pupo, Gulietta M.; Yang, Jean Y. H.; Menzies, Alexander M.; Carlino, Matteo S. et al. (2017): PD-L1 Expression and Immune Escape in Melanoma Resistance to MAPK Inhibitors. In *Clin Cancer Res* 23 (20), pp. 6054–6061. DOI: 10.1158/1078-0432.CCR-16-1688.

Kartikasari, Apriliana E. R.; Huertas, Cesar S.; Mitchell, Arnan; Plebanski, Magdalena (2021): Tumor-induced inflammatory cytokines and the emerging diagnostic devices for cancer detection and prognosis. In *Frontiers in Oncology* 11, p. 692142.

Khan, Faiz M.; Marquardt, Stephan; Gupta, Shailendra K.; Knoll, Susanne; Schmitz, Ulf; Spitschak, Alf et al. (2017): Unraveling a tumor type-specific regulatory core underlying E2F1-mediated epithelial-mesenchymal transition to predict receptor protein signatures. In *Nat Commun* 8 (1), p. 198. DOI: 10.1038/s41467-017-00268-2.

Kim, Byung-Seok; Kuen, Da-Sol; Koh, Choong-Hyun; Kim, Hyung-Don; Chang, Seon Hee; Kim, Sehui et al. (2021): Type 17 immunity promotes the exhaustion of CD8+ T cells in cancer. In *Journal for Immunotherapy of Cancer* 9 (6).

References

Kim, Seong Keun; Cho, Sun Wook (2022): The Evasion Mechanisms of Cancer Immunity and Drug Intervention in the Tumor Microenvironment. In *Frontiers in pharmacology* 13, p. 868695. DOI: 10.3389/fphar.2022.868695.

Kitamura, Takanori; Qian, Bin-Zhi; Pollard, Jeffrey W. (2015): Immune cell promotion of metastasis. In *Nature Reviews Immunology* 15 (2), pp. 73–86.

Knight, Andrew; Karapetyan, Lilit; Kirkwood, John M. (2023): Immunotherapy in melanoma: recent advances and future directions. In *Cancers* 15 (4), p. 1106.

Knoll, Susanne; Fürst, Katharina; Kowtharapu, Bhavani; Schmitz, Ulf; Marquardt, Stephan; Wolkenhauer, Olaf et al. (2014): E2F1 induces miR-224/452 expression to drive EMT through TXNIP downregulation. In *EMBO reports* 15 (12), pp. 1315–1329.

Koczan, Dirk; Fitzner, Brit; Zettl, Uwe Klaus; Hecker, Michael (2018): Microarray data of transcriptome shifts in blood cell subsets during S1P receptor modulator therapy. In *Scientific Data* 5 (1), pp. 1–9.

Kuehnemuth, Benjamin; Piseddu, Ignazio; Wiedemann, Gabriela M.; Lauseker, Michael; Kuhn, Christina; Hofmann, Simone et al. (2018): CCL1 is a major regulatory T cell attracting factor in human breast cancer. In *BMC cancer* 18, pp. 1–6.

Leong, Stanley P.; Naxerova, Kamila; Keller, Laura; Pantel, Klaus; Witte, Marlys (2022): Molecular mechanisms of cancer metastasis via the lymphatic versus the blood vessels. In *Clinical & Experimental Metastasis* 39 (1), pp. 159–179.

Li, Chong; Zuo, Wenwei (2019): IL-10 in vitro could enhance IFNγ expression and suppress PD-1 expression in CD8 T cells from esophageal cancer patients. In *Experimental Cell Research* 379 (2), pp. 159–165.

Li, Jiali; Zeng, Zihang; Wu, Qiuji; Chen, Jiarui; Liu, Xingyu; Zhang, Jianguo et al. (2021): Immunological modulation of the Th1/Th2 shift by ionizing radiation in tumors. In *International journal of oncology* 59 (1), pp. 1–12.

Li, Jingjing; Bi, Wen; Lu, Fang; Pan, Bei; Xiong, Mengqiu; Nasifu, Lubanga et al. (2023): Prognostic role of E2F1 gene expression in human cancer: a meta-analysis. In *BMC cancer* 23 (1), p. 509.

Li, Li; Ma, Yan; Xu, Yuan (2019): Follicular regulatory T cells infiltrated the ovarian carcinoma and resulted in CD8 T cell dysfunction dependent on IL-10 pathway. In *International immunopharmacology* 68, pp. 81–87.

Liu, Limin; Shi, Wenjuan; Xiao, Xiao; Wu, Xuemei; Hu, Haiyan; Yuan, Shixin et al. (2021): BCG immunotherapy inhibits cancer progression by promoting the M1 macrophage differentiation of THP-1 cells via the Rb/E2F1 pathway in cervical carcinoma. In *Oncology Reports* 46 (5), pp. 1–13. DOI: 10.3892/or.2021.8196.

Liu, Peishan; Zhang, Xiaoyue; Li, Zhengshuo; Wei, Lingyu; Peng, Qiu; Liu, Can et al. (2020): A significant role of transcription factors E2F in inflammation and tumorigenesis of nasopharyngeal carcinoma. In *Biochemical and Biophysical Research Communications* 524 (4), pp. 816–824.

References

Logotheti, Stella; Marquardt, Stephan; Gupta, Shailendra K.; Richter, Christin; Edelhäuser, Berdien A. H.; Engelmann, David et al. (2020): LncRNA-SLC16A1-AS1 induces metabolic reprogramming during Bladder Cancer progression as target and co-activator of E2F1. In *Theranostics* 10 (21), p. 9620.

Luke, Jason J.; Bao, Riyue; Sweis, Randy F.; Spranger, Stefani; Gajewski, Thomas F. (2019): WNT/β-catenin Pathway Activation Correlates with Immune Exclusion across Human Cancers. In *Clin Cancer Res* 25 (10), pp. 3074–3083. DOI: 10.1158/1078-0432.CCR-18-1942.

Manickavinayaham, Swarnalatha; Velez-Cruz, Renier; Biswas, Anup K.; Chen, Jie; Guo, Ruifeng; Johnson, David G. (2020): The E2F1 transcription factor and RB tumor suppressor moonlight as DNA repair factors. In *Cell Cycle* 19 (18), pp. 2260–2269. DOI: 10.1080/15384101.2020.1801190.

Marshall, Jean S.; Warrington, Richard; Watson, Wade; Kim, Harold L. (2018): An introduction to immunology and immunopathology. In *Allergy, Asthma & Clinical Immunology* 14, pp. 1–10.

Matthews, Natalie H.; Li, Wen-Qing; Qureshi, Abrar A.; Weinstock, Martin A.; Cho, Eunyoung (2017): Cutaneous Melanoma: Etiology and Therapy. Epidemiology of Melanoma. In *1*, pp. 3–22. DOI: 10.15586/codon.cutaneousmelanoma.2017.ch1.

McArthur, Grant A.; Chapman, Paul B.; Robert, Caroline; Larkin, James; Haanen, John B.; Dummer, Reinhard et al. (2014): Safety and efficacy of vemurafenib in BRAF(V600E) and BRAF(V600K) mutation-positive melanoma (BRIM-3): extended follow-up of a phase 3, randomised, open-label study. In *The Lancet Oncology* 15 (3), pp. 323–332. DOI: 10.1016/S1470-2045(14)70012-9.

Medzhitov, Ruslan; Janeway Jr, Charles (2000): Innate immunity. In *New England Journal of Medicine* 343 (5), pp. 338–344.

Meier, Claudia; Spitschak, Alf; Abshagen, Kerstin; Gupta, Shailendra; Mor, Joel M.; Wolkenhauer, Olaf et al. (2014): Association of RHAMM with E2F1 promotes tumour cell extravasation by transcriptional up-regulation of fibronectin. In *The Journal of pathology* 234 (3), pp. 351–364.

Murakami, Masaaki; Kamimura, Daisuke; Hirano, Toshio (2019): Pleiotropy and specificity: insights from the interleukin 6 family of cytokines. In *Immunity* 50 (4), pp. 812–831.

Na, Yi-Rang; Lee, Jin-Sub; Lee, Seok-Jong; Seok, Seung-Hyeok (2013): Interleukin-6-induced Twist and N-cadherin enhance melanoma cell metastasis. In *Melanoma research* 23 (6), pp. 434–443.

Nagarsheth, Nisha; Wicha, Max S.; Zou, Weiping (2017): Chemokines in the cancer microenvironment and their relevance in cancer immunotherapy. In *Nature Reviews Immunology* 17 (9), pp. 559–572.

Naing, Aung; Infante, Jeffrey R.; Papadopoulos, Kyriakos P.; Chan, Ivan H.; Shen, Cong; Ratti, Navneet P. et al. (2018): PEGylated IL-10 (Pegilodecakin) induces systemic immune

activation, CD8+ T cell invigoration and polyclonal T cell expansion in cancer patients. In *Cancer Cell* 34 (5), pp. 775–791.

Nelson, Joel D.; Denisenko, Oleg; Bomsztyk, Karol (2006): Protocol for the fast chromatin immunoprecipitation (ChIP) method. In *Nature protocols* 1 (1), pp. 179–185.

Nishimura, Takashi; Nakui, Minoru; Sato, Marimo; Iwakabe, Kenji; Kitamura, Hidemitsu; Sekimoto, Masashi et al. (2000): The critical role of Th1-dominant immunity in tumor immunology. In *Cancer chemotherapy and pharmacology* 46, S52-S61.

Niu, W.; Guo, L-Y; Zhang, J-Y; Ji, T.; Mao, D.; Li, X-F; Du, X-X (2020): E2F1-induced upregulation of lncRNA HCG18 stimulates proliferation and migration in gastric cancer by binding to miR-197-3p. In *European Review for Medical & Pharmacological Sciences* 24 (19).

Ozga, Aleksandra J.; Chow, Melvyn T.; Luster, Andrew D. (2021): Chemokines and the immune response to cancer. In *Immunity* 54 (5), pp. 859–874.

Philip, Mary; Schietinger, Andrea (2022): CD8+ T cell differentiation and dysfunction in cancer. In *Nature Reviews Immunology* 22 (4), pp. 209–223.

Polager, S.; Ofir, M.; Ginsberg, D. (2008): E2F1 regulates autophagy and the transcription of autophagy genes. In *Oncogene* 27 (35), pp. 4860–4864. DOI: 10.1038/onc.2008.117.

Poncette, Lucia; Bluhm, Julia; Blankenstein, Thomas (2022): The role of CD4 T cells in rejection of solid tumors. In *Current Opinion in Immunology* 74, pp. 18–24.

Qiao, Jian; Liu, Zhida; Dong, Chunbo; Luan, Yan; Zhang, Anli; Moore, Casey et al. (2019): Targeting tumors with IL-10 prevents dendritic cell-mediated CD8+ T cell apoptosis. In *Cancer Cell* 35 (6), pp. 901–915.

Qiao, Lijun; Zhang, Qiangnu; Sun, Zhe; Liu, Quan; Wu, Zongze; Hu, Weibin et al. (2021): The E2F1/USP11 positive feedback loop promotes hepatocellular carcinoma metastasis and inhibits autophagy by activating ERK/mTOR pathway. In *Cancer letters* 514, pp. 63–78.

Real, Sebastian; Meo-Evoli, Nathalie; Espada, Lilia; Tauler, Albert (2011): E2F1 regulates cellular growth by mTORC1 signaling. In *PLOS ONE* 6 (1), e16163.

Rehan Akbani; Kadir C. Akdemir; B. Arman Aksoy; Monique Albert; Adrian Ally; Samirkumar B. Amin et al. (2015): Genomic Classification of Cutaneous Melanoma. In *Cell* 161 (7), pp. 1681–1696. DOI: 10.1016/j.cell.2015.05.044.

Richter, Christin; Marquardt, Stephan; Li, Fanghua; Spitschak, Alf; Murr, Nico; Edelhäuser, Berdien A. H. et al. (2019): Rewiring E2F1 with classical NHEJ via APLF suppression promotes bladder cancer invasiveness. In *Journal of experimental & clinical cancer research : CR* 38 (1), p. 292. DOI: 10.1186/s13046-019-1286-9.

Ritchie, Shona; Reed, Daniel A.; Pereira, Brooke A.; Timpson, Paul (2021): The cancer cell secretome drives cooperative manipulation of the tumour microenvironment to accelerate tumourigenesis. In *Faculty Reviews* 10.

References

Roncati, Luca; Figueiredo, Carlos R. (2023): Hallmark of cancer: tumor promoting inflammation. In *Frontiers in Oncology* 13.

Rosenfeldt, M. T.; La Bell; Long, J. S.; O'prey, J.; Nixon, C.; Roberts, F. et al. (2014): E2F1 drives chemotherapeutic drug resistance via ABCG2. In *Oncogene* 33 (32), pp. 4164–4172.

Rouaud, Florian; Hamouda-Tekaya, Nedra; Cerezo, Michaël; Abbe, Patricia; Zangari, Joséphine; Hofman, Veronique et al. (2018): E2F1 inhibition mediates cell death of metastatic melanoma. In *Cell death & disease* 9 (5), p. 527. DOI: 10.1038/s41419-018-0566-1.

Salemme, Vincenzo; Centonze, Giorgia; Cavallo, Federica; Defilippi, Paola; Conti, Laura (2021): The crosstalk between tumor cells and the immune microenvironment in breast cancer: implications for immunotherapy. In *Frontiers in Oncology* 11, p. 610303.

Sanlorenzo, Martina; Vujic, Igor; Posch, Christian; Dajee, Akshay; Yen, Adam; Kim, Sarasa et al. (2014): Melanoma immunotherapy. In *Cancer Biology & Therapy* 15 (6), pp. 665–674.

Saraiva, Margarida; Vieira, Paulo; O'garra, Anne (2019): Biology and therapeutic potential of interleukin-10. In *The Journal of experimental medicine* 217 (1), e20190418.

Schildberg, Frank A.; Klein, Sarah R.; Freeman, Gordon J.; Sharpe, Arlene H. (2016): Coinhibitory pathways in the B7-CD28 ligand-receptor family. In *Immunity* 44 (5), pp. 955–972.

Seliger, Barbara; Massa, Chiara (2021): Immune therapy resistance and immune escape of tumors. In *Cancers* 13 (3), p. 551.

Shang, Qihang; Yu, Xiaoyun; Sun, Qi; Li, Huayao; Sun, Changgang; Liu, Lijuan (2024): Polysaccharides regulate Th1/Th2 balance: a new strategy for tumor immunotherapy. In *Biomedicine & Pharmacotherapy* 170, p. 115976.

Siegel, Rebecca L.; Miller, Kimberly D.; Wagle, Nikita Sandeep; Jemal, Ahmedin (2023): Cancer statistics, 2023. In *CA A Cancer J Clinicians* 73 (1), pp. 17–48. DOI: 10.3322/caac.21763.

Song, Liang; Dong, Guangyu; Guo, Lijia; Graves, Dana T. (2018): The function of dendritic cells in modulating the host response. In *Molecular oral microbiology* 33 (1), pp. 13–21.

Speiser, Daniel E.; Chijioke, Obinna; Schaeuble, Karin; Münz, Christian (2023): CD4+ T cells in cancer. In *Nature cancer* 4 (3), pp. 317–329.

Spitschak, Alf; Dhar, Prabir; Singh, Krishna P.; Garduño, Rosaely Casalegno; Gupta, Shailendra K.; Vera, Julio et al. (2024): E2F1-induced autocrine IL-6 inflammatory loop mediates cancer-immune crosstalk that predicts T cell phenotype switching and therapeutic responsiveness. In *Front. Immunol.* 15, p. 1470368.

Stevens, Craig; La Thangue, Nicholas B. (2004): The emerging role of E2F-1 in the DNA damage response and checkpoint control. In *DNA Repair* 3 (8-9), pp. 1071–1079. DOI: 10.1016/j.dnarep.2004.03.034.

References

Strazzulla, Lauren C.; Li, Xiaoxue; Zhu, Kathleen; Okhovat, Jean-Phillip; Lee, Sandra J.; Kim, Caroline C. (2019): Clinicopathologic, misdiagnosis, and survival differences between clinically amelanotic melanomas and pigmented melanomas. In *Journal of the American Academy of Dermatology* 80 (5), pp. 1292–1298. DOI: 10.1016/j.jaad.2019.01.012.

Subramanya, Deepthi; Grivas, Petros D. (2008): HPV and cervical cancer: updates on an established relationship. In *Postgraduate Medicine* 120 (4), pp. 7–13. DOI: 10.3810/pgm.2008.11.1928.

Sumimoto, Hidetoshi; Imabayashi, Fumie; Iwata, Tomoko; Kawakami, Yutaka (2006): The BRAF-MAPK signaling pathway is essential for cancer-immune evasion in human melanoma cells. In *The Journal of experimental medicine* 203 (7), pp. 1651–1656. DOI: 10.1084/jem.20051848.

Sun, Lina; Su, Yanhong; Jiao, Anjun; Wang, Xin; Zhang, Baojun (2023): T cells in health and disease. In *Signal Transduction and Targeted Therapy* 8 (1), p. 235.

Tan, Rongying; Nie, Manhua; Long, Wang (2022): The role of B cells in cancer development. In *Frontiers in Oncology* 12, p. 958756.

Tannir, Nizar M.; Naing, Aung; Infante, Jeffrey R.; Papadopoulos, Kyriakos P.; Wong, Deborah J. L.; Korn, Michael et al. (2018): Pegilodecakin with nivolumab (nivo) or pembrolizumab (pembro) in patients (pts) with metastatic renal cell carcinoma (RCC): American Society of Clinical Oncology.

Tannir, Nizar M.; Papadopoulos, Kyriakos P.; Wong, Deborah J.; Aljumaily, Raid; Hung, Annie; Afable, Manuel et al. (2021): Pegilodecakin as monotherapy or in combination with anti-PD-1 or tyrosine kinase inhibitor in heavily pretreated patients with advanced renal cell carcinoma: Final results of cohorts A, G, H and I of IVY Phase I study. In *International journal of cancer* 149 (2), pp. 403–408.

Tawara, Ken; Scott, Hannah; Emathinger, Jacqueline; Wolf, Cody; LaJoie, Dollie; Hedeen, Danielle et al. (2019): HIGH expression of OSM and IL-6 are associated with decreased breast cancer survival: synergistic induction of IL-6 secretion by OSM and IL-1β. In *Oncotarget* 10 (21), p. 2068.

Terai, Mizue; Eto, Masumi; Young, Garbo D.; Berd, David; Mastrangelo, Michael J.; Tamura, Yutaka et al. (2012): Interleukin 6 mediates production of interleukin 10 in metastatic melanoma. In *Cancer Immunology, Immunotherapy* 61, pp. 145–155.

Tímár, József; Ladányi, Andrea (2022): Molecular Pathology of Skin Melanoma: Epidemiology, Differential Diagnostics, Prognosis and Therapy Prediction. In *International Journal of Molecular Sciences* 23 (10), p. 5384. DOI: 10.3390/ijms23105384.

Truffi, Marta; Sorrentino, Luca; Corsi, Fabio (2020): Fibroblasts in the tumor microenvironment. In *Tumor Microenvironment: Non-Hematopoietic Cells*, pp. 15–29.

Tsukamoto, Hirotake; Fujieda, Koji; Senju, Satoru; Ikeda, Tokunori; Oshiumi, Hiroyuki; Nishimura, Yasuharu (2018): Immune-suppressive effects of interleukin-6 on T-cell-mediated anti-tumor immunity. In *Cancer science* 109 (3), pp. 523–530.

References

Ugurel, S.; Rappl, G.; Tilgen, W.; Reinhold, U. (2001): Increased serum concentration of angiogenic factors in malignant melanoma patients correlates with tumor progression and survival. In *Journal of clinical oncology : official journal of the American Society of Clinical Oncology* 19 (2), pp. 577–583. DOI: 10.1200/JCO.2001.19.2.577.

Van den Eeckhout, Bram; Huyghe, Leander; van Lint, Sandra; Burg, Elianne; Plaisance, Stéphane; Peelman, Frank et al. (2021): Selective IL-1 activity on CD8+ T cells empowers antitumor immunity and synergizes with neovasculature-targeted TNF for full tumor eradication. In *Journal for Immunotherapy of Cancer* 9 (11).

Vera, Julio; Schmitz, Ulf; Lai, Xin; Engelmann, David; Khan, Faiz M.; Wolkenhauer, Olaf; Pützer, Brigitte M. (2013): Kinetic modeling-based detection of genetic signatures that provide chemoresistance via the E2F1-p73/DNp73-miR-205 network. In *Cancer research* 73 (12), pp. 3511–3524. DOI: 10.1158/0008-5472.CAN-12-4095.

Wan, Yisong Y. (2010): Multi-tasking of helper T cells. In *Immunology* 130 (2), pp. 166–171.

Wang, Dan; Yu, Weina; Lian, Jingyao; Wu, Qian; Liu, Shasha; Yang, Li et al. (2020): Th17 cells inhibit CD8+ T cell migration by systematically downregulating CXCR3 expression via IL-17A/STAT3 in advanced-stage colorectal cancer patients. In *Journal of hematology & oncology* 13, pp. 1–15.

Wang, Hua; Lafdil, Fouad; Kong, Xiaoni; Gao, Bin (2011): Signal transducer and activator of transcription 3 in liver diseases: a novel therapeutic target. In *International journal of biological sciences* 7 (5), p. 536.

Wang, Xiaoting; Wong, Kit; Ouyang, Wenjun; Rutz, Sascha (2019): Targeting IL-10 family cytokines for the treatment of human diseases. In *Cold Spring Harbor perspectives in biology* 11 (2), a028548.

Wang, Yajie; Alla, Vijay; Goody, Deborah; Gupta, Shailendra K.; Spitschak, Alf; Wolkenhauer, Olaf et al. (2016): Epigenetic factor EPC1 is a master regulator of DNA damage response by interacting with E2F1 to silence death and activate metastasis-related gene signatures. In *Nucleic acids research* 44 (1), pp. 117–133.

Wolchok, Jedd D.; Chiarion-Sileni, Vanna; Gonzalez, Rene; Rutkowski, Piotr; Grob, Jean-Jacques; Cowey, C. Lance et al. (2017): Overall survival with combined nivolumab and ipilimumab in advanced melanoma. In *New England Journal of Medicine* 377 (14), pp. 1345–1356.

Wu, Ting; Dai, Yun (2017): Tumor microenvironment and therapeutic response. In *Cancer letters* 387, pp. 61–68.

Xiao, Weihua; Hodge, David R.; Wang, Lihua; Yang, Xiaoyi; Zhang, Xiaohu; Farrar, William L. (2004): NF-kappaB activates IL-6 expression through cooperation with c-Jun and IL6-AP1 site, but is independent of its IL6-NFkappaB regulatory site in autocrine human multiple myeloma cells. In *Cancer Biology & Therapy* 3 (10), pp. 1007–1017.

References

Xu, Qinyang; Ge, Qiulin; Zhou, Yang; Yang, Bikang; Yang, Qin; Jiang, Shuheng et al. (2020): MELK promotes Endometrial carcinoma progression via activating mTOR signaling pathway. In *EBioMedicine* 51.

Xu, Yu-Dong; Cheng, Mi; Shang, Pan-Pan; Yang, Yong-Qing (2022): Role of IL-6 in dendritic cell functions. In *Journal of leukocyte biology* 111 (3), pp. 695–709. DOI: 10.1002/JLB.3MR0621-616RR.

Yan, Lin-Hai; Wei, Wei-Yuan; Cao, Wen-Long; Zhang, Xiao-Shi; Xie, Yu-Bo; Xiao, Qiang (2014): Overexpression of E2F1 in human gastric carcinoma is involved in anti-cancer drug resistance. In *BMC cancer* 14, pp. 1–10.

Yao, Yixin; Dai, Wei (2014): Genomic Instability and Cancer. In *Journal of carcinogenesis & mutagenesis* 5. DOI: 10.4172/2157-2518.1000165.

Yasukawa, Hideo; Ohishi, Masanobu; Mori, Hiroyuki; Murakami, Masaaki; Chinen, Takatoshi; Aki, Daisuke et al. (2003): IL-6 induces an anti-inflammatory response in the absence of SOCS3 in macrophages. In *Nature immunology* 4 (6), pp. 551–556.

Yoon, Jeehyun; Grinchuk, Oleg V.; Tirado-Magallanes, Roberto; Ngian, Zhen Kai; Tay, Emmy Xue Yun; Chuah, You Heng et al. (2022): E2F and STAT3 provide transcriptional synergy for histone variant H2AZ activation to sustain glioblastoma chromatin accessibility and tumorigenicity. In *Cell Death & Differentiation* 29 (7), pp. 1379–1394.

Zbytek, Blazej; Carlson, J. Andrew; Granese, Jacqueline; Ross, Jeffrey; Mihm, Martin C.; Slominski, Andrzej (2008): Current concepts of metastasis in melanoma. In *Expert Review of Dermatology* 3 (5), pp. 569–585. DOI: 10.1586/17469872.3.5.569.

Zhang, Hongyu; Li, Ruochen; Cao, Yifan; Gu, Yun; Lin, Chao; Liu, Xin et al. (2022): Poor clinical outcomes and immunoevasive contexture in intratumoral IL-10-producing macrophages enriched gastric cancer patients. In *Annals of surgery* 275 (4), e626-e635.

Zhang, Jun; Veeramachaneni, Nirmal (2022): Targeting interleukin-1β and inflammation in lung cancer. In *Biomarker research* 10 (1), p. 5. DOI: 10.1186/s40364-021-00341-5.

Zhang, Ke-Wei; Wang, Dong; Cai, Hao; Cao, Man-Qing; Zhang, Yuan-Yuan; Zhuang, Peng-Yuan; Shen, Jun (2021): IL-6 plays a crucial role in epithelial-mesenchymal transition and pro-metastasis induced by sorafenib in liver cancer. In *Oncology Reports* 45 (3), pp. 1105–1117.

Appendix

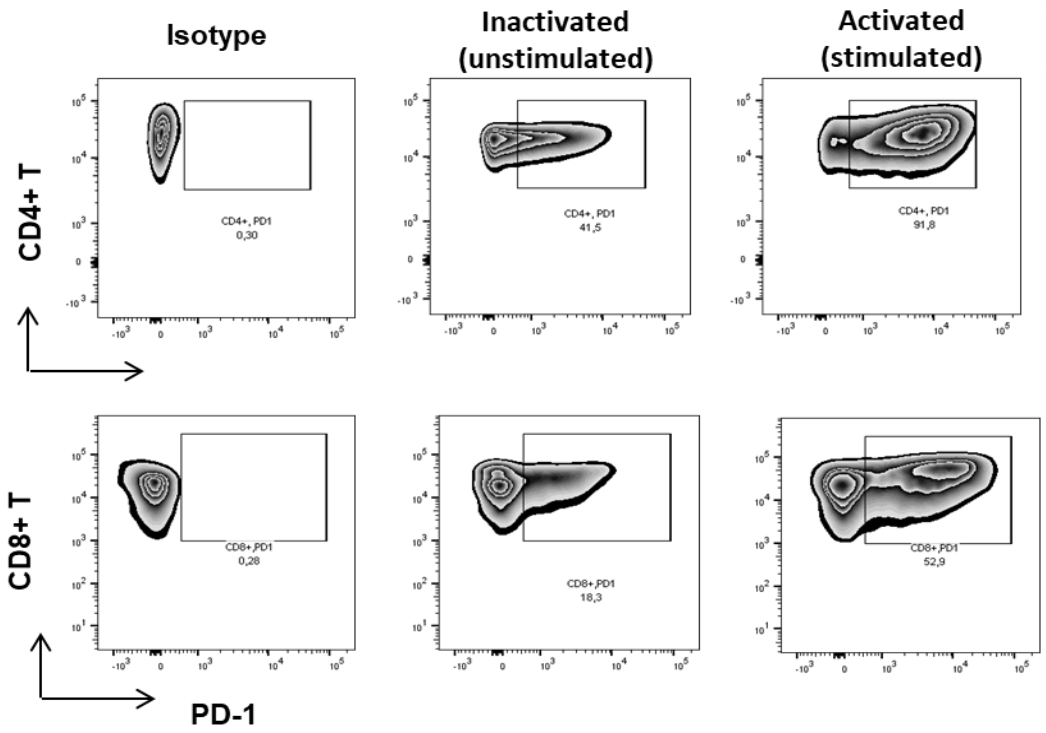

Figure 18: The gating strategies for PD-1 expression on CD4+ and CD8+ T cells.

Plasmid map

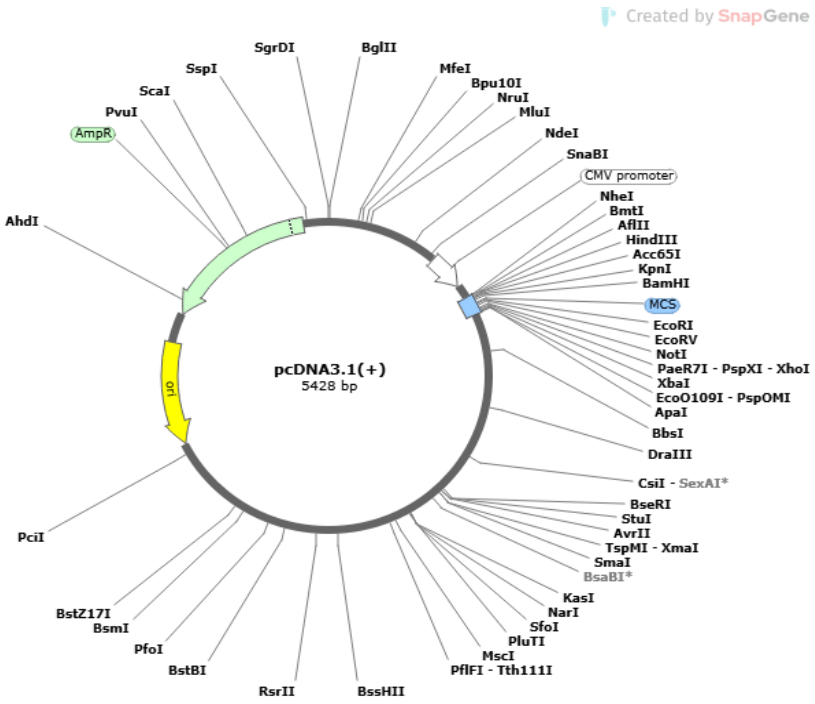

pcDNA3.1(+)

Appendix

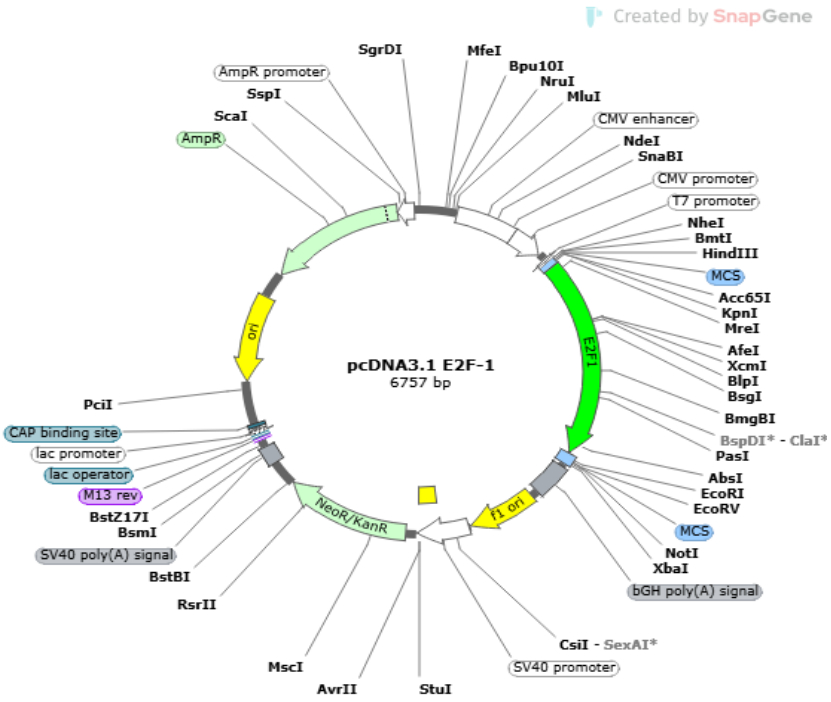

pcDNA3.1 E2F1

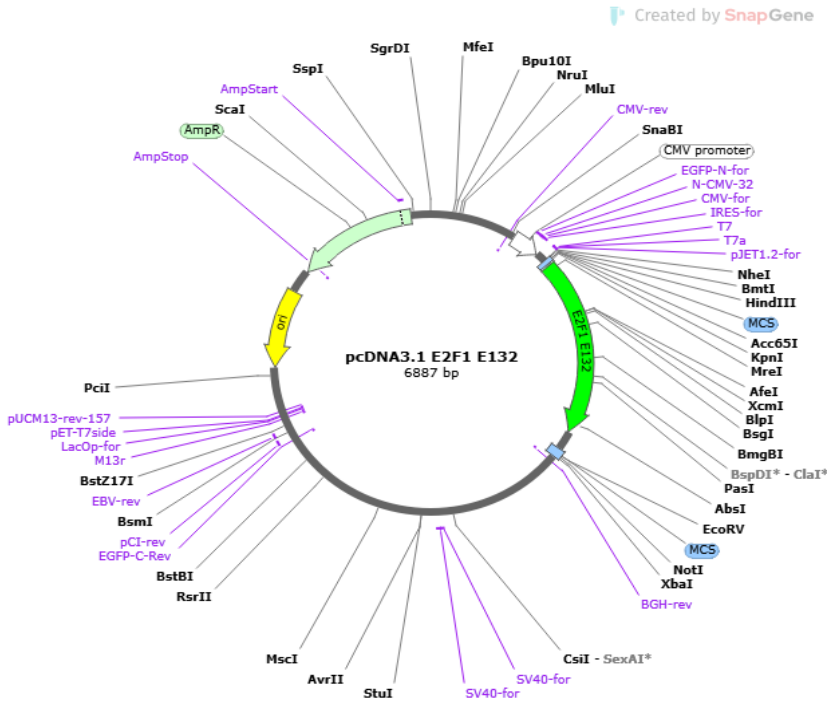

pcDNA3.1 E2F1-E132

Appendix

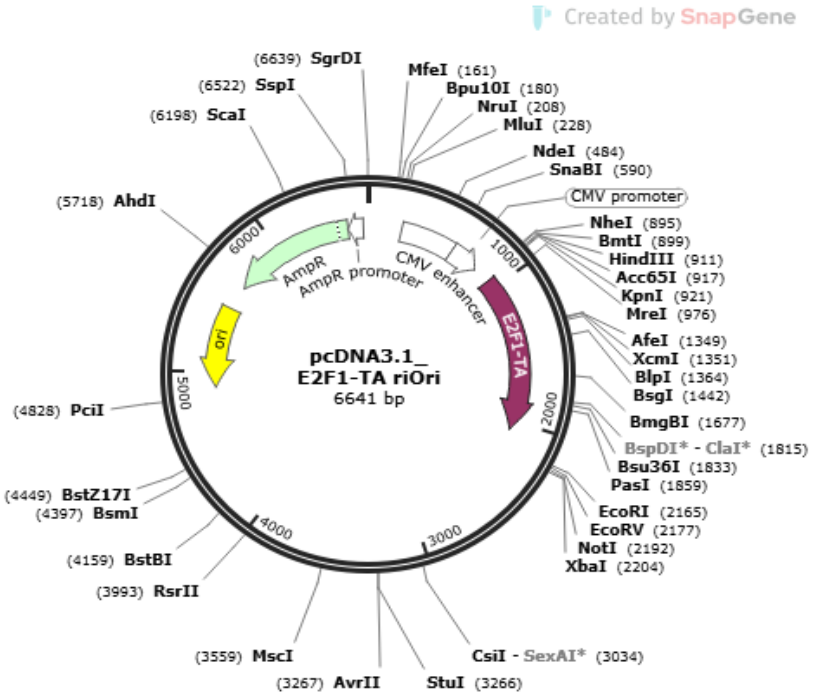

pcDNA3.1 E2F1-TA

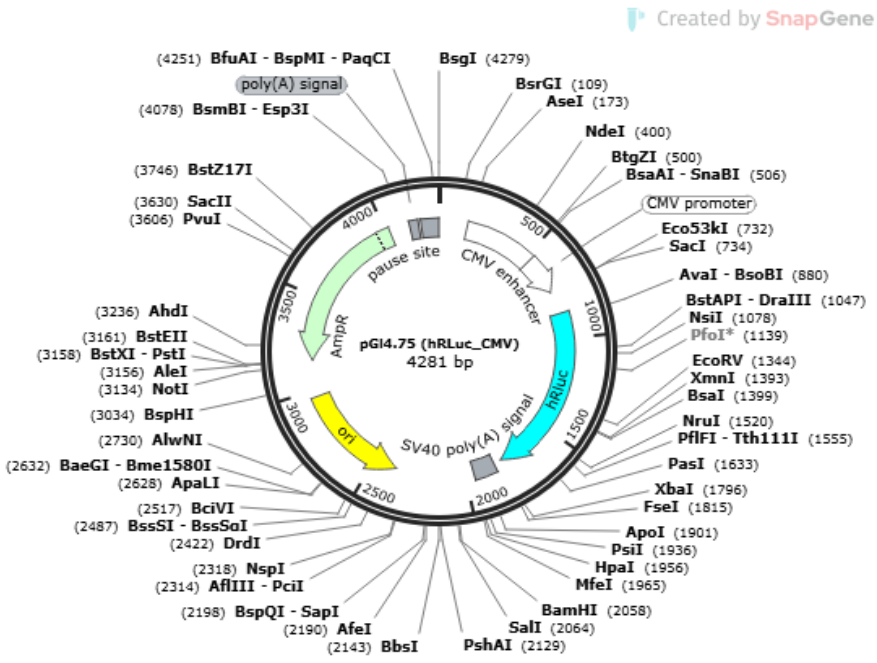

pGL4.75(hRluc_CMV)

Appendix

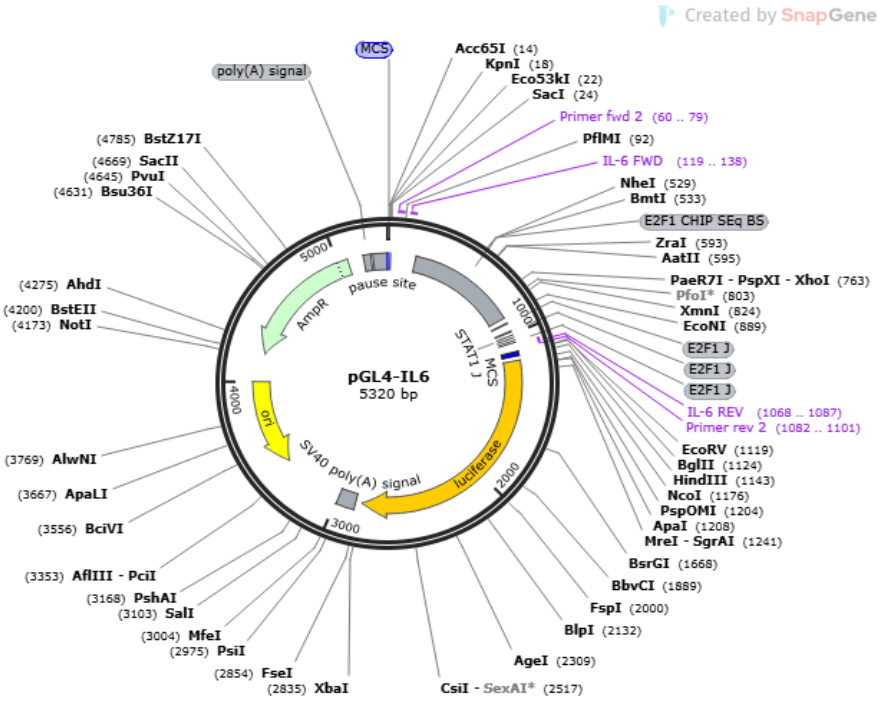

pGL4-IL6-promoter

Appendix

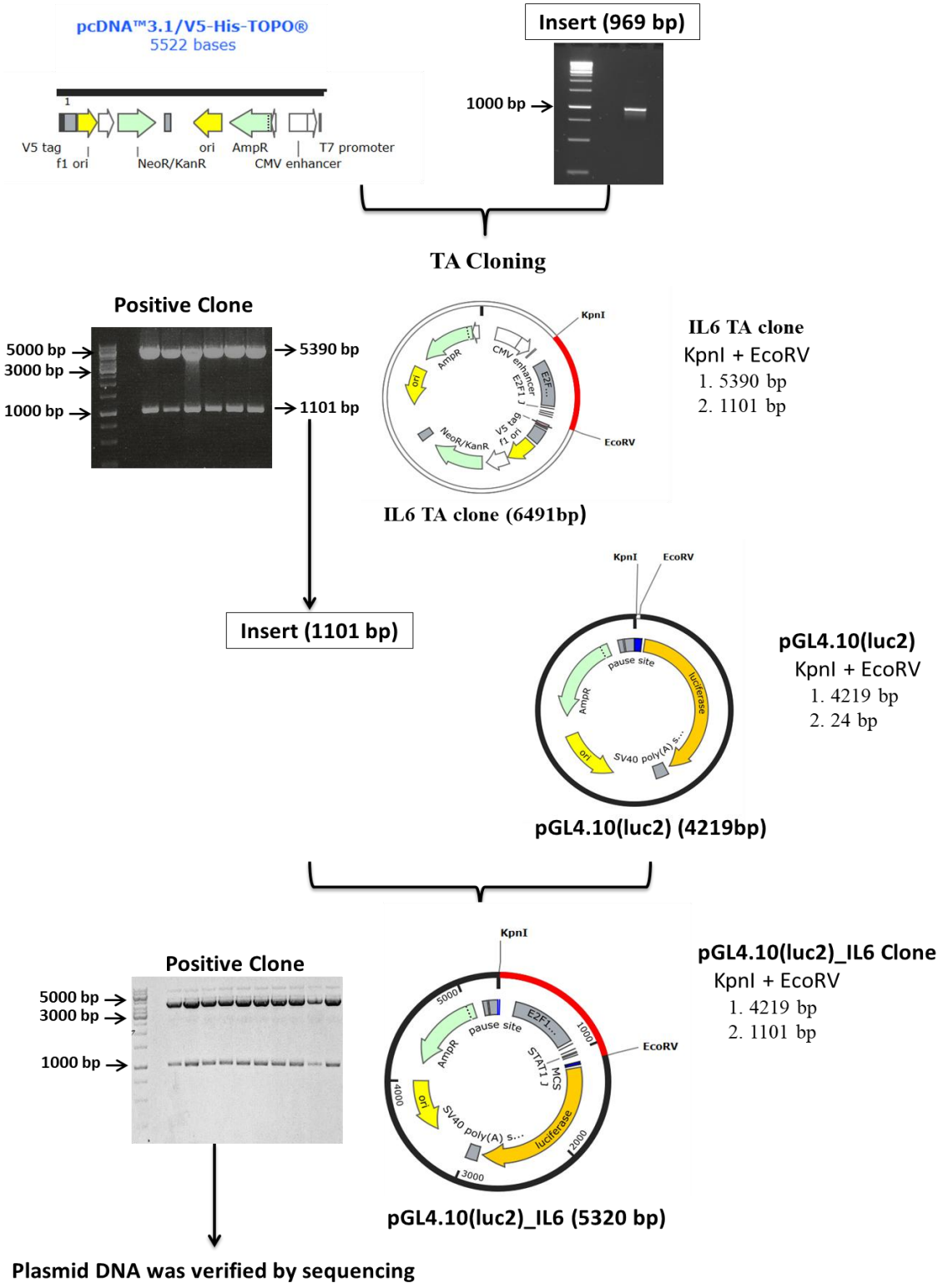

Figure 19: Outline of the cloning strategy for the pGL4-IL6 promoter plasmid.

Appendix

Table 10: List of E2F1-regulated immunomodulatory genes

Number	Gene Name	Number	Gene Name	Number	Gene Name
1.	AKAP12	**19.**	HSPD1	**37.**	POLR3G
2.	ALDH1A2	**20.**	IL1A	**38.**	PRDM5
3.	ATF2	**21.**	IL6	**39.**	PTGER1
4.	C4A	**22.**	INPP5D	**40.**	PTPN1
5.	CALCOCO2	**23.**	ITGAV	**41.**	ROCK2
6.	CEBPG	**24.**	KDM5B	**42.**	SCNN1B
7.	COL3A1	**25.**	LSM14A	**43.**	SIRT1
8.	CTSC	**26.**	MCL1	**44.**	SLC12A2
9.	CXCR4	**27.**	MFHAS1	**45.**	SOCS2
10.	DFFA	**28.**	MME	**46.**	SOS1
11.	DROSHA	**29.**	NAV3	**47.**	SP100
12.	EDN1	**30.**	NFKB2	**48.**	STK39
13.	EZH2	**31.**	NR1H3	**49.**	SYT11
14.	FOXP1	**32.**	NUB1	**50.**	TACR1
15.	GSK3B	**33.**	NUPR1	**51.**	TGFB2
16.	HAS2	**34.**	PAWR	**52.**	UPF1
17.	HNRNPU	**35.**	PLA2G2D	**53.**	WNK4
18.	HSP90AB1	**36.**	PLCG2	**54.**	ZYX

Appendix

Table 11: List of microarray generated for this study

Description	No of Array
SK-Mel-147 Ctl (E2F1 high expression) monoculture	3
SK-Mel-147 KD (E2F1 knockdown) monoculture	3
$CD4^+$ T cells monoculture	3
$CD8^+$ T cells monoculture	3
SK-Mel-147 Ctl co-cultured with $CD4^+$ T cells (SK-Mel-147 Ctl)	3
SK-Mel-147 Ctl co-cultured with $CD4^+$ T cells ($CD4^+$ T)	3
SK-Mel-147 KD co-cultured with $CD4^+$ T cells (SK-Mel-147 KD)	3
SK-Mel-147 KD co-cultured with $CD4^+$ T cells ($CD4^+$ T)	3
SK-Mel-147 Ctl co-cultured with $CD8^+$ T cells (SK-Mel-147 Ctl)	3
SK-Mel-147 Ctl co-cultured with $CD8^+$ T cells ($CD8^+$ T)	3
SK-Mel-147 KD co-cultured with $CD8^+$ T cells (SK-Mel-147 KD)	3
SK-Mel-147 KD co-cultured with $CD8^+$ T cells ($CD8^+$ T)	3

Declaration of Originality

I hereby declare that this doctoral thesis titled –E2F1-induced IL6 mediates cancer-immune cell crosstalk by modulating T cell response in tumor microenvironment that regulates metastatic properties in melanoma" represents my own, original work and was carried out under the supervision of Prof. Dr. Brigitte M. Pützer, Institute of Experimental Gene Therapy and Cancer Research, University of Rostock.

All data, tables, figures, and text citations that have been reproduced from other sources, including the internet, are explicitly acknowledged, and I have used no sources except those cited.

Furthermore, I confirm that no academic degree has been awarded to me for this Ph.D. thesis or any part of it before, either at the University of Rostock or at any other University or Institution.

I am familiar with the publicly available Regulations for the Award of Doctoral Degrees of the Medical Faculty at the University of Rostock, and I am aware of the consequences of submitting a false affidavit.

Rostock**,** _____ Prabir Dhar _____

Acknowledgement

First and foremost, I wish to express my profound gratitude to my supervisor, Prof. Dr. Brigitte M. Pützer, for granting me the opportunity to pursue my PhD in her lab. Her unwavering guidance and invaluable insights have been instrumental throughout my doctoral journey. I would like to express my heartfelt thanks to my co-supervisor, Dr. Stella Logotheti, for her exceptional supervision and encouragement, which significantly strengthened my research. Additionally, I extend my thanks to Dr. Alf Spitschak for his constructive comments and suggestions that enriched my thesis. I would like to acknowledge Wendy Bergmann, Core facility for cell sorting and cell analysis (Rostock University Medical Center), for her technical support with flow cytometry experiments, as well as Dr. Dirk Koczan, Core Facility Genomics (Rostock University Medical Center), for his expertise in micro array analysis and Dr. Krishna Pal Singh, Department of Systems Biology and Bioinformatics (University of Rostock), for his contributions to transcriptomic data analysis. Special thanks to Ingrid Winkler and Anja Stoll for their cordial cooperation and generous help whenever I needed support with chemicals, laboratory facilities, and other resources. I wish to express my thanks to all of the lab members of IEGT for their helpfulness and pleasant working atmosphere. Above all, I would like to express my deepest gratitude to my beloved parents, my wife Boishakhi Banik, and my son Pranshu Dhar for their endless sacrifices, heartiest blessings, and constant support throughout my life.

Curriculum Vitae

Personal data

Name: Prabir Dhar
Place and Date of birth: Chittagong, Bangladesh 16.10.1987
Nationality: Bangladeshi

Education

10/2018 – Present	**PhD Candidate**
Rostock, Germany	University of Rostock
PhD Thesis	E2F1-induced IL6 mediates cancer-immune cell crosstalk by modulating T cell response in tumor microenvironment that regulates metastatic properties in melanoma. Supervisor: Prof. Dr. Brigitte M. Pützer. Institute of Experimental Gene Therapy and Cancer Research.
10/2014 – 10/2017	**Master of Science in Biology**
Munich, Germany	Ludwig-Maximilians-Universität München
Master Thesis	Analysis of the immune evasive function of the Epstein-Barr virus protein BRRF1. Supervisor: PD Dr. Josef Mautner. Helmholtz Zentrum München, Research Unit Gene Vectors.
12/2005 – 05/2011	**B.Sc. (Honors) in Genetic Engineering & Biotechnology**
Sylhet, Bangladesh	Shahjalal University of Science & Technology
Bachelor Thesis	Identification of salt tolerant rice genotypes using SSR markers and their genetic diversity analysis. Supervisor: Dr. Md. Asrafuzzaman. Bangladesh Institute of Nuclear Agriculture, Bangladesh.

Language Proficiency

- **Bengali:** Native
- **English:** Fluent
- **German:** B1 level

Academic Award and Certifications

- **04/2016 – 01/2017:** Bavarian State Scholarship for international students of Ludwig-Maximilians-Universität München.
- **22nd – 23rd June, 2020:** "Good Scientific Practice" course, Graduate Academy, University of Rostock.

List of Publications

Spitschak, Alf, **Prabir Dhar**, Krishna P. Singh, Rosaely Casalegno Garduño, Shailendra K. Gupta, Julio Vera, Luca Musella, Nico Murr, Anja Stoll, and Brigitte M. Pützer. "E2F1-induced autocrine IL-6 inflammatory loop mediates cancer-immune crosstalk that predicts T cell phenotype switching and therapeutic responsiveness." Frontiers in Immunology 15 (2024): 1470368.

Marquardt, Stephan, Athanasia Pavlopoulou, Işıl Takan, **Prabir Dhar**, Brigitte M. Pützer, and Stella Logotheti. "A systems-based key innovation-driven approach infers co-option of jaw developmental programs during cancer progression." *Frontiers in cell and developmental biology* 9 (2021): 682619.

Stellberger, Thorsten, Iris Stockmar, Johannes Draxler, **Prabir Dhar**, Melanie Pavlovic, Martina Anton, Nina Koehler et al. "Characterization of retroviral vector derived DNA-isoforms by PCR and sequencing." *Journal of Consumer Protection and Food Safety* 14 (2019): 157-165.

Dhar, P., Ashrafuzzaman, M., Begum, SN, Islam, MM, & Chowdhury, MMH (2012). Identification of salt tolerant rice genotypes and their genetic diversity analysis using SSR markers. *International Journal of Biological Science 2* (9), 45-50.

Chowdhury, M. M. H., M. Ashrafuzzaman, S. N. Begum, M. M. Islam, and **P. Dhar**. "Regeneration of plantlets from grape (Vitis vinifera L.) through different explants." *International Journal of Sustainable Crop Production* 7, no. 2 (2012): 12-18.

Proceedings & Abstracts

Prabir Dhar, Krishna P. Singh, Shailendra K. Gupta, Dhanya Peringot, Alf Spitschak, and Brigitte M. Pützer. "E2F1-induced autocrine IL-6 inflammatory loop mediates cancer-immune cell crosstalk that regulates metastatic properties in melanoma." *Cancer Research* 84, no. 6_Supplement (2024): 6814-6814.

Prabir Dhar, Shailendra K. Gupta, Stephan Marquardt, Krishna P Singh, Julio Vera, Styliani Logotheti, Brigitte M Pützer. "E2F1 induced cancer secretome modulates the T cells response in Melanoma microenvironment."*VIB conference (Translational Immunology);* 22-23 November, 2021.

Prabir Dhar, Shailendra K. Gupta, Stephan Marquardt, Krishna P Singh, Martin Eberhardt, Julio Vera, Brigitte M Pützer, Styliani Logotheti1. "Reprogramming the melanoma-immune cell interface by tumor-intrinsic E2F1 and its implications for autoimmunity upon cancer immunotherapy." *eMed Meeting on Systems Medicine conference–virtual,* 20-22 September, 2021.

Oral Presentations

Prabir Dhar, "Vector Technology at the forefront of Cardiac Reprogramming: Mission Accomplished". Research network iRhythmics final meeting**,** University of Rostock. 5th May, 2022.

Prabir Dhar, "iRhythmics: Programming pacemaker cells for in vitro drug testing". Research network irhythmic meeting**,** University of Rostock. 14th January, 2020.